Upper Water Column Nitrification Processes and the Implications of Euphotic Zone Nitrification for Estimates of New Production

by

Damian Grundle
B.Sc. Honours, University of Tasmania, 2004
M.Sc., University of Victoria, 2007

A Dissertation Submitted in Partial Fulfillment
of the Requirements for the Degree of

DOCTOR OF PHILOSOPHY

in the Department of Biology

Supervisory Committee

Upper Water Column Nitrification Processes and the Implications of Euphotic Zone Nitrification for Estimates of New Production

by

Damian Grundle
B.Sc. Honors, University of Tasmania, 2004
M.Sc., University of Victoria, 2007

Supervisory Committee

Dr. S. Kim Juniper (Department of Biology and School of Earth and Ocean Sciences)
Supervisor

Dr. Diana E. Varela (Department of Biology and School of Earth and Ocean Sciences)
Departmental Member

Dr. Jay T. Cullen (School of Earth and Ocean Sciences)
Outside Member

Dr. James R. Christian (Canadian Centre for Climate Modelling and Analysis)
Outside Member

Supervisory Committee
Dr. S. Kim Juniper (Department of Biology and School of Earth and Ocean Sciences)
Supervisor
Dr. Diana E. Varela (Department of Biology and School of Earth and Ocean Sciences)
Departmental Member
Dr. Jay T. Cullen (School of Earth and Ocean Sciences)
Outside Member
Dr. James R. Christian (Canadian Centre for Climate Modelling and Analysis)
Outside Member

Abstract

I used a specific inhibitor approach to systematically measure NH_4^+ oxidation rates through the euphotic zone of three distinct oceanographic regimes. Study sites included Saanich Inlet, a highly productive British Columbia fjord, the Line P oceanographic transect in the NE subarctic pacific, and the Bermuda Atlantic Time-series Study (BATS) station in the oligotrophic, sub-tropical Sargasso Sea. Nitrate uptake rates were also measured at select stations on a number of research cruises. NH_4^+ oxidation rates were found to proceed throughout the euphotic zone in each of my study regions, and, overall, euphotic zone NH_4^+ oxidation rates ranged from undetectable to 203 nmol L^{-1} d^{-1}. A general characterization of the rates observed in each of my study regions shows that euphotic zone NH_4^+ oxidation rates were typically highest in Saanich Inlet, intermediate along Line P, and lowest at BATS. The observation that NH_4^+ oxidation occurred throughout the euphotic zone in each of my study regions was in contrast to the traditional assumption of no euphotic zone nitrification, and it should now be considered a ubiquitous process in the euphotic regions of the ocean. Results found that euphotic zone nitrification could have potentially supported, on average, 15, 53 and 79% of the phytoplankton NO_3^- requirements in Saanich Inlet, and along Line P and at BATS, respectively, and this underscores the need for a major re-evaluation of the new production paradigm. Light, substrate concentrations, and potentially substrate supply

rates were all found to play a role in regulating NH_4^+ oxidation, albeit to varying degrees, and I discuss the influence that each of these variables may have had on controlling NH_4^+ oxidation rates at regionally specific scales in Chapters 2 (Saanich Inlet), 3 (Line P) and 4 (BATS). Finally, a cross study-region comparison of results showed that the relative degree by which new production estimates were reduced, when euphotic zone nitrification was taken into consideration, decreased exponentially as total NO_3^- uptake rates increased; the relationship I describe between these two variables may potentially provide a simple and rapid means of estimating the extent to which new production may have been overestimated at regionally specific and global scales.

My Line P sampling program also provided me with an opportunity to conduct the first investigation of intermediate depth N_2O distributions along the Line P oceanographic transect. My results demonstrated that nitrification is the predominant production pathway for N_2O in the NE subarctic Pacific. N_2O distributions along Line P were variable, however, and I also consider the role of different transiting water masses and potential far-field denitrification in contributing to this variability. Finally, I estimated sea-to-air fluxes of N_2O and based on these results I have demonstrated that the NE subarctic Pacific is a "hotspot" for N_2O emissions to the atmosphere.

Table of Contents

List of Tables

List of Figures

Acknowledgments

I would like to start by thanking my supervisor, Dr. Kim Juniper, for all of the support and guidance you have given me throughout my Ph.D. work. In particular, thank you for the independent freedom you gave me to pursue the topics and field studies that interested me, and for providing me with so many opportunities to expand my scientific horizons through travel to conduct research at the Bermuda Institute of Ocean Science and to participate in conferences. It was through these opportunities that I have developed many valuable working relationships which I hope will continue throughout my career. In short, it has been an absolute pleasure and a great experience working with you. I would also like to thank my committee members, Dr. Diana Varela, Dr. Jay Cullen, and Dr. James Christian for all your input and advice over the past several years. Furthermore, thank you to Dr. Roxane Maranger and Dr. Mike Lomas for all of your input and advice on our Line P N_2O and BATS manuscripts, respectively.

Thanks also to Dr. John Dower and Dr. Verena Tunnicliffe, your mentoring and friendship throughout my time at UVic has been tremendous. Thanks to Jon Rose for all your help in so many areas they are too numerous to list. I am also grateful to Sheryl Murdock for helping me in the lab and for running nutrient samples, and of course to every other member of the Juniper Lab.

My Ph.D. research would not have been possible without ship-time and field support, and for that I have many people to thank. Saanich Inlet work was supported by an *MSV John Strickland* ship-time grant awarded to Dr. Kim Juniper; Line P work was supported by the Institute of Ocean Sciences (IOS), DFO Canada, and sampling opportunities were facilitated by Marie Robert (Chief Scientist); BATS work was

organized by Dr. Mike Lomas and facilitated by the BATS team at the Bermuda Institute of Ocean Sciences. I am also grateful to Dr. Maureen Conte for providing me with an additional cruise opportunity to BATS. Thanks to Captain Ken Brown of the *MSV John Strickland* and all of the other fantastic officers and crew of the *CCGS John P. Tully* and *RV Atlantic Explorer*. Thanks also to Ian Beveridge for all your help during Saanich Inlet cruises. For the Line P work I would also like to thank all members of the science groups for all your help during cruises. The BATS work would not have been possible without equipment and field support, so thank you once again to Dr. Mike Lomas, as well as Deb Lomas, for all your support and for making me feel welcome in the lab. Thanks also to John Casey and Charlotte Best for help at sea, and to Doug Bell for being so accommodating with the spectrophotometer and for allowing me to ask more than two questions per day. Furthermore, my research trips to Bermuda would not have been so enjoyable without all of the people listed above, as well as Marlene Jefferies, Jason Ness, and Jerome Aucan. We had many a good night at The Wind.

Thank you also to Dr. Debbie Bronk and Dr. Mark Altabet for all the research proposal writing advice you have given me over the last year and a half of my Ph.D.. It undoubtedly paved the way for my next endeavour.

Finally, I would like to thank my Mum and Dad for all of the support and opportunities you have given me for as long as I can remember. I love you both very much.

Chapter 1 : Introduction

1.1 Carbon Export in the Ocean

The ocean is a major sink for atmospheric CO_2 and at timescales of hundreds to thousands of years it is the largest active carbon reservoir on earth (Takahashi et al. 2002; Yool et al. 2007). Large fractions of anthropogenic CO_2 can be sequestered by the ocean. Up to 30% of the anthropogenic CO_2 produced during the industrial revolution has been removed from the atmosphere into the ocean (Raven and Falkowski 1999). One of the principle driving forces behind the capacity of the ocean to remove CO_2 from the atmosphere is the solubility pump which is driven by physico-chemical processes that respond on timescales of years to decades. At longer timescales (i.e. hundreds to thousands of years), biological responses also play an important role in atmospheric CO_2 removal by sequestering carbon to deep waters and sediments via the biological pump (Sarmiento and Bender 1994). Of the ~45 gigatons of organic carbon produced by marine primary production on an annual basis ~35% is exported to the ocean interior via the biological pump (Falkowski et al. 1998), and although this pump typically responds at timescales ranging from hundreds to thousands of years, anthropogenic influences are capable of speeding up the response time. For example, while most of the anthropogenic CO_2 from the industrial revolution that entered the ocean was a result of the solubility pump, some was also a result of increased primary production caused by contemporaneous anthropogenic inputs of N, P and Fe (Raven and Falkowski 1999). Given the role that the biological pump plays in sequestering CO_2 from the atmosphere to the deep ocean and sediments, and the critical need to determine how it will respond to both natural and anthropogenically induced changes, a great deal of research has gone into understanding the factors which regulate carbon export via this biological pathway.

Because direct carbon export measurements via the biological pump are difficult to obtain at high spatio-temporal resolutions, indirect proxies which estimate the fraction of total primary production which is available for export are often used instead (Yool et al. 2007). One common proxy that has been used to estimate carbon export via the biological pump, and determine the factors which influence it, is the new production paradigm (discussed below).

1.2 The New Production Paradigm

Nitrogen is one of the key limiting elements for biological productivity in the ocean, and plays a critical role in regulating marine primary production (Gruber 2008). Of the various forms of nitrogen that are available to phytoplankton, NO_3^- has received the greatest attention (Mulholland and Lomas 2009), and is considered to be the primary nitrogen species supporting new production in most oceanic regions (Dore and Karl 1996; Eppley and Peterson 1979). As such, the biologically mediated two-step process of nitrification, which oxidizes NH_4^+ to NO_2^- (ammonium oxidation; Eq. 1A) and then NO_2^- to NO_3^- (nitrite oxidation; Eq. 1B) is a critical component of the marine nitrogen cycle[1].

$$NH_3 + 1.5O_2 \rightarrow NO_2^- + H_2O + H^+ \quad \text{1A}$$

$$NO_2^- + 0.5O_2 \rightarrow NO_3^- \quad \text{1B}$$

The new production paradigm, originally put forward by Dugdale and Goering (1967), has played a central role in the way we have viewed biological nutrient cycling over the past several decades. These authors defined NO_2^- and NO_3^- as sources of 'new' nitrogen, and NH_4^+ and DON as sources of 'regenerated' nitrogen, and they characterized

[1] Note: although the first step of nitrification is commonly referred to as NH_4^+ oxidation, it is the uncharged NH_3 that is the substrate for the first step of nitrification.

any primary production based on the utilization of these nitrogen sources as 'new' and 'regenerated' production, respectively. The basis for these designations was the fundamental assumption that although particulate organic nitrogen (PON) is remineralized to NH_4^+ throughout the euphotic zone, nitrification was confined to the disphotic and aphotic regions (hereinafter collectively referred to as aphotic) of the water column. Thus, it was presumed that any NO_3^- present within the euphotic zone was a direct result of upwelling or upward mixing. Eppley and Peterson (1979) expanded this concept by suggesting that because dissolved nitrogen does not build up within the euphotic zone, any upward flux of NO_3^- must be balanced by a downward flux of PON, and concluded that over spatio-temporal scales approaching steady-state conditions new production should be quantitatively equivalent to export production. Consequently, measurements of new production became a widely used proxy for estimating the efficiency and quantitative importance of the biological carbon pump.

1.3 Light Inhibition of Nitrification

The original assumption that nitrification was confined to depths below the euphotic zone stemmed from evidence that nitrification was light inhibited. Early evidence for this came from experiments with soil nitrifying bacteria (Mueller-Neugluck and Engel 1961). Later work by Horrigan et al. (1981) supported the theory of photo-inhibition for marine nitrifying bacteria. The Horrigan et al. (1981) study used enrichment cultures of nitrifying bacteria collected from the sea-surface film, and found that NH_4^+ oxidation was at least partially inhibited by light, while NO_2^- oxidation was completely inhibited by light. Based on these results it was concluded that NH_4^+ and NO_2^- oxidation displayed differential photo-inhibition, such that NO_2^- oxidation was more susceptible to light

inhibition that NH_4^+ oxidation (Guerrero and Jones 1996a; Vanzella et al. 1989). In contrast, however, Lomas and Lipschultz (2006) have since suggested that NO_2^- oxidation may actually exceed NH_4^+ oxidation in the euphotic zone. Further complicating our understanding as to the precise effect of light on nitrification activities are culture study results which show that: 1) the inhibitory effect of light is wavelength dependent (Guerrero and Jones 1996a; Vanzella et al. 1989); 2) increased cell concentrations of NO_2^- oxidizing bacteria lead to greater photosensitivity of NO_2^- oxidizing activity (Guerrero and Jones 1996a); 3) NH_4^+ oxidizing bacteria display greater photo-resistance as substrate concentration increases (Guerrero and Jones 1996a; Hooper and Terry 1973; Vanzella et al. 1989, 1990); 4) species specific responses to light may make generalizations difficult (Guerrero and Jones 1996a) and 5) isolates of estuarine NH_4^+ oxidizing bacteria are less sensitive to photo-inhibition than oceanic isolates (Horrigan and Springer 1990). Another confounding factor is that many of the cultures used to study the effects of light on nitrifying bacteria were initially maintained in the dark, which may have biased results by selecting dark-adapted nitrifying bacteria (Horrigan et al. 1981). More recently, NH_4^+ oxidizing archaea have also been discovered (Könneke et al. 2005), but the potential role of light in controlling NH_4^+ oxidation through the archaeal oxidation pathway remains to be determined (Ward 2008). Many of the factors discussed above, which can lead to variations in the degree of photosensitivity of nitrifying communities, are likely the cause of conflicting field observations. For example, while some studies have shown that *in situ* NH_4^+ oxidation rates increase with decreasing light intensity throughout the euphotic zone (e.g. Olson 1981; Ward 2005), others have found no clear increase in NH_4^+ oxidation rates with decreasing light through

much of this region (e.g. Bianchi et al. 1999a; Diaz and Raimbault 2000). Furthermore, Yool et al. (2007) recently compiled a total of 431 NH_4^+ oxidation rate measurements between the surface waters of the ocean and ~250m depth. These authors concluded that light inhibition of NH_4^+ oxidation was not significant as they did not observe a notable increase in specific NH_4^+ oxidation rates (i.e. NH_4^+ oxidation rate:NH_4^+ concentration) with increasing depth. This conclusion, based on a meta-analysis, should be treated with caution as many of the data points were based on NH_4^+ oxidation rates made near or below the base of the euphotic zone. Furthermore, the cross regional comparison which Yool et al. (2007) employed, is likely inappropriate given the potential for inter-regional differences in NH_4^+ oxidizing communities and ultimately the role that light may play in controlling NH_4^+ oxidation rates.

Although there is clearly plenty of evidence to support the notion of photo-inhibition of marine nitrification, the effect of light on this process appears to be highly variable and dependent on a number of extrinsic factors. The fact remains that both field and laboratory studies have shown that nitrification is capable of occurring to varying degrees within the illuminated region of the water column.

1.4 The Need to Re-evaluate the New Production Paradigm

Despite the increasing recognition that nitrification may be capable of proceeding to various degrees within the euphotic zone, studies continue to conduct new production measurements under the assumption that all NO_3^- within the euphotic zone is new nitrogen, an assumption which has undoubtedly resulted in overestimates of new production. Furthermore, although model simulations of new production often include nitrification parameters, these are often restricted to light intensity thresholds that are

lower than those which may actually inhibit nitrification, thus underplaying the potential importance of euphotic zone NO_3^- regeneration. The exclusion or misrepresentation of euphotic zone NO_3^- regeneration estimates from both field and modeled estimates of new production does not reflect a failure on the studies themselves, but is rather a reflection of our poor understanding of euphotic zone nitrification at regionally specific scales. The incorporation of euphotic zone nitrification rates into estimates of new production will not refute the new production paradigm, as conceptually it can accommodate such modifications (Mulholland and Lomas 2009). To improve the value of new production measurements and their use to estimate potential carbon export via the biological pump, modifications to the new production paradigm are necessary. *To achieve this, it is critical that we first gain a more comprehensive understanding as to the magnitude of euphotic zone nitrification and its inter-regional variability, as well as determine the factors which influence euphotic zone nitrification rates.*

1.5 Primary Research Objectives

The primary objectives of my Ph.D. research were to quantify the magnitude of euphotic zone nitrification, and estimate the extent by which estimates of new production are reduced as a result of euphotic zone NO_3^- regeneration, in three distinct oceanographic regions. These regions included: 1) a highly productive fjord (Saanich Inlet, British Columbia; Grundle and Juniper 2011 [Chapter 2]), 2) a transect spanning the upwelling region just off the continental shelf to the open ocean high-nutrient, low-chlorophyll (HNLC) region of the subarctic Pacific Ocean (Line P; Chapter 3), and 3) the oligotrophic sub-tropical Bermuda Atlantic Time-series study (BATS) site in the Sargasso Sea (Chapter 4).

Saanich Inlet was selected as it represents a highly productive coastal region. High primary productivity within the inlet has the potential to elevate particulate organic nitrogen (PON) flux. High PON flux could support high rates of PON remineralization and subsequent NH_4^+ oxidation. Saanich Inlet was also the site of a recent new production study (Grundle et al. 2009), and measurements of euphotic zone nitrification have allowed us to assess the degree to which these authors may have overestimated this important nitrogen cycling parameter. In addition, although many aspects of physical and biological nutrient cycling have been studied in Saanich Inlet, very little is known about nitrification within the inlet, and this study has provided important new insights into the role that *in situ* nitrification plays in recycling and supplying NO_3^- within Sannich Inlet.

The principle underlying rationale for selecting Line P and BATS as study regions for my Ph.D. research was that both of these areas have long served as locations for oceanographic time-series studies. Oceanographic sampling at OSP (Ocean Station Papa, also known as P26), the western most station along Line P, has been ongoing since 1949, and spatial sampling along Line P began in 1959. Sampling at the BATS site in the oligotrophic Sargasso Sea began in 1989, however, time-series sampling at nearby Hydrostation S started in 1954. The physical, chemical and biological time-series data, including new production measurements, which have been measured at Line P and BATS/Hydrostation S have played a key role in our understanding of oceanographic processes. In particular the Sargasso Sea served as the site for the first measurements of new production (Dugdale and Goering 1967). As such, it was felt that Line P and BATS deserved particular attention for the investigation of euphotic zone nitrification and the results I present in this thesis have significantly improved our understanding of upper

water column nitrogen cycling in these regions, and has, for the first time, quantified the extent by which new production may have been overestimated in these two key oceanographic sampling regions.

To estimate the potential role that nitrification plays in regenerating NO_3^- within the euphotic zone, I focused on the first and rate-limiting step of nitrification (i.e. NH_4^+ oxidation). The exception to this was Saanich Inlet, where simultaneous measurements of both NH_4^+ and NO_2^- oxidation rates were conducted. Determination of the extent by which euphotic zone nitrification reduced estimates of new production was assessed either indirectly or directly. In Saanich Inlet I relied on earlier measurements of phytoplankton NO_3^- uptake rates, whereas for the Line P and BATS studies I conducted simultaneous NO_3^- uptake measurements. Ultimately, the results from these three studies have allowed us to evaluate the extent to which new production is overestimated as a result of assuming no euphotic zone nitrification, both within and between regions which continue to serve as important sites for understanding marine biogeochemical processes. Developing a comprehensive understanding of the 'between-region' implications of euphotic zone nitrification is an important first step toward determining the extent to which new production may have been overestimated at the global scale.

1.6 Additional Study Objectives

1.6.1 Impact of Nitrification on the Development of Hypoxia

Understanding the effect that specific microbial processes have upon oxygen consumption is of significant importance given the expansion of coastal hypoxic and oceanic oxygen minimum zones. The presence of a shallow sill in Saanich Inlet results in periods of water mass isolation, and hypoxia periodically develops at depths >70 m.

Hypoxia is reversed when dense oxygenated water spills over the sill and re-supplies oxygen to the deep basin of the inlet. Influxes of oxygenated water followed by the development of hypoxia makes Saanich Inlet an ideal "model system" in which to study the contribution of microbial activities to the development of hypoxia, as following an oxygen renewal event, the temporal build-up of hypoxia can be tracked in conjunction with the activity of specific microbial processes. To this end, I also assessed the contribution of nitrification to the development of hypoxia in Saanich Inlet following an oxygen renewal event (Chapter 2).

1.6.2 Nitrous Oxide Distributions and Potential Production by Nitrification in the NE subarctic Pacific

Nitrous oxide (N_2O) is an important greenhouse gas and, over a 100 year time span it has a per mole global warming footprint which is ~300 times that of CO_2 (Crutzen 1970; de Bie et al. 2002), and NH_4^+ oxidation is one of the major sources of N_2O in the ocean. During NH_4^+ oxidation, N_2O can be produced via hydroxylamine, an intermediary product in the oxidation of NH_4^+ to NO_2^-(Bange 2008). The relative magnitude of N_2O production by NH_4^+ oxidation increases as dissolved oxygen concentrations decrease (Codispoti and Christensen 1985; de Bie et al. 2002; Goreau et al. 1980; Naqvi et al. 2010). The subarctic Pacific has experienced declining dissolved oxygen concentrations over the past several decades (Emerson et al. 2004; Whitney et al. 2007), and this may have led to an increase in N_2O production. Even if dissolved oxygen concentrations have not yet decreased to the extent which promotes increased N_2O production, dissolved oxygen concentrations are predicted to continue declining through this century (Keeling et al. 2010), and, as such, it is possible that N_2O production will also increase. Given the

absence of any N_2O measurements from the Line P region of the NE subarctic Pacific, I therefore took advantage of the opportunity to also quantify the distribution and magnitude of N_2O concentrations and potential production at intermediate depths along the Line P transect during cruises in 2009 (Chapter 5). Results from this study have provided important insights into the water masses which contribute N_2O to the different regions along Line P, and have provided an important baseline from which future studies will be able to determine how further decreases in dissolved oxygen will impact N_2O pools and production in the NE subarctic Pacific.

1.7 Sampling Regime

Sampling in Saanich Inlet was conducted on a monthly basis from April to October 2008, onboard the *MSV John Strickland*. This sampling regime allowed us to assess the overall importance of *in situ* nitrification to Saanich Inlet NO_3^- supply and the role that nitrification plays in euphotic zone NO_3^- regeneration during the highly productive Saanich Inlet growing season (Grundle et al. 2009). Water sampling and NH_4^+ oxidation rate measurements were conducted at a range of depths spanning the lower euphotic zone to the sub-oxic waters of the inlet, thus allowing me to assess how nitrification rates vary across well-defined environmental gradients that are characterized by large bulk changes in oxygen and nutrient concentrations.

Sampling along Line P was conducted during winter (February), spring (June) and late-summer (August) cruises in 2009, onboard the *CCGS John P. Tully*. NH_4^+ oxidation and NO_3^- uptake rates were measured from the surface to the base of the euphotic zone (i.e. 1% of surface incident irradiance; I_o). The Line P transect provided an opportunity to determine how NH_4^+ oxidation rates, and the contribution of euphotic zone nitrification

to phytoplankton NO_3^- requirements, varies across regions characterized by different nutrient conditions, as well as between seasons when changes in light intensity may contribute to NH_4^+ oxidation rate variability. These cruises also allowed us to opportunistically examine the distribution of N_2O and O_2 concentrations at intermediate depths along an east-west gradient in the NE subarctic Pacific. Different water masses contribute to the longitudinal variability of intermediate depth chemical and physical properties of the NE subarctic Pacific, and thus, the Line P east-west gradient enabled us to assess the potential role that these water masses play in the distribution of NE subarctic Pacific N_2O at intermediate depths.

Sampling in the Sargasso Sea was conducted at BATS during two cruises in April 2009 and two cruises in November 2009, onboard the *RV Atlantic Explorer*. NH_4^+ oxidation and NO_3^- uptake rates were measured from the surface to the base of the euphotic zone (i.e. 1% I_o). Our sampling regime allowed us to estimate the degree to which euphotic zone nitrification contributes to phytoplankton NO_3^- requirements during the Sargasso Sea oligotrophic period when surface stratification minimizes upward intrusions of truly new NO_3^- (Lipschultz et al. 2002).

1.8 Ammonium Oxidation Rate Measurements

A number of approaches have been used to measure NH_4^+ oxidation rates in the ocean and these have been outlined in detail by Ward (2008, 2011). Two of the most frequently used methods include the use of either ^{15}N tracer or specific-inhibitor techniques. Tracer techniques involve adding a ^{15}N enriched substrate (e.g. ^{15}N-labelled NH_4^+) to incubation bottles, and then tracing the evolution of the enriched isotope signal from the substrate to the product pool. Of course, the ^{15}N enriched substrate must be added in sufficient

quantities to be able to detect its transfer into the product pool. In highly oligotrophic regions this can lead to enrichments which are in excess of the ambient *in situ* substrate pool and may cause significant positive perturbations to the rates being measured (e.g. Ward 2005). On the other hand, NH_4^+ regeneration, in the case of NH_4^+ oxidation rates measurements for example, will dilute the ^{15}N enriched substrate pool, thus leading to underestimates of rate processes. Because my Ph.D. research involved a comparative analysis of NH_4^+ oxidation rates across regions which are characterized by distinctly different nutrient conditions, and probably NH_4^+ regeneration rates, I therefore opted to use a specific-inhibitor based approach to measure NH_4^+ oxidation rates.

The inhibitor technique I used during my Ph.D. research involved the use of allylthiourea (ATU), which specifically inhibits NH_4^+ oxidizing bacteria, to measure NH_4^+ oxidation rates. This is a well-established method which requires no alteration of the ambient substrate pool and has been successfully used to measure NH_4^+ oxidation rates under a range of environmental and oceanic conditions (e.g. Bianchi et al. 1994a, 1994b, 1997; de Bie et al. 2002; Feliatra and Bianchi 1993; Iriarte et al. 1996; Lam et al. 2004; Santoro et al. 2010). The ATU method involves incubating replicate treatment (treated with 10 mg L^{-1} of ATU) and unamended control bottles. Because ATU inhibits NH_4^+, but not NO_2^-, oxidizing bacteria, any increase of NO_2^- in the control bottles vs. the treatment bottles at the end of the incubation will be due to NH_4^+ oxidation (Ward 2011). Of course, this method also has its drawbacks. The foremost drawback is related to the recommended need to conduct incubations in the dark in order to prevent, or at least minimize, autotrophic NO_2^- uptake (Ward 2008). The use of dark incubations could have 1) provided the NH_4^+ oxidizing organisms with additional relief from photo-inhibition

(i.e. greater than that which would be naturally provided to them during the night) and 2) resulted in decreased substrate competition between NH_4^+ oxidizing organisms and phytoplankton. Ultimately, these perturbations to the natural conditions could have led to overestimations of AO rates. Indeed, field studies in the N Pacific using ^{15}N tracer additions and 24 hr light and dark incubations have demonstrated that light incubations resulted in AO rates which were 70 and 96% of those measured in the dark (Olson 1981). Thus, the dark incubations used during my Ph.D. research could have resulted in NH_4^+ oxidation rates being overestimated by as much as 30%. Another potential source of error involved with the use of ATU relates to the presence of NH_4^+ oxidizing archaea. NH_4^+ oxidizing archaea were only recently discovered (Könneke et al. 2005), and even more recently Santoro et al. (2010) showed that ATU only inhibited ~60-75% of AO activity in mixed AO organism assemblages collected from the euphotic zone of the California current. Thus, while ATU completely inhibits AO bacteria, it may only partially inhibit AO archaea and could lead to NH_4^+ oxidation rates being underestimated if archaea are actively oxidizing NH_4^+. Unfortunately, this came to light after the completion of my Ph.D field studies and, as such, I was unable to resolve this problem. Still, given that the use of dark incubations may lead to NH_4^+ oxidation rates being overestimated by up to 30%, while the use of ATU could cause underestimates of up to 40%, it is likely that these positive and negative sources of error would have countered each other to some degree.

All of the AO rate measurements conducted during my Ph.D. research were run in duplicate and the overall average error between all duplicate measurements was 15%. The study specific AO rate measurement errors were 17, 15 and 15% for Saanich Inlet

(Chapter 2), Line P (Chapter 3) and BATS (Chapter 4), respectively. Finally, while the nitrification rate results from Saanich Inlet, Line P and BATS are summarized in figures in chapters 2, 3 and 4, respectively, a complete list of the nitrification rates measured throughout my Ph.D. research are also included in Tables A1 (Saanich Inlet), A2 (Line P) and A3 (BATS) in Appendix 1.

Chapter 2 : Nitrification from the lower euphotic zone to the sub-oxic waters of a highly productive British Columbia fjord

Citation:

Grundle, D.S., and S. K. Juniper. 2011. Nitrification from the lower euphotic zone to the sub-oxic waters of a highly productive British Columbia fjord. *Marine Chemistry* 126: 173-181.

Abstract

Nitrification rates were measured monthly from April to October 2008, at depths ranging from the lower euphotic zone to the sub-oxic waters of Saanich Inlet. Ammonium (NH_4^+) and nitrite (NO_2^-) oxidation rates ranged from undetectable to 0.319 and 0.478 μmol L^{-1} d^{-1}, respectively. NH_4^+ oxidation rates and concentrations were positively correlated at substrate concentrations less than 0.8 μmol NH_4^+ L^{-1}. Positive correlations between NH_4^+ oxidation rates, NO_2^- concentrations, and NO_2^- oxidation rates were also observed, highlighting the important role that NH_4^+ oxidation plays in supporting NO_2^- oxidation in Saanich Inlet. Despite the apparent dependence of NO_2^- oxidation rates on NH_4^+ oxidation rates, the former was still 44% higher than the latter and we concluded that Saanich Inlet NO_2^- oxidation rates were augmented by fortnightly spring-tide nutrient renewal. From May to October, sub-oxic zone waters were isolated from any significant mixing events, and we estimated that nitrification was responsible for approximately 25% of dissolved oxygen consumption. This estimate is in close agreement with that calculated using Redfield stoichiometry, and as such highlights the accuracy with which nitrification rates can be quantified using incubation techniques. Finally, nitrification rates in the euphotic zone were at times substantial, and we suggest that earlier estimates of new production in Saanich Inlet may have been overestimated by approximately 15%.

2.1 Introduction

Saanich Inlet, a silled fjord on southern Vancouver Island, British Columbia (Fig. 2.1) is well known for its high primary productivity (Grundle et al. 2009; Timothy and Soon 2001), which is largely driven by NO_3^- based diatom growth (Grundle et al. 2009). The shallow (~70 m) sill restricts the movement of deep water between the basin of the fjord and neighboring Satellite Channel, which in combination with vertical organic matter flux, results in deep-water anoxia (Cohen 1978; Herlinveaux 1962). However, unlike a number of other British Columbia fjords that develop deep-water anoxia, Saanich Inlet periodically experiences renewal events that re-supply oxygenated water to its deep basin (Anderson and Devol 1973).

The high rates of NO_3^- driven primary production in Saanich Inlet have been attributed to a somewhat unusual but regular nutrient delivery mechanism (described in detail by Gargett et al. 2003). Briefly, during spring tides, when tidal currents are strong, increased mixing seaward of Saanich Inlet causes a breakdown of surface-water stratification in adjacent Satellite Channel. The ensuing density gradient causes NO_3^- depleted water from the upper portion of the euphotic zone to flow out through the mouth of Saanich Inlet and into Satellite Channel. This outflow is replaced by a sub-surface inflow of well mixed nutrient-rich water, which re-supplies nutrients to the euphotic zone of Saanich Inlet and promotes increased phytoplankton growth several days later during the neap tide period (Parsons et al. 1983; Takahashi et al. 1977).

Although horizontal transport of new nutrients (i.e. NO_3^- and NO_2^-) into Saanich Inlet is fairly well understood, very little is known about the *in situ* production of these inorganic nitrogen anions. The only previous study of nitrification in Saanich Inlet

limited *in situ* NH_4^+ oxidation rate measurements to 9 depths between ~30 and 140 m in August 1986 and 3 depths between 30 and 112 m in September 1986 (Ward and Kilpatrick 1990). The main goal of Ward and Kilpatrick (1990) was to investigate possible relationships between NH_4^+ and CH_4 oxidation rates and substrate concentrations. The temporal variability of nitrification and its relative impact on overall NO_3^- supply to Saanich Inlet remain poorly understood. The primary focus of the present study was to evaluate the quantitative importance of *in situ* nitrification processes in Saanich Inlet during the highly productive growing season (April to October; Grundle et al. 2009) of 2008, at a sampling station near the mouth of the inlet. Relationships between experimentally derived nitrification rates and a number of environmental and physical processes were also examined.

Our study also provided an opportunity to contribute to an emerging understanding of the occurrence of nitrification within the euphotic zone, and its broader implications for our understanding of nitrogen and carbon cycling. Dugdale and Goering (1967) originally defined NO_3^- as a "new" source of nitrogen to the euphotic zone, and NO_3^- based primary production as "new" production. This designation was founded upon the assumption that nitrification was restricted to the aphotic water column, and that any NO_3^- in the euphotic zone was a result of upwelling or upward mixing. Eppley and Peterson (1979) later pointed out that because dissolved nitrogen does not accumulate within euphotic zone waters, upward fluxes of NO_3^- must be balanced by downward fluxes of PON, and concluded that new production was quantitatively equivalent to export production. The assumption that nitrification was restricted to aphotic depths seemed reasonable given evidence for photo-inhibition of nitrification (Horrigan et al. 1981; Mueller-Neugluck

and Engel 1961; Schon and Engel 1962). However, the potential for nitrification to occur within the euphotic zone has since been demonstrated (Ward 1987). Nevertheless, measurements of new production have continued under the assumption of no euphotic zone nitrification, and as such studies may have substantially overestimated new production and potential carbon export (Yool et al. 2007).

2.2 Methods

2.2.1 Sampling regime

Monthly sampling was conducted from the *MSV John Strickland* at station SI-2 near the mouth of Saanich Inlet (Fig. 2.1), from April to October 2008. This sampling period has previously been shown to span the highly productive phytoplankton growing season in Saanich Inlet (Grundle et al. 2009), and station SI-2 has been the focus of phytoplankton and nutrient dynamic studies in the past (Grundle et al. 2009; Timothy et al. 2003; Timothy and Soon 2001). Water samples for biological and chemical measurements were collected using acid-cleaned Niskin bottles on a Rosette sampler with an attached SeaBird Electronics SBE 19+ conductivity, temperature and depth (CTD) profiler. Discrete water samples were collected from depths corresponding to 55, 10 and 1% of surface incident irradiance (I_o), as determined using an integrated Biospherical QSP-200L photosynthetically active radiation (PAR) sensor, and from 30, 45, 60, 75, 90, 105 and 120 m.

2.2.2 Automated CTD measurements and dissolved nutrient concentrations

Vertical profiles of temperature and salinity were measured with the CTD profiler. A SeaBird Electronics SBE 43 dissolved oxygen sensor was also attached to the CTD to

obtain continuous vertical measurements of dissolved oxygen (DO) concentrations.Water samples for the measurement of dissolved NO_3^-, NO_2^-, and NH_4^+ concentrations were collected at each of the previously stated sampling depths. Dissolved NH_4^+ concentrations were measured using the fluorometric technique of Holmes et al. (1999) immediately following collection, whereas dissolved NO_3^- and NO_2^- samples were stored at -20°C until analysis using an Astoria-Pacific autoanalyzer (Barwell-Clarke and Whitney 1996).

2.2.3 Nitrification rates

Samples for nitrification rate measurements were collected from depths corresponding to 10 and 1% I_o, and from 30, 60, 90 and 120 m depths. The exception to this was during April when nitrification rates were only measured at 10% I_o, and 30 and 90 m depths. NH_4^+ oxidation (AO) and NO_2^- oxidation (NO) rates were measured using the well-recognized AO and NO inhibitors allylthiourea (ATU; final concentration 10 mg L^{-1}) and $NaClO_3$ (final concentration 10 mmol L^{-1}), respectively (Bianchi et al. 1994a, 1994b). Water from each depth was split into 6 x 500 ml acid-cleaned polycarbonate bottles: 2 non-amended (control), 2 amended with ATU, and 2 amended with $NaClO_3$. Given that ATU inhibits AO but not NO, any increase of NO_2^- in the control compared to the ATU treatment was due to AO; whereas $NaClO_3$ inhibits NO but not AO, such that any decrease of NO_2^- in the control relative to the $NaClO_3$ treatment was a result of NO. Following the addition of inhibitors, samples were incubated in the dark under controlled temperature conditions (within 1°C of *in situ* sampling depth temperature). Dissolved NO_2^- concentrations in the control and treatment bottles were measured every 3-4 h, to a maximum of 24 h, and rates were derived from the linear increase or decrease of NO_2^- in

the replicate control bottles vs. the replicate treatment bottles. For the nitrification rate measurements, NO_2^- concentrations were determined by the colorimetric method outlined by Bendschneider and Robinson (1952) at 543 nm, using 10 cm pathlength cells to permit detection of nanomolar concentrations.

Trapezoidal integration from the depth of 10% I_o to 120 m depth was used to estimate depth-integrated AO and NO rates. For our April sampling date, when the deepest sampling depth was 90 m, we extrapolated the 90 m AO and NO rates to 120 m, so as to maintain consistency with the depth range used for integrations from May to October. For the period of May to October, AO and NO decreased from 90 to 120 m by an average of 62% and 31%, respectively. We therefore assumed that during April, AO and NO rates would have decreased to a similar extent over the same depth range. The extrapolation used for AO and NO rates at 120 m depth, accounted for 30 and 29%, respectively, of the integrated rates for April.

2.3 Results and Discussion

2.3.1 Automated CTD measurements and dissolved nutrient concentrations

2.3.1.1 Density, Temperature and Salinity

Consistent with previous studies of Saanich Inlet (e.g. Grundle et al. 2009; Herlinveaux 1962; Timothy and Soon 2001), density gradients always extended from ~70 m depth to the surface, indicating that the surface waters of the fjord were stratified throughout the study (Fig. 2.2a). Although the surface waters at station SI-2 were permanently stratified during the present study, to maintain consistency with previous

studies of Saanich Inlet (e.g. Gargett et al. 2003; Grundle et al. 2009), we used the mean of 1 m binned temperature and salinity intervals (Fig. 2.2b and 2.2c) through the upper 20 m of the water column to estimate surface temperature and salinity. Surface temperature ranged from 8.1 to 12.5°C (Fig. 2.2b inset), and the monthly variability closely matched the monthly air temperature variability measured at Victoria International Airport. Surface salinity reached a maximum of 29.8 in May and then decreased to a minimum of 29.0 in September (Fig. 2.2c inset). External seaward influences need to be considered when interpreting variations in surface salinity in Saanich Inlet, as the major sources of freshwater to the inlet are from the Fraser River in spring and summer, and from the Cowichan River in winter (Herlinveaux 1962). In 2008, Fraser River flow was highest between mid-May and early September, with peak flow (~10,000 m^3 s^{-1}) occurring between May and early June (flow data obtained from Environment Canada; Fraser River Hope station). Thus, the decrease in surface salinity between May and September was likely caused by the Fraser River freshet.

2.3.1.2 Dissolved Oxygen

DO concentrations in Saanich Inlet are influenced by a number of biological and physical factors. Photoautotrophic oxygen production, along with gas exchange at the sea-air interface, produces high DO concentrations in the near surface waters; while remineralization and oxidative processes consume DO at greater depths (Fig. 2.3). The effect of sub-surface metabolism on DO concentrations accrues below the depth of the sill (~70 m) that separates the deep waters of Saanich Inlet from the well-mixed oxygenated waters of Satellite Channel. Mid-water (~90 -110 m) oxygen renewal occasionally occurs when oxygenated water, with a density greater than that of the

resident deep water, spills over the sill and subsequently sinks to its equivalent density level within the inlet (Anderson and Devol 1973). Such an event probably occurred between our April and May sampling dates, as the depth of the hypoxic boundary, defined as DO concentrations <2.0 ml L^{-1} (Diaz and Rosenberg 1995), deepened from 90 – 110 m during this period (Fig. 2.3 inset). Following May, the hypoxic boundary progressively shoaled to a minimum of 67 m in October, indicating that there were no additional intrusions of oxygenated water between the depth of the sill and our deepest sampling depth during this period. This is consistent with previous observations of oxygen depletion within this depth range in Saanich Inlet (Anderson and Devol 1973). It is important to note that even though anoxia (i.e. 0 ml O_2 L^{-1}) is a common feature in the deep basin of Saanich Inlet during summer (Tunnicliffe et al. 2003), the lowest DO concentrations recorded by the DO sensor on our CTD were ~0.1 ml L^{-1}. This sensor is known to be accurate to within 0.13 to 0.2 ml L^{-1} (Manning et al. 2010). Thus, any CTD-DO concentrations <0.20 ml L^{-1} should be considered potentially anoxic.

2.3.1.3 Dissolved Nutrients

At depths spanning the lower euphotic zone to the sub-oxic waters (i.e. 120 m) of Saanich Inlet, dissolved NO_3^-, NO_2^-, and NH_4^+ concentrations ranged from undetectable to 28.9 µmol L^{-1}, 0.015 to 1.12 µmol L^{-1}, and from undetectable to 4.9 µmol L^{-1}, respectively (Fig. 2.4). Typically, NO_3^- concentrations increased with depth to ~90 m, before decreasing to 120 m depth (Fig. 2.4a). NO_2^- concentrations tended to increase with depth from 55% to 1% I_o, after which there were only minor vertical variations (Fig. 2.4b). A notable exception to this occurred during October when NO_2^- concentrations were greatest in the upper 45 m of the water column, with a large peak occurring at 10%

I_o. Although NH_4^+ concentrations showed a high degree of vertical and temporal variability, highest concentrations were often observed at mid-water depths between the base of the euphotic zone (1% I_o) and 60 m, and probably represented the zone of highest ammonification (Fig.2. 4C). The overall highest NH_4^+ concentrations were observed in May and September and likely resulted from the remineralization of spring and summer phytoplankton blooms, which are characteristic features of Saanich Inlet (Grundle et al. 2009)

2.3.2 Nitrification Rates

2.3.2.1 Ammonium and Nitrite Oxidation Rates and Substrate Concentrations

AO and NO rates displayed a high degree of vertical and temporal variability, ranging from undetectable to 0.319 µmol L^{-1} d^{-1} and undetectable to 0.478 µmol L^{-1} d^{-1}, respectively (Fig. 2.5). The upper range of the nitrification rates reported here are an order of magnitude higher than those reported for several pelagic coastal NE Pacific regions (Ward 1987, 2005; Ward et al. 1984), but are similar to those observed in other estuarine waters (Bianchi et al. 1999a, 1999b; Iriarte et al. 1996). Furthermore, with the exception of our two highest measurements in October (Fig. 2.5), the range and considerable vertical variability of our AO rates were similar to those reported for Saanich Inlet by Ward and Kilpatrick (1990). In the Rhone River estuary (NW Mediterranean), high NH_4^+ concentrations were found to drive high AO rates, which in turn allowed for high rates of NO (Bianchi et al. 1999a). Although we observed no relationship between AO rates and NH_4^+ concentrations (Fig. 2.6a), we did find that both NO_2^- concentrations and NO rates were positively correlated with AO rates (Fig. 2.6b and 2.6c, respectively), and that NO rates were positively correlated with NO_2^- concentrations

(Fig. 2.6d). This indicates that, similar to the scenario in the Rhone River plume, NO rates were at least partly driven by AO through the production of NO_2^-. Given the observation that NO rates were correlated with NO_2^- concentrations, we attempted to fit a one-site saturation Michaelis-Menten type model to the results; however, given the linearity of the data, this model was found to be inappropriate. This may indicate that NO_2^- concentrations in Saanich Inlet were not saturating and that the NO communities were able to respond to changes in substrate concentration. Conversely, our observation that AO rates were not correlated to substrate concentrations may indicate that NH_4^+ concentrations in Saanich Inlet were saturating. Olson (1981) estimated that the K_s value for a natural population of AO bacteria was <0.1 µmol NH_4^+ L^{-1}, a concentration less that that of the ambient NH_4^+ concentrations corresponding to many of our AO rate measurements. However, the results reported by Olson (1981) were based on NH_4^+ addition incubations lasting 24 hours or less. Given that we were unable to determine the resident time of the ambient NH_4^+ pools measured during this study, it is difficult to compare results from kinetic studies such as Olson (1981) with those observed during the present study, for two primary reasons. Firstly, AO bacteria possess constitutive Calvin cycle and chemolithotrophic pathways, and the enzymes associated with these pathways do not respond to changes in substrate concentrations over short time periods (Ward and Kilpatrick 1990). To this end, there would likely be a lag period between NH_4^+ addition and the potential maximum AO rate. As such, NH_4^+ addition incubations lasting 24 hours or less likely underestimate potential maximum daily AO rates and K_s values. Secondly, even when grown under laboratory conditions, the maximum growth rate of common AO bacteria is approximately one division per day (Ward et al. 1982). Kinetic experiments of

24 hours or less therefore assume a relatively static population size. As we do not know the residence time of the ambient NH_4^+ pools measured during the present study, we cannot discount the possibility that AO organisms in Saanich Inlet were able to undergo population growth, and thus achieve higher community wide K_s values. It is important to note however, that at NH_4^+ concentrations <0.80 µmol L^{-1} these two variables were significantly positively correlated (Spearman Rank Correlation test: p <0.01; r = 0.514; n =25), whereas at higher concentrations of NH_4^+ no correlation was observed. This indicates that, at the lower range of NH_4^+ concentrations (i.e. <0.80 µmol L^{-1}), the AO communities sampled in Saanich Inlet had been afforded sufficient time to respond to changes in substrate concentrations. Conversely, the higher range of NH_4^+ concentrations may have been representative of fresh NH_4^+ inputs to which the AO communities had not yet had time to react. In summary, while AO rates were likely partly controlled by NH_4^+ concentrations during the present study, single time-point comparisons following what may have been rapid inputs of NH_4^+ did not always show a direct relationship between these two variables.

2.3.2.2 Nitrification and Dissolved Oxygen Concentrations

At 120 m, the sampling depth at which DO concentrations were lowest, both AO and NO rates were at times greater than those at depths with higher DO concentrations, and no significant correlation between nitrification rates and DO concentrations was found (i.e. p >0.05). This is not surprising, as it is unlikely that any relationship between nitrification rates and DO concentrations would be observed unless rates were measured across the transition zone between limiting and non-limiting DO concentrations. Our observations, together with those from previous studies, lead us to conclude that AO was

not oxygen limited within the upper 120 m during the present study. AO has been shown to proceed in Saanich Inlet (Ward and Kilpatrick 1990), and other regions (Lipschultz et al. 1990; Ward et al. 1989), at DO concentrations <~0.1 ml L^{-1}, concentrations which were lower than those found at our deepest sampling depth. Furthermore, although AO is more tolerant of reduced DO than NO, AO bacteria do not typically outcompete NO bacteria until DO concentrations fall below 0.7 ml L^{-1} or less (Brockmann and Morgenroth (2010). DO values less that 0.7 ml L^{-1} were only observed at our sub-oxic sampling depths during October of the present study. Therefore, while it is possible that NO may have been DO-limited during the final month of the study, we conclude that it was not DO-limited in the sampling months preceding October.

Although DO concentrations did not appear to influence nitrification rates during this study, there is evidence for a significant impact of nitrification on oxygen consumption within Saanich Inlet. Apparent oxygen utilization (AOU) is one method of estimating the amount of oxygen consumed by biogeochemical processes in the ocean (Bange 2008). In the absence of biological oxygen production or physical oxygen re-supply, AOU will increase as water masses age. Between May and October, water at our "below sill" sampling depths (i.e. 90 and 120 m) appeared to have been cutoff from any intrusions from Satellite Channel, as oxygen concentrations decreased while average AOU in this region of the water column increased from 203 to 271 µmol L^{-1}. The O_2:N molar ratios for AO and NO are 1.5 and 0.5 respectively (Ward 2008), and if these processes are significant contributors to DO consumption it should be possible, in the absence of oxygen renewal, to detect a correlation between nitrifier DO consumption and AOU. However, because AOU was cumulative from May to October, comparing single time-

point measurements of DO consumption by nitrification to monthly estimates of AOU is not appropriate. Instead, to determine the effect of nitrification on AOU, cumulative DO consumption by nitrification should be calculated. To this end, we determined average monthly stoichiometric DO consumption based on AO and NO rates at 90 and 120 m, temporally interpolated them between sampling dates, and then cumulatively added them from month to month. Finally, we compared average (90 and 120 m) monthly AOU estimates to cumulative DO consumption from May to October using simple linear regression, and found a significant positive linear relationship between these two variables (Fig. 2.7). Based on the slope of the regression line used to describe the relationship between AOU and cumulative DO consumption, we estimated that within the "below sill" (90 – 120 m) depth interval, the combined effects of AO and NO were responsible for ~25% of the oxygen utilization from May to October 2008. Our estimate of combined oxygen consumption by AO and NO is remarkably close to that calculated using Redfield stoichiometry, which attributes 23% of marine oxygen consumption to AO and NO processes (Ward 2008). The close agreement between our estimate of oxygen consumption by AO and NO, and that based on Redfield stoichiometry, underlines the accuracy with which the inhibitor based methods, employed during this study, can be used to estimate nitrification rates. In addition, it also demonstrates the accuracy with which oxygen consumption processes, and their impact on the development of hypoxia, can be quantified in Saanich Inlet during post-oxygen renewal periods of water mass isolation. This latter point highlights the potential for Saanich Inlet to serve as a model system to investigate the processes involved in, and affected by, the

development of hypoxia, a topic which is gaining considerable attention given the worldwide expansion of oxygen minimum zones (e.g. Keeling et al. 2010).

2.3.2.3 Differences between Ammonium and Nitrite Oxidation Rates

Depth-integrated (10% I_o to 120 m) AO and NO rates ranged from 4.52 to 23.9 mmol NH_4^+ m^{-2} d^{-1} and from 6.02 to 18.3 mmol NO_2^- m^{-2} d^{-1}. A temporal extrapolation of the monthly depth-integrated nitrification rates showed that, for the duration of the study period, AO and NO accounted for 1.58 and 2.28 mol N oxidized m^{-2}, respectively, such that NO was 44% higher than AO. Furthermore, subsequent analysis of the data revealed that all of the observed difference between AO and NO was accounted for by rates measured above the depth of the sill (i.e. <70 m). A paired t-test confirmed that AO rates were significantly lower than NO rates (p = 0.022; n = 26) between 10% I_o and 60 m depth.

The finding that AO rates were significantly lower than NO rates at depths above the sill was somewhat surprising given that the former provides the substrate for the latter. Our finding either points towards a methodological artifact, or a deviation from steady-state nitrification conditions (i.e. where NO is ≤ AO) at depths above the sill in Saanich Inlet. This study measured AO and NO rates in dark incubations which may have artificially altered the two processes, causing NO to be greater than AO, in samples collected from the euphotic zone. For example, NO could be photo-inhibited to a greater degree than AO, however over diurnal cycles the two processes may remain balanced because NO is quicker to recover from photo-inhibition than AO. If this were the case, our use of dark incubations for euphotic zone samples may have led to an increase in NO rates over AO rates. While we cannot conclusively discount this possibility, there is no

definitive evidence to support it, as studies which have investigated differential photo-inhibition of AO and NO have reported conflicting results (Guerrero and Jones 1996a; Horrigan et al. 1981; Vanzella et al. 1989). Another natural phenomenon that may have resulted in NO rates being greater than AO rates is that of phytoplankton NO_2^- release. Under low light conditions, such as those experienced near the base of the euphotic zone, phytoplankton may release NO_2^- as a result of incomplete NO_3^- to NH_4^+ reduction. This phenomenon is often thought to be responsible for the occurrence of a primary nitrite maxima at the base of mixed layers or euphotic zones (Lomas and Lipschultz 2006). If irradiance near the base of the stratified euphotic zone in Saanich Inlet had been insufficient for photoautotrophic cells to achieve complete NO_3^- reduction, then phytoplankton NO_2^- release may have led to NO rates increasing relative to AO rates. While either of the points discussed so far (i.e. differential recovery from photo-inhibition by AO and NO organisms, or phytoplankton NO_2^- release) may have potentially led to an increase of NO over AO, any enhancement would have been restricted to our euphotic zone samples. However, as was previously pointed out, NO was significantly greater than AO at both euphotic and aphotic depths above the sill in Saanich Inlet. We therefore conclude that the enhancement of NO rates, relative to AO rates, was a result of some other natural perturbation that affected rates at both euphotic and aphotic depths.

As described in section 2.1, spring tide mixing outside of Saanich Inlet causes new nitrogen to be horizontally transported into Saanich Inlet (Gargett et al. 2003). In addition to the affect that it has on other biogeochemical processes in Saanich Inlet, such as primary production (Parsons et al. 1983), spring tide NO_2^- and NO_3^- supply could enhance NO rates over AO rates. As previously shown, NO rates in Saanich Inlet were

positively correlated to NO_2^- concentrations, and thus it seems reasonable that during spring tides, when more NO_2^- would be available for NO than would be contributed by *in situ* AO alone, NO would increase over AO. Spring tides are characterized by increased maximum daily tidal exchange (MDX). As such, if the increase in NO rates over AO rates was in fact linked to spring tide mixing, then the magnitude by which NO is enhanced over AO should increase as the MDX increases. To test this hypothesis we compared the difference between average daily NO and AO rates above the depth of the sill with the corresponding MDX of each sampling date (MDX_{SD}; Fig. 2.8). Results showed that there was little difference between NO and AO rates during periods of low MDX, however as the MDX increased, signifying maximum spring tide periods, NO rates became increasingly greater than AO rates, and simple linear regression confirmed that the relationship shown in Fig. 2.8 was statistically significant ($p = 0.013$; $R^2 = 0.74$). The cyclicity of the maximum difference between NO and AO is therefore opposite to that of the fortnightly phytoplankton biomass periodicity, and our results further emphasize the important role of spring tide mixing in biogeochemical processes in Saanich Inlet. Finally, given that NO rates were greater than AO rates above the depth of the sill, and that there was no difference between these rates below sill depth, we can conclude that complete nitrification occurs in Saanich Inlet (i.e. all NH_4^+ which is oxidized to NO_2^- is eventually oxidized to NO_3^-) within the depth range sampled. Thus, any further discussion, as to the rate and relative importance of *in situ* NO_3^- production from NH_4^+, will focus solely on the magnitude of AO.

2.3.2.4 Importance of *in situ* Ammonium Oxidation to Nitrate Supply

To determine the overall importance of *in situ* AO as a NO_3^- source to Saanich Inlet we used simple linear regression to compare changes in temporally interpolated (between sampling dates) depth-integrated AO rates to changes in depth-integrated NO_3^- concentrations from month to month. Briefly, depth-integrated AO rates interpolated between April and May were plotted against depth-integrated May NO_3^- concentrations, depth-integrated AO rates interpolated between May and June were plotted against depth-integrated June NO_3^- concentrations, and so on (Fig. 2.9). These two variables were significantly positively correlated ($p < 0.01$; $R^2 = 0.89$), and based on the slope of the regression line it appears that temporally interpolated AO rates were responsible for ~48% of the change in depth-integrated NO_3^- concentrations. While this result clearly implies that *in situ* AO is responsible for a substantial portion of the NO_3^- flux to Saanich Inlet over monthly or seasonal time scales, in should be interpreted with some caution when considering its relative importance over shorter time periods. That is, during spring tides when sub-surface NO_3^- rich waters are horizontally advected into Saanich Inlet (see section 2.1), the relative contribution of *in situ* NO_3^- production by AO, to total NO_3^- supply (i.e. NO_3^- supplied from the oxidation of NH_4^+ within Saanich Inlet plus the NO_3^- supplied through horizontal advection), would be lower than during neap tides when little or no NO_3^- is supplied to Saanich Inlet via horizontal advection.

2.3.2.5 Euphotic Zone Ammonium Oxidation

Average euphotic zone (10 and 1% I_o) AO rates ranged from 0.021 to 0.203 μmol L^{-1} d^{-1} (study period mean, 0.100 μmol L^{-1} d^{-1}; median, 0.078 μmol L^{-1} d^{-1}), and were similar

to the range of AO rates reported for the surface waters of the Rhone river estuary (Bianchi et al. 1999a). However, it is important to point out that if *in situ* AO rates were photo-inhibited at our euphotic zone sampling depths, our use of dark incubations may have led to recovery from photo-inhibition, which would have resulted in overestimates of the rates. Although photo-inhibition of AO has been well documented (Ward 2008), the precise effect of light on mixed assemblages of AO organisms has not been well defined, and contrasting results have been reported for factors such as the effect of light on *in situ* AO rates through the euphotic zone, intensity of light required to induce photo-inhibition of AO bacteria, and the "dark-time" required for recovery from photo-inhibition. Studies of cultured AO bacteria have found that light intensities of 5 (Vanzella et al. 1989) and 15 W m^{-2} (Guerrero and Jones 1996b) were required to induce sufficient photo-inhibition (i.e. greater than ~60% inhibition). The light intensities we recorded close to mid-day during each of our sampling dates at 10% I_o (range, 0.14 to 1.1 W m^{-2}) were far below the lower threshold value of Vanzella et al. (1989). Based on the measured light intensities at our 10% I_o sampling depths, and the results of Vanzella et al. (1989) and Guerrero and Jones (1996b), we believe it is unlikely that AO was photo-inhibited at our 10 and 1% sampling depths, and as such dark incubations should not have resulted in a significant overestimate of the rates. This assumption is further supported by the vertical profiles of AO rates reported by Ward (2005) for Monterey Bay, California, which showed no notable increase in AO rates between 17 and 1% I_o. Ward (2005) did, however, observe decreases in AO at depths shallower than 17% I_o, and thus it is likely that photo-inhibition of AO occurs in Saanich Inlet at euphotic zone depths shallower than those sampled during this study. Still, the degree of photo-inhibition in the upper

region of the Saanich Inlet euphotic zone is likely less than that which has been observed in pelagic coastal regions such as those studied by Ward (2005), as 1) photo-inhibition of AO appears to be less important in estuarine regions (Horrigan and Springer 1990), possibly due to increased turbidity (Guerrero and Jones 1996a), and 2) periodic high rates of NH_4^+ regeneration in Saanich Inlet, originating from the decomposition of fortnightly phytoplankton blooms, may act to alleviate the effects of photo-inhibition as increased NH_4^+ availability has been shown to reduce the effects of light on AO bacteria (Guerrero and Jones 1996a; Vanzella et al. 1989).

The finding that AO occurred within the euphotic zone of Saanich Inlet highlights that not all NO_3^- present in this region of the water column should be considered "new" nitrogen, and has important implications for studies of new production. The only new production study to date in Saanich Inlet was conducted by Grundle et al. (2009) and was based on $^{15}NO_3^-$ uptake incubations. These authors reported that, in terms of carbon, new production at station SI-2 ranged from 0.08 to 3.1 g C m^{-2} d^{-1} (mean, 1.1 g C m^{-2} d^{-1}) during the growing season (April to October) of 2006, and they calculated an average growing season *f*-ratio of 0.58. Following the rationale of Eppley and Peterson (1979), that new production is quantitatively equivalent to carbon export, the *f*-ratio reported by Grundle et al. (2009) suggests that ~60% of growing season POC production is vertically exported from the euphotic zone of Saanich Inlet. However, this value assumes no euphotic zone NO_3^- regeneration. Given that we did not measure AO rates at depths spanning the full depth range of the euphotic zone, we cannot be certain of the role that AO plays in supplying regenerated NO_3^- to primary producers throughout the entire illuminated region of the water column. Still, by applying our median euphotic zone AO

rate to the data of Grundle (2009) we can produce a first order estimate as to the degree by which new production may have been overestimated in Saanich Inlet, as a result of assuming no euphotic zone NO_3^- regeneration. We recognize that by applying our median euphotic zone AO rate, which was calculated from rates measured at 10 and 1% I_o, to the full depth range of the euphotic zone, we are introducing additional error which may lead to an overestimate of the potential role that AO plays in regenerating NO_3^- within the euphotic zone. However, considering the previous discussion that the degree of photo-inhibition in Saanich Inlet is likely lower than that which has been observed in many other coastal and open ocean regions, and because our median euphotic zone AO estimate is more conservative than our mean estimate, we feel that any error should tend towards the lower end rather than the higher. Estimated in this way, AO, and subsequent NO_3^- regeneration, could have supported between 2 and 130% of the daily phytoplankton NO_3^- demand reported by Grundle et al. (2009). This would have resulted in a 15% reduction in the growing season mean new production rate, and a newly calculated seasonal *f*-ratio of 0.50. In conclusion, these results clearly highlight the importance of including AO rate measurements into estimates of new production, and draw further attention to the need for a comprehensive understanding of euphotic zone AO in regions where new production has been or will be measured.

2.4 Conclusions

This study is the first to report simultaneous AO and NO rates for Saanich Inlet, and is one of only a few studies to investigate these processes in NE Pacific coastal waters (see Ward 2008 for a review of global nitrification rates). Its findings have significantly enhanced our understanding of nitrogen cycling within the fjord, and our observation

linking enhancements of NO over AO, to increased MDX, provides further evidence that horizontal spring tide nutrient transport into Saanich Inlet plays an important role in the support of *in situ* biogeochemical processes. Furthermore, the accuracy with which nitrification rates were measured during the present study was demonstrated by the close agreement between estimates of oxygen consumption based upon our measured AO and NO rates, and those based upon Redfield stoichiometry. Finally, of particular importance was the observation that AO was at times substantial in the lower region of the euphotic zone, and that new production in Saanich Inlet may have previously been overestimated by approximately 15%.

Figures

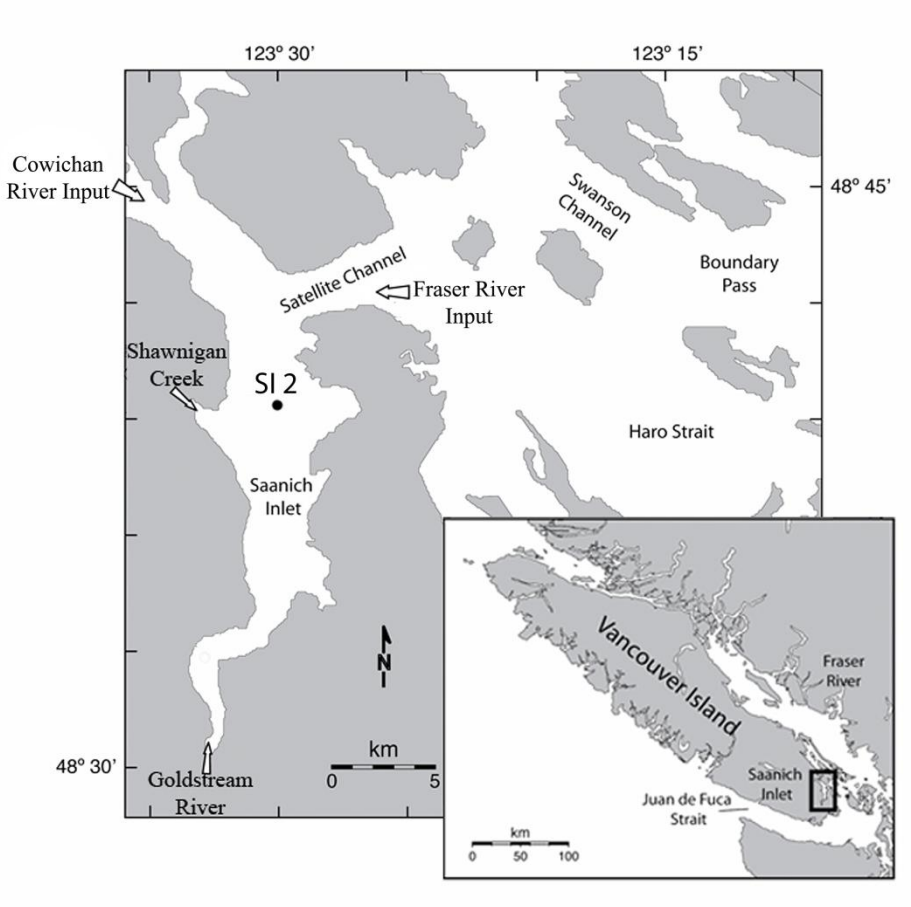

Figure 2.1. Location of sampling station SI-2 in Saanich Inlet, southeastern Vancouver Island, British Columbia, Canada. Also shown are the discharge points of Shawnigan Creek and Goldstream River, and the direction of freshwater flow from the Cowichan and Fraser Rivers (reproduced from Grundle et al. 2009).

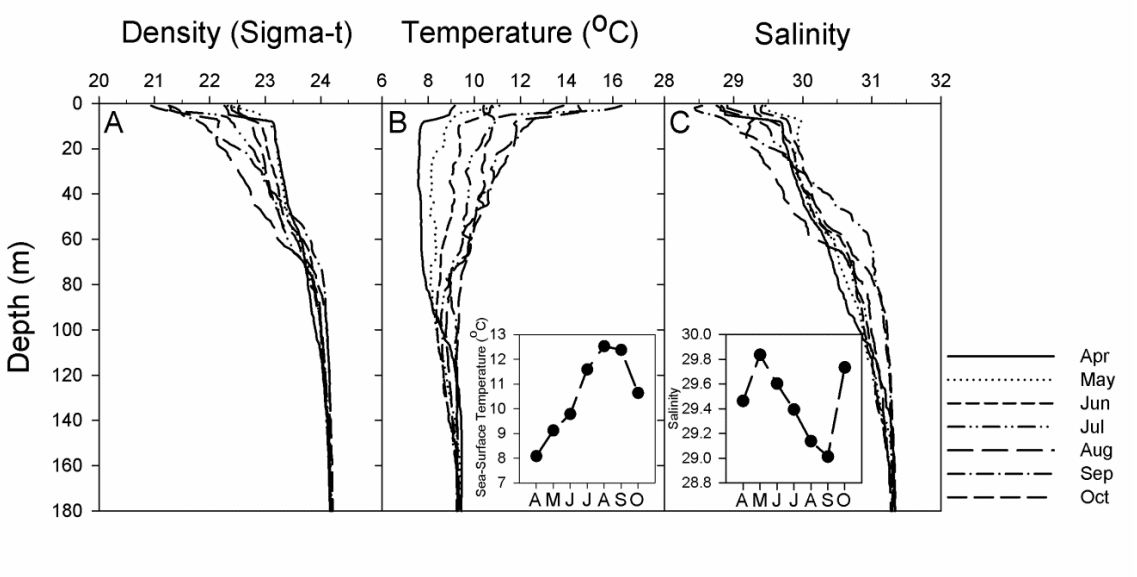

Figure 2.2. Vertical profiles of (A) density (B) temperature and (C) salinity from the surface to 180 m depth at station SI-2 in Saanich Inlet, for the period April to October 2008. Also shown are monthly sea-surface temperature and surface salinity values, calculated from the average temperature and salinity of the upper water column (inset).

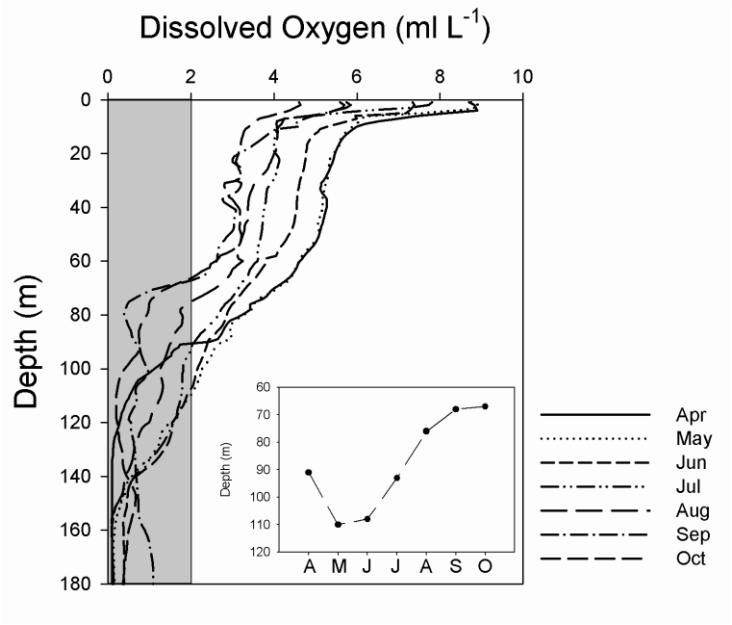

Figure 2.3. Vertical profiles of dissolved oxygen (DO) concentrations from the surface to 180 m depth at station SI-2 in Saanich Inlet, for the period April to October 2008. The shaded area represents hypoxic DO concentrations, defined as concentrations ≤2.0 ml O_2 L^{-1} (Diaz and Rosenberg 1995). Also shown is the depth of the hypoxic boundary for the same time period (inset).

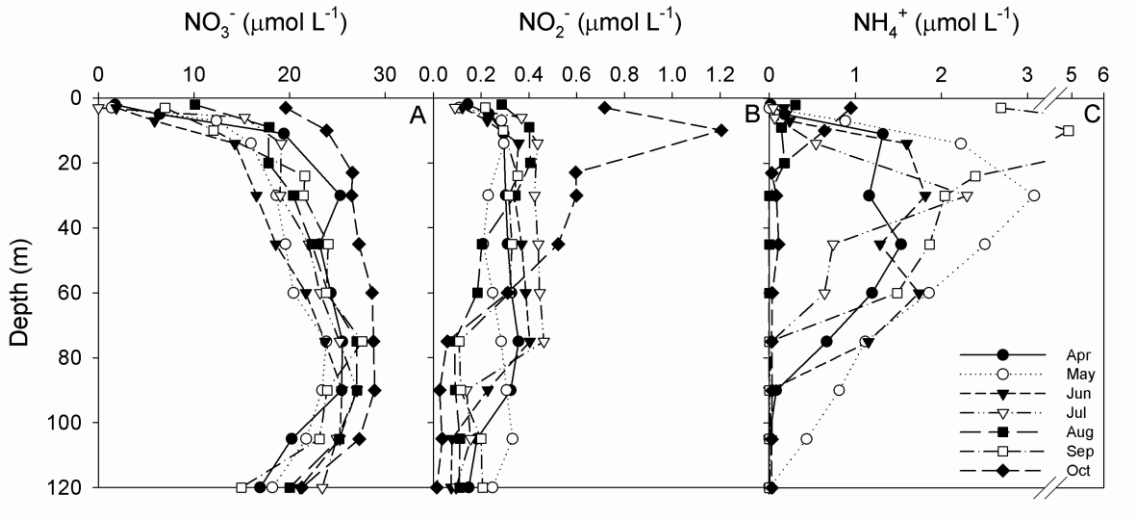

Figure 2.4. Vertical profiles of (A) NO_3^-, (B) NO_2^- and (C) NH_4^+ at station SI-2 in Saanich Inlet, for the period April to October 2008. Euphotic zone measurements were conducted at 55, 10, and 1% I_o (the depths of which are indicated by the first three data points in each profile), while aphotic zone measurements were conducted at 30, 45, 60, 75, 90, 105 and 120 m.

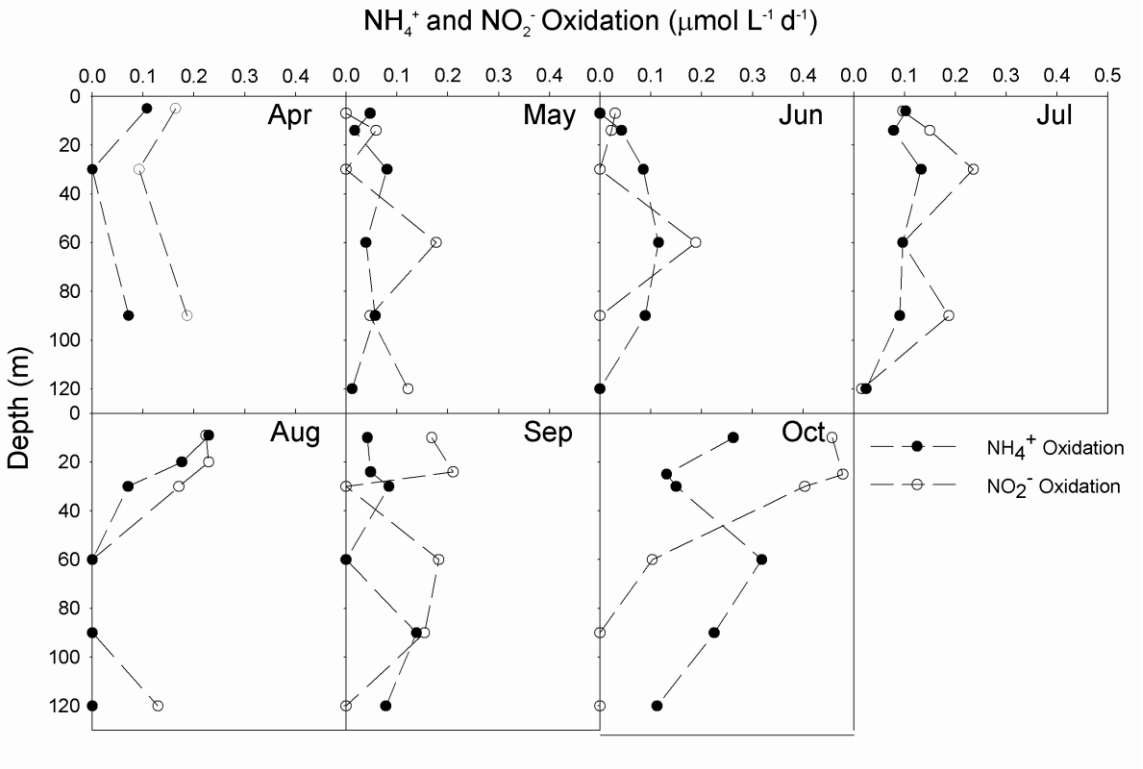

Figure 2.5. Vertical profiles of NH_4^+ and NO_2^- oxidation rates at station SI-2 in Saanich Inlet, for the period April to October 2008. Euphotic zone measurements were conducted at 10 and 1% I_o (the depths of which are indicated by the first two data points in each profile), while aphotic zone measurements were conducted at 30, 60, 90 and 120 m (the exception to this was during April when measurements were only conducted at 10% I_o, and 30 and 90 m depth).

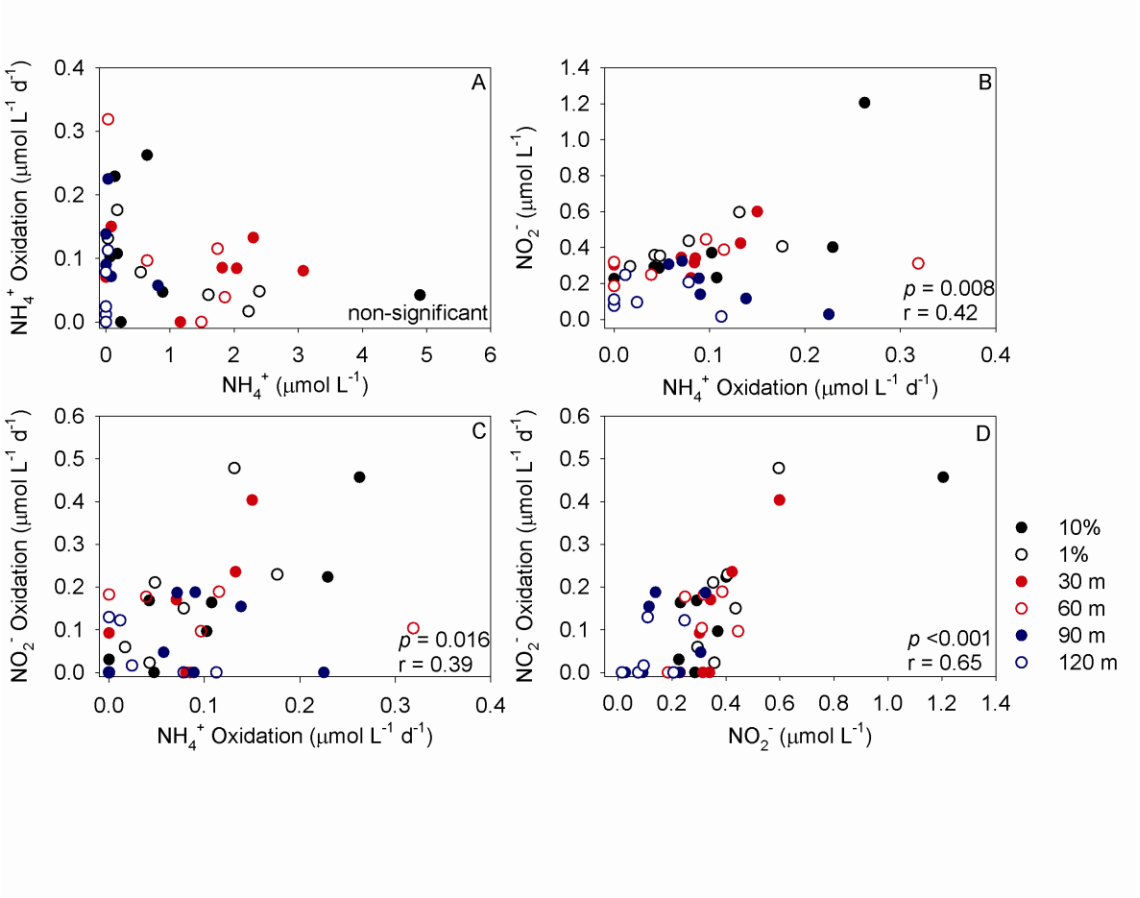

Figure 2.6. (A) NH_4^+ oxidation rates vs. NH_4^+ concentration, (B) NO_2^- concentrations vs. NH_4^+ oxidation rates, (C) NO_2^- oxidation rates vs. NH_4^+ oxidation rates, and (D) NO_2^- oxidation rates vs. NO_2^- concentrations, for the period April to October 2008 at depths corresponding to 10 and 1% I_o, and at 30, 60, 90 and 120 m. Also shown are the results from the Spearman Rank correlation tests. Note: data from all sampling depths were pooled for the correlations tests.

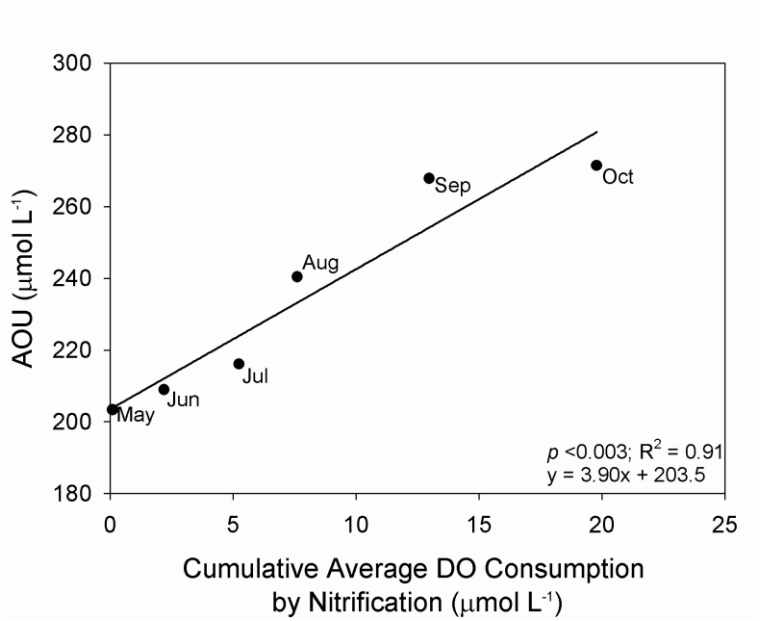

Figure 2.7. Average apparent oxygen utilization (AOU) vs. cumulative average dissolved oxygen (DO) consumption by nitrification at station SI-2 in Saanich Inlet, for the period May to October 2008. Average calculations were based on measurements made at 90 and 120 m depth. Cumulative average DO consumption was calculated by (1) estimating the daily oxygen consumption rates due to the combined effects of NH_4^+ and NO_2^- oxidation for each sampling date, assuming a 2:3 and 2:1 $N:O_2$ molar ratio (Ward 2008), (2) temporally integrating the DO consumption rates between each sampling date, and (3) cumulatively adding the temporally integrated DO consumption rates from month to month.

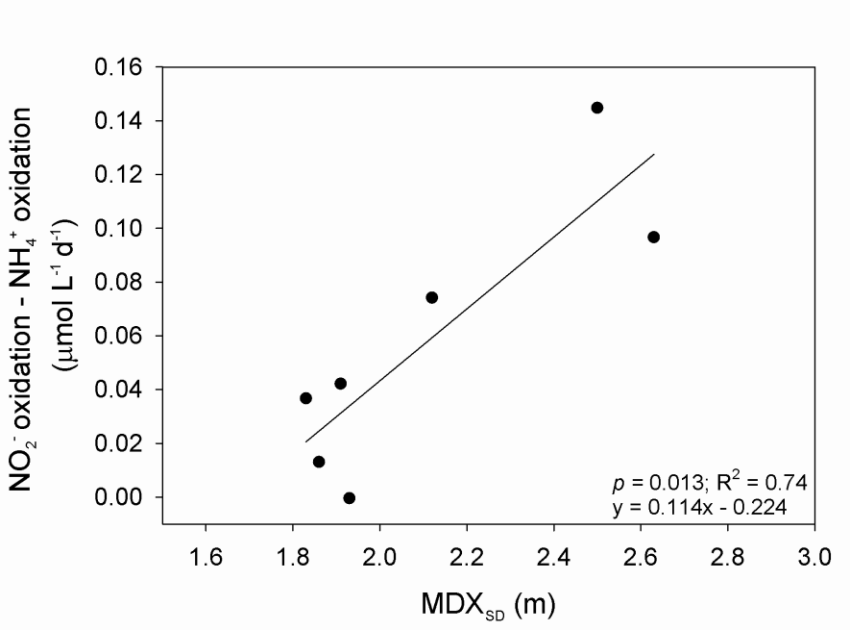

Figure 2.8. Difference between average monthly NO_2^- and NH_4^+ oxidation rates in the upper 60 m of the water column at station SI-2 vs. the maximum daily tidal exchange of the corresponding sampling date (MDX_{SD}).

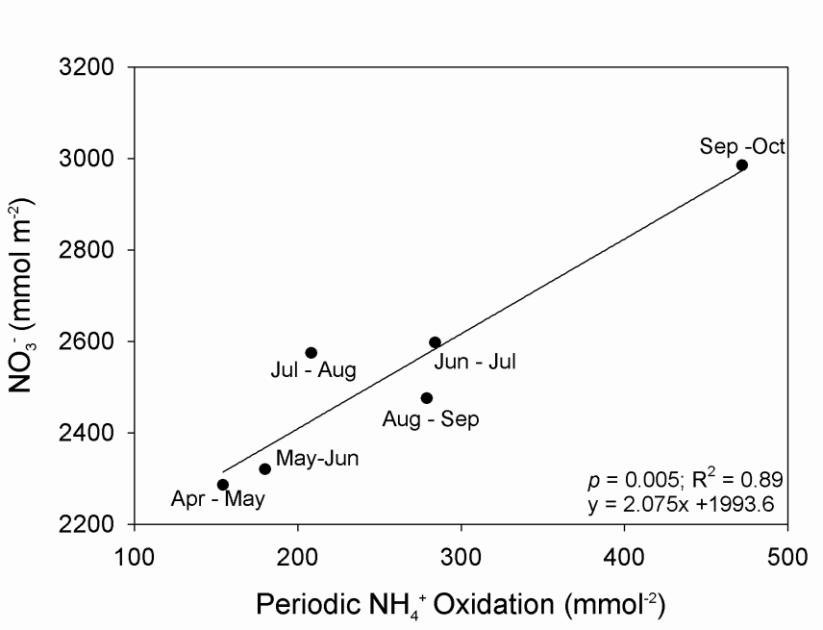

Figure 2.9. Monthly depth-integrated (depth of 10% I_o to 120 m) NO_3^- concentrations vs. periodically interpolated depth-integrated NH_4^+ oxidation at station SI-2 in Saanich Inlet, for the period April to October 2008. For clarification, depth-integrated NH_4^+ oxidation rates interpolated from April to May were compared to May depth-integrated NO_3^- concentrations, while depth-integrated NH_4^+ oxidation rates interpolated from May to June were compared to June depth-integrated NO_3^- concentrations, and so on.

Chapter 3 : Euphotic zone nitrification in the NE subarctic Pacific: Implications for measurements of new production

Citation:

Grundle, D.S., S. K. Juniper, and K.E. Giesbrecht. In revision. Euphotic zone nitrification in the NE subarctic Pacific: Implications for measurements of new production. *Marine Chemistry.*

Abstract

Ammonium (NH_4^+) oxidation rates, nitrate (NO_3^-) uptake rates and dissolved nutrient concentrations were measured throughout the euphotic zone along the Line P time-series transect in the northeast subarctic Pacific, on three cruises (winter, spring and late-summer) in 2009. NH_4^+ oxidation occurred throughout the euphotic zone and rates ranged from undetectable to 97 nmol L^{-1} d^{-1}. Evidence was found to suggest that both light and NH_4^+ concentrations played a role in regulating NH_4^+ oxidation rates, with rates increasing as light decreased and NH_4^+ concentrations increased. The observation that NH_4^+ oxidation was a ubiquitous process throughout the euphotic zone demonstrates that not all NO_3^- present in the euphotic zone should be considered new nitrogen, and has important implications for estimates of new production in the northeast subarctic Pacific. Depth-integrated NO_3^- uptake rates ranged from 0.65 to 6.0 mmol m^{-2} d^{-1}, and we found that euphotic zone NH_4^+ oxidation could have supported between 3 and 100% of the phytoplankton NO_3^- demands along Line P. Taking potential euphotic zone NO_3^- regeneration into account resulted in new production estimates being reduced by an average of ~50%. During spring and late-summer, the degree by which new production was reduced, when euphotic zone NO_3^- regeneration was taken into consideration, was tightly anti-correlated to total NO_3^- uptake rates. This indicates that the implications of euphotic zone nitrification for estimates of new production are greatest in the less productive regions of the oceans.

3.1 Introduction

Understanding factors influencing biologically mediated oceanic carbon export (hereinafter referred to as C-export) are critical to accurately determining how potential anthropogenically and naturally induced environmental shifts may affect the efficiency by which the "biological pump" sequesters carbon from the atmosphere to deep waters and sediments. One of the first challenges is to obtain accurate estimates of export production, and subsequently examine how changes to different environmental parameters affect this process. Over the past several decades one extensively used approach to estimating potential C-export in the ocean has involved the new production paradigm. The new production paradigm is based on a concept developed by Dugdale and Goering (1967), who proposed that, in contrast to regenerated forms of nitrogen (e.g. NH_4^+ and urea; N_{reg}), NO_3^- should be considered a form of "new" nitrogen (N_{new}) to the euphotic zone, and, in turn, any primary production based on the utilization of NO_3^- should be termed "new" production (NP). The rationale behind the designation of NO_3^- as a form of N_{new} relied upon the assumption that nitrification (i.e. the biological oxidation of NH_4^+ to NO_3^-, via NO_2^-) was restricted to the aphotic zone, and as such any NO_3^- present in the euphotic region of the water column was presumed to be a result of physical transport mechanisms (e.g. upward mixing). It was later pointed out that to remain in equilibrium, any upward flux of NO_3^- must be balanced by a downward flux of particulate organic matter, and, thus, any primary production based on the utilization of NO_3^- (i.e. NP) should be quantitatively equivalent to potential C-export via the biological pump (Eppley and Peterson 1979). Following this, measurements of NP became widely used and they have become central to our understanding of potential C-export in the

ocean. Oceanographic time-series have played a particularly important role in this respect, as they allow for repeated measurements of NP and the assessment of how changes to various environmental variables affect it.

As pointed out above, the new production paradigm is underlain by the fundamental assumption that nitrification only occurs in the aphotic regions of the ocean. This was a reasonable assumption given evidence for photo-inhibition of nitrification (Horrigan et al. 1981; Mueller-Neugluck and Engel 1961; Schon and Engel (1962). Still, as Dugdale and Goering (1967) noted, "*if nitrification rates are eventually shown to be sufficiently higher than has been assumed, the assumption that nitrate is a nonregenerated nutrient form in the euphotic zone would have to be modified*". Indeed, nitrification has since been shown to occur within the euphotic zone (Ward 1987). Thus, some fraction of euphotic zone NO_3^- should be included in the N_{reg}, rather than the N_{new}, pool. As such, any primary production based on the utilization of regenerated NO_3^- should not be considered NP. However, NP studies have proceeded under the assumption that nitrification does not occur within the illuminated region of the water column, and as Yool et al. (2007) demonstrated, this may have led to substantial overestimates in the rates and magnitude of global oceanic C-export.

The Line P sampling transect (Fig. 3.1) is a long-standing oceanographic time-series that has played an important role in our understanding of NP and potential C-export in the NE subarctic Pacific. Sampling along Line P has been ongoing since 1959, and sampling at the terminal station, P26 (also known as Ocean Station Papa), began in 1949. During the Canadian JGOFS I (1992 to 1994) and II (1995 to 1997), and SERIES (2002) programs, NP (i.e. NO_3^- uptake) dynamics along Line P were studied extensively, and the

variability associated with this process and the factors which affect it have been discussed in detail (e.g. Boyd et al. 1996; Maldonado et al. 1999; Marchetti et al. 2006; Peña and Varela 2007; Varela and Harrison 1999). However, in light of evidence that nitrification can occur within the euphotic zone, it is possible that interpretations of NP studies conducted along Line P, may have led to overestimations of potential C-export in the NE subarctic Pacific. To this end, the present study aimed to quantify and describe euphotic zone nitrification rates along Line P during three cruises (winter, spring and late-summer) in 2009. To estimate the potential amount of NO_3^-, which may be produced by nitrification in the euphotic zone, we focused on the first and rate-limiting step of nitrification: NH_4^+ oxidation (AO). AO is also the step which separates what has traditionally been considered N_{reg} from N_{new}. NO_3^- uptake rates were also measured during these cruises, and we estimate and discuss the maximum potential degree by which new production and potential C-export rates are reduced along the east-west Line P gradient when euphotic zone NO_3^- regeneration is taken into consideration. Line P spans a range of oceanographic regimes, from the highly productive waters off the west coast of Vancouver Island to the High-Nitrate Low-Chlorophyll (HNLC) waters at the terminal end of the transect (Boyd et al. 1996, Whitney et al. 1998). As such, the present study afforded us the opportunity to determine the implications of euphotic zone nitrification for estimates of NP across this range of oceanographic regimes.

3.2 Methods

3.2.1 Sampling Regime

Sampling was conducted at 5 stations along the Line P oceanographic transect (Fig. 3.1) during the winter (February), spring (June) and late-summer (August) of 2009,

onboard the *CCGS John P. Tully*. Water samples for biological and chemical measurements were collected using a rosette configuration of Niskin bottles with an attached SeaBird Electronics SBE 911 conductivity, temperature and depth (CTD) profiler. A Biospherical QSP-400L photosynthetically active radiation (PAR) sensor was also attached to the CTD to measure underwater irradiance. Water samples for AO rate measurements and dissolved nutrient concentrations (NO_3^-, NO_2^- and NH_4^+) were collected at the surface and from 10, 20, 30, 40 and 75m below the surface on the winter cruise. The % surface incident irradiances (I_o) recorded at each sampling depth along Line P during winter are shown in Table 3.1. During the spring and late-summer cruises, water samples for measuring AO rates and dissolved nutrients were collected from depths corresponding to 100, 55, 33, 10 and 1% I_o. On all three cruises, water samples were also collected from depths corresponding to 100, 55, 33, 10 and 1% I_o for the purpose of measuring NO_3^- uptake rates. AO and NO_3^- uptake rates were therefore measured at the same depths during the spring and late-summer cruises, but at different depths during the winter cruise.

3.2.2 Physical and Chemical Measurements

Continuous vertical profiles of temperature, salinity and PAR were measured at stations P4, P12, P16, P20 and P26 (Fig. 3.1) across the depth ranges which were pertinent to each of our station/cruise specific sampling depths. Density (σ_θ) was derived from temperature and salinity, and the base of the mixed layer was defined as the depth at which a change of 0.125 σ_θ, relative to the surface, was observed (Levitus 1982). Immediately following collection, water samples for the measurement of dissolved NO_3^- and NO_2^- were stored at -20°C until analysis ashore using an Astoria-Pacific autoanalyzer

and following the protocol of Barwell-Clarke and Whitney (1996). Dissolved NH_4^+ concentrations were measured fresh at sea using a Turner Designs TD-700 fluorometer (Holmes et al. 1999).

3.2.3 Ammonium Oxidation Rates

AO rates were measured at stations P4, P12, P16, P20 and P26 (Fig. 3.1) using an inhibitor based method previously described by Grundle and Juniper (2011[Chapter 2]). Seawater samples were collected from each sampling depth and transferred into 4 x 500 ml acid-cleaned polycarbonate bottles. Immediately following this, two of the samples were treated with allylthiourea (ATU; final concentration 10 mg L^{-1}), a well-recognized AO inhibitor (Bianchi et al. 1994a,b), while the remaining two samples were left untreated (control). Samples were then incubated in the dark under controlled temperature conditions (within ~2°C of *in situ* sampling depth temperature) for ~24h, and any increase in NO_2^- concentrations in the control samples, compared to the ATU treated samples, were considered to be a result of AO. Finally, for our AO rate measurements, changes in NO_2^- concentrations between the control and ATU treated samples were determined using the colorimetric method outlined by Bendschneider and Robinson (1952) at 543 nm, using 10 cm pathlength cells to allow for nanomolar detection of NO_2^-.

3.2.4 Nitrate Uptake Rates

In contrast to the physical, chemical and AO rate measurements previously described, NO_3^- uptake rates were only measured at stations P4, P16 and P26. The NO_3^- uptake rates reported here were also incorporated into the results of Giesbrecht et al. (in review), and these authors have provided a detailed description of the methods that were used. Briefly, seawater samples were collected in 1-L acid-cleaned polycarbonate bottles and inoculated

with ^{15}N-labelled KNO_3 (99 atom% ^{15}N) at ~10% of ambient NO_3^- concentrations. Samples were then covered with neutral density screening to simulate the irradiance at each collection depth, and incubated in an on-deck polycarbonate tank for 24 h. Incubation temperatures were maintained by continuously flowing surface supplied seawater through the tanks. At the end of 24 h, incubations were terminated by gentle vacuum filtration through pre-combusted, 0.7 µm pore-size borosilicate filters. The particulate organic nitrogen retained on these filters and the atom% ^{15}N were measured by continuous flow isotope ratio mass spectrometry at the University of California, Davis, Stable Isotope Facility. Finally, specific and absolute NO_3^- uptake rates were calculated according to Eqs. (6) and (3), respectively, of Dugdale and Wilkerson (1986).

3.3 Results and Discussion

3.3.1 Physical Properties

Mixed layer (ML) and euphotic zone base (1% I_o) depths were deepest in winter and shallowest in spring and late-summer (Table 3.2). During winter, the depth of the ML was always deeper than the base of the euphotic zone, whereas in spring and late-summer the pycnocline intersected the euphotic zone at all stations, leaving only the upper layers of the euphotic zone mixed. Spatially, ML and euphotic zone depths were shallowest at P4 and then increased at the more distal stations. ML temperatures displayed expected seasonal variations: lowest in winter, intermediate in spring, and highest in late-summer (Table 3.2). Spatially, ML temperatures decreased with increasing distance from P4 during winter and spring. In late-summer, ML temperatures peaked at P12 and P16. Variations in ML salinity were minimal (<0.2%) and no spatial or seasonal trends were apparent (Table 3.2).

3.3.2 Dissolved Nutrients

Dissolved NO_3^-, NO_2^- and NH_4^+ concentrations ranged from undetectable to 18.1, 0.500 and 1.3 µmol L^{-1}, respectively (Fig. 3.2). With the exception of relatively high NO_2^- concentrations at P4 and P20 during late-summer, NO_3^- and NO_2^- concentrations were often highest in winter. There was no obvious spatial trend in NO_3^- distributions between P4 and P16, however, west of P16 NO_3^- increased, reaching maximum concentrations at P20 and P26. This is consistent with the concept that NO_3^- draw down at the far-offshore stations of Line P is iron limited, and the classification of this area as an HNLC region (Boyd et al. 1996, 1998; Varela and Harrison 1999). The spatial distributions of NO_2^- on the other hand were much more variable. In contrast to the seasonal variability of NO_3^- and NO_2^-, NH_4^+ concentrations were often lowest in winter and highest in spring and late-summer. No longitudinal trends in NH_4^+ concentrations were observed, and this is consistent with other studies that have examined upper water column NH_4^+ concentrations along Line P (e.g. Varela and Harrison 1999). Finally, excluding winter data, when, for the most part, there was little vertical variability, concentrations of all three N species were typically highest at the base of the euphotic zone (i.e. 1% I_o).

3.3.3 Ammonium Oxidation Rates

AO rates ranged from undetectable to 97 nmol L^{-1} d^{-1} (Fig. 3.3; mean, 20 ±19 nmol L^{-1} d^{-1}). The highest rates measured during this study were an order of magnitude lower than the highest euphotic zone rates recently reported for Saanich Inlet (Grundle and Juniper 2011[Chapter 2]), a highly productive British Columbia fjord that lies at a similar latitude to the Line P sampling stations. The range of AO rates that we observed were

instead similar to those measured in the euphotic zone of more pelagic coastal and open ocean regions of the N pacific (Dore and Karl 1996; Santoro et al. 2010; Ward 2005, Ward et al. 1984).

Temporally, the highest AO rates were typically observed in winter. A notable exception to this was at P12, where AO rates were undetectable throughout the euphotic zone. This observation may have been caused by substrate limitation, as NH_4^+ concentrations were also undetectable throughout the euphotic zone at P12 during winter (Fig. 3.2). This is difficult to definitively conclude though, as undetectable NH_4^+ concentrations did not always result in undetectable AO rates. The rate of NH_4^+ supply (i.e. ammonification) may, at times, also play an important role in controlling AO rates (Ward 2005). Thus, the complete lack of detectable AO rates through the euphotic zone at P12 during winter may have resulted from limiting substrate concentrations combined with insufficient substrate supply rates.

Depth-integrated AO rates (DI-AO; trapezoidal integration from the surface to depth of 1% I_o integration) ranged from undetectable to 2.37 mmol m^{-2} d^{-1} (Fig. 3.4), and the mean DI-AO rate for the entire study was 1.16 ±0.66 mmol m^{-2} d^{-1}. The east-west variability of DI-AO rates was much more variable in winter (mean, 1.29 ±1.06 mmol m^{-2} d^{-1}) than during the spring/late summer period (mean, 1.09 ±0.41 mmol m^{-2} d^{-1}). Still, with the exception of the undetectable DI-AO rate at P12, a general decreasing trend in winter DI-AO rates was evident between P4 and P26 (Fig. 3.4). This trend was reversed in spring and late-summer, with DI-AO rates displaying a general increase with increasing distance along Line P (Fig. 3.4).

The observation that AO occurred throughout the euphotic zone along Line P adds to a growing body of work which has demonstrated that AO is not completely photo-inhibited (e.g. Clark et al. 2008; Diaz and Raimbault 2000; Dore and Karl 1996; Grundle and Juniper 2011[Chapter 2]; Santoro et al. 2010; Ward 1987, 2005; Ward et al. 1984; Yool et al. 2007), and highlights that not all NO_3^- in the illuminated portion of the water column should be considered new nitrogen. To this end, measurements of NP in the NE subarctic Pacific, which followed the traditional assumption of no euphotic zone NO_3^- regeneration, would have overestimated NP and potential C-export (discussed further in section 3.3.5). It is important to note that, as discussed in Chapter 1 (section 1.7), the use of dark incubations may have resulted in partial recovery of photo-inhibition of AO organisms, thus resulting in euphotic zone AO rates being overestimated. Conversely, the use of ATU may have led to underestimations of AO rates due to incomplete inhibition of AO archaea. However, given that the use of dark incubations may lead to NH_4^+ oxidation rates being overestimated by up to 30%, while the use of ATU could cause underestimates of up to 40%, it is likely that these positive and negative sources of error would have countered each other to some degree. Finally, our postulation that the positive and negative errors that may have been introduced through our use of dark incubations and ATU, respectively, would have countered each other to some degree is backed up by the high degree of similarity between the rates measured during the present study and those measured in other regions of the N Pacific.

3.3.4 Factors Controlling Ammonium Oxidation

Light: Although we have demonstrated that AO occurs throughout the euphotic zone of the NE subarctic Pacific, changes in light intensity through the water column probably

still play an important role in regulating AO rates in the euphotic zone. This was recently highlighted by Ward (2005), who showed that, although low AO rates occurred at all light intensities in Monterey Bay, highest AO rates were usually associated with light intensities <20% I_o. We also found evidence to indicate that light played a role in regulating euphotic zone AO rates along Line P. Excluding station P12 during winter, where AO rates throughout the euphotic zone were undetectable, 12 of the remaining 14 vertical AO rate profiles displayed maximum rates at light intensities <20% (Fig. 3.3; see Table 1 for the $\%I_o$ at each winter sampling depth). Furthermore, when data from all cruises and stations were pooled, we found that the median AO rates at light intensities <20% I_o and >20% I_o were 25 and 15 nmol L^{-1} d^{-1}, respectively, and a Mann-Whitney U test demonstrated that the difference in median AO rates above and below 20% I_o was significantly different (p <0.01). Additional evidence to support the notion that light plays a role in influencing AO rates comes from examining the AO vs. relative light intensity relationship. Similar to Ward (2005), we found that low rates occurred at all light intensities, but the highest AO rates were observed at the lowest light intensities, and the overall trend of the relationship showed that AO rates increased exponentially with decreasing relative light intensity (p <0.01, R^2 = 0.10; Fig. 3.5). In addition to supporting the notion of partial photo-inhibition of AO, the results shown here also indicate that our use of dark incubations did not interfere with the potential impact of light on AO through the euphotic zone.

Finally, although the non-linear regression between relative light intensity and AO was statistically significant, it explained only 10% (i.e. R^2 =0.10) of the variability in AO rates. This is probably not surprising for at least a couple of reasons. Firstly, we

compared AO rates to relative light intensity, whereas the absolute light intensity is probably more important when considering photo-inhibition of AO. Laboratory studies have shown that light intensities between 5 (Vanzella et al. 1989) and 15 W m^{-2} (Guerrero and Jones 1996) are required to induced significant photo-inhibition of AO bacteria. Given that factors such as spatial and temporal changes in cloud albedo, light attenuation, and the angle of the sun would all play a role in causing "between station" and "between cruise" differences in the amount of absolute light reaching depths of the same relative light intensity, it is not surprising that only a small fraction of AO variability is explained by $\%I_o$. Secondly, while light undoubtedly plays a role in controlling AO rates through the illuminated portion of the water column, there are likely a number of other controlling factors as well (discussed further below).

Substrate availability: In addition to light, we also found that substrate availability, to varying degrees, played a role in maintaining AO rates throughout the euphotic zone. To assess the effect of varying NH_4^+ concentrations on AO rates, a Spearman Rank correlation test was used to compare the relationship between these two variables. However, because the response of AO to changes in NH_4^+ availability appeared to be higher in winter than during the spring/late-summer period (Fig. 3.6), we ran separate correlation tests for these two temporal periods. Results showed that AO rates were significantly positively correlated to NH_4^+ concentrations during both the winter (p = 0.02; r = 0.42) and spring/late-summer (p = 0.02; r = 0.32) periods. The general observation that increases in substrate concentrations correlated to higher AO rates is consistent with a number of other studies which have shown that *in situ* substrate availability can play an important role in regulating AO rates under natural conditions

(e.g. Bianchi et al. 1999; Grundle and Juniper 2011[Chapter 2]; Olson 1981). An explanation for the apparently different AO vs. NH_4^+ concentration relationships during winter and spring/late summer, probably involves the different amounts of *in situ* irradiance that AO organisms may have been exposed to during these periods. Shorter day-lengths and lower irradiance during winter may have provided AO organisms with some degree of relief from photo-inhibition, thus allowing for more efficient substrate utilization. This would certainly explain the apparent enhanced response of AO to changes in NH_4^+ concentrations in winter compared to spring/late-summer (Fig. 3.6). Of course, an additional explanation for the apparently higher substrate utilization efficiency by AO organisms during winter may have involved a reduction in substrate competition with phytoplankton, as irradiance is lower during winter and phytoplankton are likely light limited.

To summarize, increases in NH_4^+ concentrations generally led to higher AO rates, however, as was the case with the role that light plays in controlling AO rates, changes in AO were only partially explained by substrate availability, and there were occasions when AO proceeded when NH_4^+ was undetectable. As earlier noted, the rate of NH_4^+ supply can also regulate AO rates, and, at times, it may even be more important than ambient substrate concentrations alone (Ward 2005). AO bacteria possess constitutive Calvin cycle and chemolithotrophic pathways, and the associated enzymes are unable to respond to changes in substrate concentrations over short time periods (Ward and Kilpatrick 1990). Thus, while it is unlikely that AO rates would be able to immediately respond to rapid increases in NH_4^+ supply, these two processes could become coupled if the rate of ammonification remains somewhat constant over sufficient time periods. Such

a scenario would explain the occasional observations of measureable AO activity when NH_4^+ was undetectable.

3.3.5 Nitrate Uptake Rates and the Implications of Euphotic Zone Nitrification for Estimates of New Production

3.3.5.1 Nitrate Uptake Rates and New Production

The vertical, horizontal and temporal variability of phytoplankton NO_3^- uptake rates along Line P and at Ocean Station Papa (i.e. P26), and the factors which regulate them, have previously been discussed in detail (e.g. Boyd et al. 1996; Maldonado et al. 1999; Marchetti et al. 2006; Peña and Varela 2007; Varela and Harrison 1999). As such, our principle aim here is to use NO_3^- uptake rates observed along Line P during the winter, spring and late-summer of 2009, to estimate new production and potential C-export following the traditional assumption of no euphotic zone nitrification, and then the degree to which these estimates are reduced once we account for potential NO_3^- regeneration.

During 2009, NO_3^- uptake rates at stations P4, P16 and P26 ranged from undetectable to 730 nmol L^{-1} d^{-1} (Fig. 3.7; mean, 82 ±160 nmol L^{-1} d^{-1}). The vertical distribution of NO_3^- uptake showed that rates were typically lowest at depths corresponding to 1% I_o and highest in the upper regions of the euphotic zone. Spatially, the highest NO_3^- uptake rates were typically observed at P4, while temporally, the highest rates at each station were often observed during late-summer. With the exception of three anomalously high late-summer NO_3^- uptake rates at P4 and at depths corresponding to 100, 55, and 33 % I_o (Fig. 3.7), the range of uptake rates reported here are similar to those previously observed along Line P (Peña and Varela 2007; Varela and Harrison 1999). The late-summer P4 rates to which we refer were accompanied by NO_3^- concentrations far in excess of those

observed at P4 during spring (Fig. 3.2). During our late-summer 2009 cruise, there was evidence of an anti-cyclonic eddy, centered at station P8, whose eastern boundary appeared to encompass P4 (Line P database, Department of Fisheries and Oceans Canada; data not shown). Anti-cyclonic eddies have been shown to transport nutrient rich water offshore from the continental shelf (Whitney et al. 2005). It is therefore possible that the high late-summer P4 NO_3^- uptake rates were a result of NO_3^- rich waters being transported into this region by a transiting anti-cyclonic eddy.

Depth-integrated (DI) (surface to 1% I_o) NO_3^- uptake rates ranged from 0.65 to 6.0 mmol m^{-2} d^{-1} (Fig. 3.8). The highest DI-NO_3^- uptake rates were consistently observed at P4, after which they decreased at the more distal stations. Following the traditional assumption that nitrification does not occur within the euphotic zone, and employing the Redfield C:N ratio of 6.6, the DI-NO_3^- uptake rates equate to a DI-NP range, in terms of C, of 52 to 478 mg m^{-2} d^{-1} (Fig. 3.9 open bars). A spatio-temporal integration of these data indicates that the annual, per square km mean new production rate for the Line P region is 53,000 kg C.

3.3.5.2 Potential Contribution of Nitrification to Daily Phytoplankton NO_3^- Demands through the Euphotic Zone

The observation that AO was in fact a ubiquitous process throughout the euphotic zone of the NE subarctic Pacific, indicates that not all of the NO_3^- present within the euphotic zone was N_{new}, and instead some of the NO_3^- being utilized by phytoplankton would have been supplied by *in situ* nitrification. Here, we estimate the maximum potential contribution of nitrification to daily phytoplankton NO_3^- demands.

Given that AO and NO_3^- uptake rates were only measured at the same depths during spring and late-summer, we were unable to calculate the potential contribution of nitrification to daily phytoplankton NO_3^- demands at each depth during winter. Nevertheless, of greater importance is probably the overall impact of euphotic zone nitrification for estimates of vertically integrated new production rates (discussed in section 3.3.5.3), as it is these integrated rates that are used to approximate potential C-export from the euphotic zone. During spring and late-summer, when both AO and NO_3^- uptake rates were measured at the same depths at stations P4, P16 and P26, nitrification could have contributed between 0 and >100% of the daily phytoplankton NO_3^- requirements. The mean (data from P4, P16 and P26 pooled) potential contribution of AO to phytoplankton NO_3^- requirements at each of our relative light intensity sampling depths during spring and late-summer ranged from 28% at the surface to ~1000% at the base of the euphotic zone (i.e. 1% I_o). This is consistent with other studies which have shown that *in situ* nitrification can fuel substantial amounts of NO_3^- based primary production, particularly in the lower regions of the euphotic zone (e.g. Diaz and Raimbault 2000; Dore and Karl 1996; Raimbault et al. 1999; Ward 2005; Ward et al. 1989). The finding that nitrification may contribute quantities of NO_3^- far in excess of that required by phytoplankton at the base of the euphotic zone is also consistent with our observation that AO rates were often highest within or near this region, while NO_3^- uptake rates were lowest.

The vertical separation between the relative magnitude by which nitrification may fuel phytoplankton NO_3^- demands in the upper vs. the lower portion of the euphotic zone, is an important distinction to make when the ML depth is shallower than the base of the

euphotic zone. When the base of the euphotic zone is located within the pycnocline, high rates of *in situ* NO_3^- regeneration which exceed phytoplankton NO_3^- requirements will simply lead to accumulations of NO_3^- below the mixed layer, as the excess NO_3^- will not be immediately available to phytoplankton in the shallower, mixed regions of the euphotic zone where NO_3^- uptake rates are maximal.

3.3.5.3 Potential Implications of Euphotic Zone Nitrification for Estimates of New Production

In order to assess the overall implications of euphotic zone nitrification for estimates of new production and C-export, we estimated the maximum potential degree by which euphotic zone nitrification could have supported DI-NO_3^- uptake rates. The ML was deeper than the base of the euphotic zone during winter (Table 3.2), and, as such, we simply estimated the potential contribution of nitrification to DI-NO_3^- demands based on our DI-AO rate estimates. However, during spring and late-summer, the ML depth was shallower than the base of the euphotic zone, and, as we discussed above, in this situation it is not possible to assume that the excess NO_3^-, resulting from high AO and low NO_3^- uptake in the lower regions of the euphotic zone, will be immediately available to primary producers in the ML. We recognize that at some point in time, such as during deep mixing events, this excess regenerated NO_3^- could be transported into the upper regions of the euphotic zone. However, as we have no record of mixing events that may have occurred outside of our sampling dates, and because we do not know what the mixing ratio of lower euphotic zone regenerated NO_3^- to truly new NO_3^- (i.e. NO_3^- produced in the aphotic region of the water column) would have been, we chose to simply determine the implications of euphotic zone nitrification for estimates of new

production at time-scales relevant to our sampling strategy. As such, it was necessary to restrict the excess regenerated NO_3^- in the lower portion of the euphotic zone to the pycnocline, rather than allowing it to be simultaneously available to phytoplankton in the ML. To this end, we employed a two-step process to estimate the potential contribution of euphotic zone nitrification to DI-NO_3^- uptake rates during the spring and late-summer periods. Firstly, we estimated the potential contribution of ML-integrated AO to ML-integrated NO_3^- uptake. We then estimated the potential contribution of AO to NO_3^- uptake at our discrete sampling depths in the pycnocline. These results were then combined to determine the overall contribution of euphotic zone AO to estimates of DI-new production.

Taking into consideration the portion of phytoplankton DI-NO_3^- requirements that were potentially fuelled by regenerated NO_3^-, by following the protocols outlined above, we found that our Line P DI-NP estimates were reduced by 3 to 100% (mean, 53%). This resulted in a revised range of DI-NP rates, in terms of C, of 0 to 463 mg m^{-2} d^{-1} (Fig. 3.9 closed bars). To put this reduction into a broader perspective, our previously estimated annual, per square km mean NP rate for the Line P region was reduced from 53,000 to 30,000 kg C after accounting for potential NO_3^- regeneration in the euphotic zone. This result indicates that the failure to consider euphotic zone nitrification could result in new production and potential C-export being overestimated by ~45% in the NE subarctic Pacific. This estimated reduction is only slightly lower than the 55% global reduction that Yool et al. (2007) proposed following their inclusion of euphotic zone nitrification into a global NP model. Charette et al. (1999) used the ^{234}Thorium (Th) method to estimate *e-ratios* (ratio of exported particulate matter to total primary production) along Line P on

four cruises between February 1996 and February 1999. The mean annual Line P *e-ratio* estimate of Charette et al. (1999) was 60% lower than the contemporaneous mean annual Line P *f-ratio* estimate of Varela and Harrison (1999) based on traditional NP estimates. Charette et al. (1999) suggested that the difference between the two estimates may have been due to export of dissolved organic matter (DOM), which they concluded the NP method, but not the ^{234}Th approach, would have accounted for. However, based on the results reported in this chapter (i.e. that annual Line P NP estimates may be overestimated by ~45% when euphotic zone nitrification is not taken into account), I suggest that the difference between the *e-ratio* and *f-ratio* estimates of Charette et al. (1999) and Varela and Harrsion (1999), respectively, was likely due to a combination of both potential DOM export and the exclusion of euphotic zone NO_3^- regeneration from the NP estimates of Varela and Harrison.

3.3.5.4 Variability in the Reduction of New Production Estimates

No clear seasonal trend in the degree by which DI-NP estimates were reduced was apparent, however, a spatial trend was evident. In general, DI-NP estimates were typically reduced to a lesser extent at P4 where DI-NO_3^- uptake rates were highest, and to a greater extent at the more distal stations where DI-NO_3^- uptake rates were lowest (Fig. 3.9). Furthermore, a comparison of the relative amount by which DI-NP estimates were reduced vs. DI-NO_3^- uptake rates shows an exponential decay-type relationship ($p = 0.03$, $R^2 = 0.50$; Fig. 3.10a). It is important to note, however, that when considered independently of the pooled data-set, the winter results did not fit this relationship. DI-AO rates were much more spatially variable during winter, whereas in spring and late-summer DI-AO rates showed minimal spatial variability in comparison to the spatial

variability observed by the DI-NO_3^- uptake rates. Indeed, when the winter data were removed, the fit of the exponential decay model increased substantially (p <0.01; R^2 = 0.86; Fig. 3.10b). As such, during spring/late-summer periods, when the spatial variability of DI-AO is much lower than that of DI-NO_3^- uptake, the exponential decay model, which explained 86% of the variability associated with the relative reduction in DI-NP estimates, may prove useful when interpreting both historical and future NO_3^- measurements and estimating potential C-export in the NE subarctic Pacific. However, the non-linear exponential decay model that we have described here, should only be considered a first-order estimate of the relative amount by which DI-NP estimates are reduced as DI-NO_3^- uptake rates vary along Line P during spring and late-summer periods. Further observations of this nature are necessary to ascertain whether the relationship shown in Fig. 3.10b is reproducible. Still, the general inverse trend that we have described, for the relative reduction in DI-NP vs. DI-NO_3^- uptake rate relationship, is in keeping with observations from other studies. For example, when Yool et al. (2007) incorporated estimates of euphotic zone NO_3^- regeneration into their global NP model, they also found that estimates of new production were most reduced in regions of lower productivity. Results from other field studies also support the findings reported here. During HOT-50 at station ALOHA in the N Pacific subtropical gyre, daily DI-NO_3^- uptake was within the lower range of the DI-NO_3^- uptake rates measured during this study, and Dore and Karl (1996) estimated that euphotic zone nitrification could supply between 47 and 112% of the daily phytoplankton NO_3^- requirements. In contrast, in Saanich Inlet, one of the most highly productive fjords in the northern hemisphere, where NO_3^- based production accounts for a substantial fraction of total primary production

(~55%; Grundle et al. 2009), Grundle and Juniper (2011[Chapter 2]) demonstrated that their observations of euphotic zone nitrification may require that the DI-NP estimates of Grundle et al. (2009) be reduced by ~15%. In summary, both modeled global results, as well as field results from oligotrophic oceanic and highly productive coastal waters of the N Pacific, support our observation that the relative degree by which DI-NP estimates are reduced, when euphotic zone nitrification is taken into consideration, decreases as DI-NO_3^- uptake increases.

3.4 Summary

This study is the first to report AO rates for the Line P region of the NE subarctic Pacific, and, as such, it has furthered our understanding of nitrogen cycling processes along this important oceanographic time-series transect. The range of AO rates reported during the present study were similar to those which have previously been measured in other pelagic coastal and open ocean regions of the N Pacific, and our results add to a growing body of evidence that euphotic zone nitrification is an important and ubiquitous process. We have demonstrated that a substantial portion of the NO_3^- assimilated by phytoplankton in the NE subarctic Pacific may have been derived from nitrification occurring within the euphotic zone. The relative importance of euphotic zone nitrification for the support of NO_3^- based primary production was particularly evident near the base of the euphotic zone. This likely reflects the contrasting roles that light plays in regulating these two processes through the illuminated region of the water column. In terms of NP calculations in the NE subarctic Pacific, we found that the inclusion of euphotic zone NO_3^- regeneration into these calculations could significantly reduce estimates of NP. These results have important implications for historical NP estimates in

this region, and we warn that the failure to consider euphotic zone nitrification when interpreting both past and future NP measurements could result in potential C-export being grossly overestimated. The spatial variability in the relative degree by which NP estimates were reduced along Line P, indicates that euphotic zone NO_3^- regeneration is more important to phytoplankton in areas of low NO_3^- based production than in regions of high NO_3^- based production.

Recent recognition of the ubiquity of euphotic zone nitrification also has important inferences for other biogeochemical processes that we did not consider in the present study. For example, nitrification should be taken into consideration when interpreting N and O isotope fractionation in the euphotic zone (Wankel et al. 2007). It may also represent a previously under considered source of nitrous oxide (N_2O; Dore et al. 1998). N_2O is an important greenhouse gas which can be produced as a by-product during the oxidation of NH_4^+ to NO_2^-. Any previous exclusions of the euphotic zone from areal estimates of oceanic N_2O production, because of the original view that nitrification was photo-inhibited, could have resulted in oceanic N_2O production being underestimated. Based on contemporaneous measurements of ML N_2O at each of the same stations sampled during the present study, along with estimates of ML N_2O residence times and nitrification N_2O yields, Grundle et al. (2009 [Chapter 5]) concluded that euphotic zone nitrification was only a minor source of N_2O to the ML of the NE subarctic Pacific. However, these authors also showed that, in comparison to many other open ocean regions, the NE subarctic Pacific was somewhat of a "hotspot" for upward fluxes of N_2O into the ML and then into the atmosphere. As such, their suggestion that euphotic zone nitrification was a relatively minor contributor of N_2O to the surface waters of the NE

subarctic Pacific, was strictly region-specific, and not necessarily applicable to the global ocean. Indeed, studies from other regions have shown that euphotic zone nitrification may be an extremely important source of surface water N_2O (e.g. Dore and Karl 1996; Santoro et al. 2011).

Finally, results from the present study, as well as those of previous euphotic zone nitrification studies, should collectively transform our view of upper water column nitrogen cycling. As we have demonstrated, it is particularly important that we reconsider what has become, despite mounting evidence to the contrary, a rather stagnated view that all euphotic zone NO_3^- represents a source of N_{new} which has been mixed upwards from the aphotic region of the water column. By no means does this suggest that the new production paradigm is no longer valid. Instead, it simply implies that estimates of euphotic zone nitrification need to be incorporated into NP calculations, so as to ascertain what fraction of NO_3^- based production is attributable to truly new NO_3^- and what fraction is driven by simultaneous NO_3^- regeneration within the euphotic zone.

Tables

Table 3.1. The % surface incident irradiance recorded at each sampling depth and station during winter 2009.

Sampling Depth (m)	% Surface Irradiance				
	P4	P12	P16	P20	P26
0	100	100	100	100	100
10	14.0	50.0	27.0	43.5	38.0
20	5.0	32.5	11.5	30.0	24.0
30	2.0	27.5	4.0	13.5	16.0
40	1.5	12.5	2.5	7.0	10.0
75	0.1	1.0	0.5	1.0	1.0

Table 3.2. Depths of 1% I_o (i.e. base of the euphotic zone), mixed layer (ML) depths, ML temperature and ML salinity at each sampling station (data previously reported in Grundle et al. 2009 [Chapter 5]).

Characteristic	Station	Cruise		
		Winter	Spring	Late-Summer
1% I_o depth (m)	P4	47	27	25
	P12	75	57	65
	P16	60	61	64
	P20	75	46	64
	P26	75	46	62
ML depth (m)	P4	55	14	15
	P12	112	21	25
	P16	102	16	38
	P20	103	16	41
	P26	121	24	36
ML Temperature (°C)	P4	7.61	12.62	12.91
	P12	7.60	11.05	15.81
	P16	6.86	10.79	15.47
	P20	6.33	10.21	13.34
	P26	6.01	9.08	12.47
ML Salinity	P4	32.17	32.11	32.21
	P12	32.46	32.43	32.28
	P16	32.43	32.46	32.49
	P20	32.48	32.50	32.48
	P26	32.57	32.56	32.47

Figures

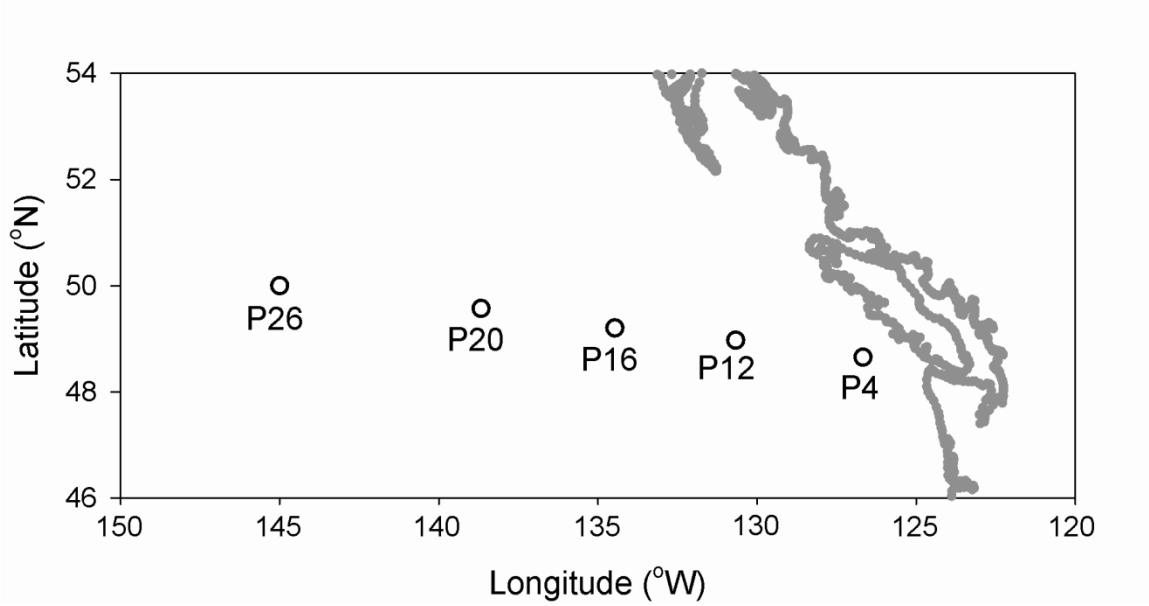

Figure 3.1. Map of the NE subarctic Pacific showing the locations of the 5 major sampling stations along Line P where seawater sampling was conducted during the present study (from Grundle et al. 2009 [Chapter 5])**.**

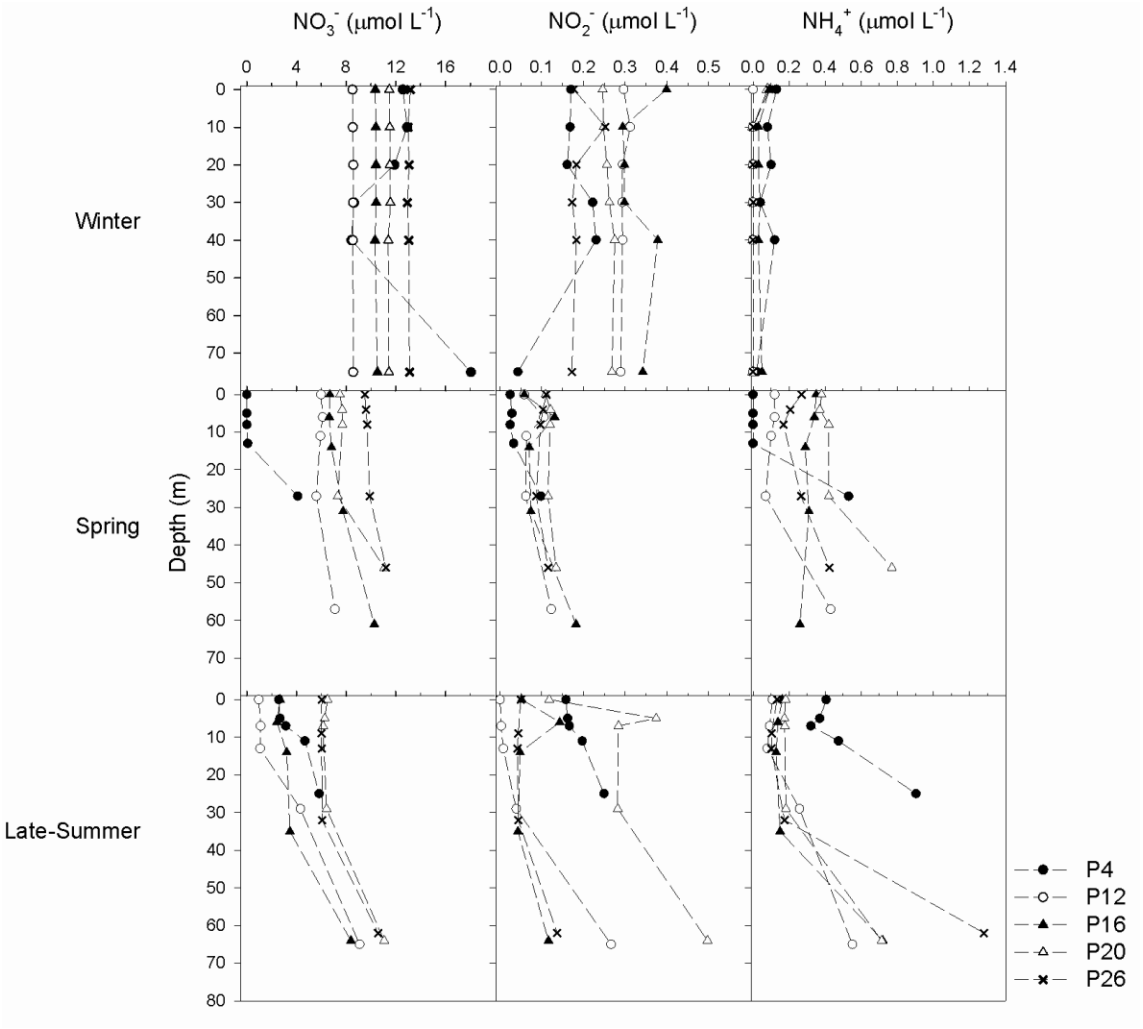

Figure 3.2. Vertical profiles of dissolved NO_3^-, NO_2^- and NH_4^+ at stations P4, P12, P16, P20 and P26 during winter, spring and late-summer 2009. During winter, dissolved nutrients were measured from the surface to 75 m, whereas during spring and late-summer measurements of dissolved nutrients were conducted from the surface to the depth of 1% I_o.

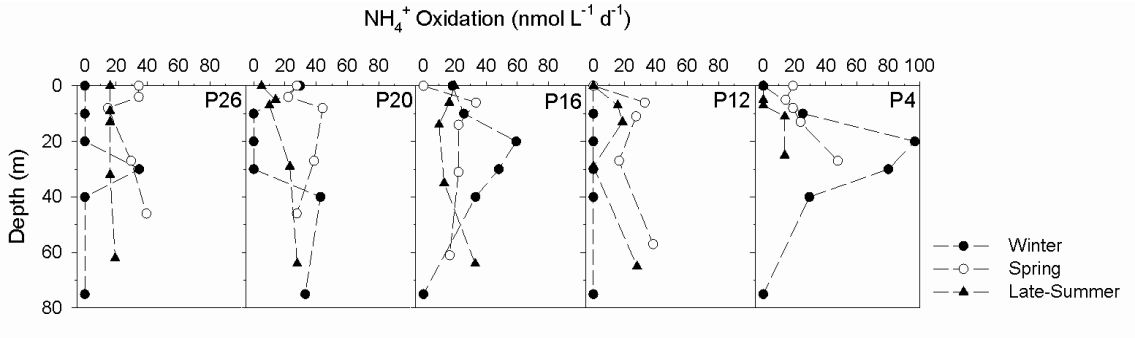

Figure 3.3. Vertical profiles of NH_4^+ oxidation (AO) rates at stations P4, P12, P16, P20 and P26 during winter, spring and late-summer 2009. During winter, AO rates were measured from the surface to 75 m, whereas during spring and late-summer AO rates were measured from the surface to the depth of 1% I_o.

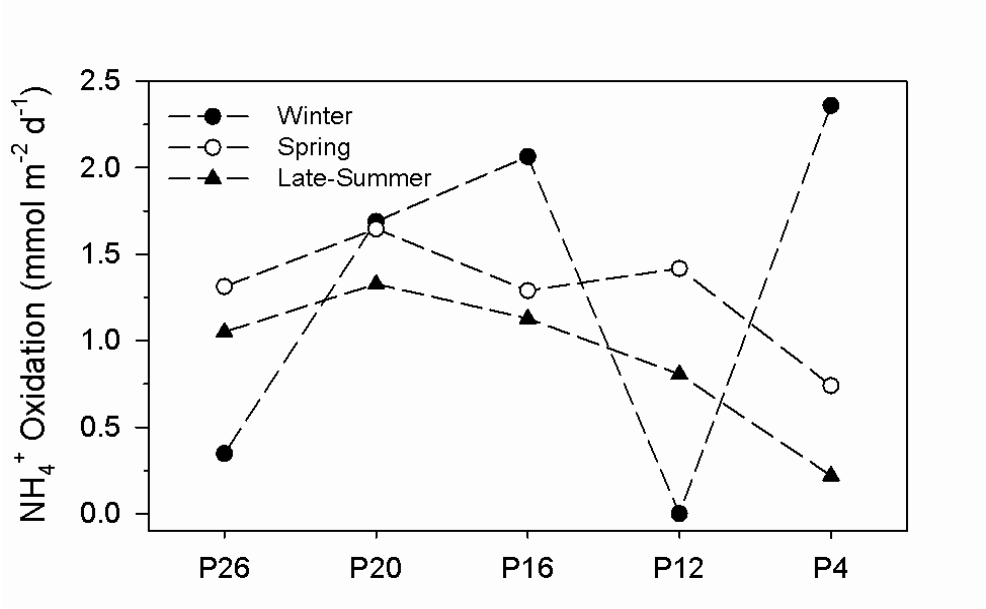

Figure 3.4. Euphotic zone integrated (i.e. surface to depth of 1% I_o integration) NH_4^+ oxidation rates at stations P4, P12, P16, P20 and P26 during winter, spring and late-summer 2009.

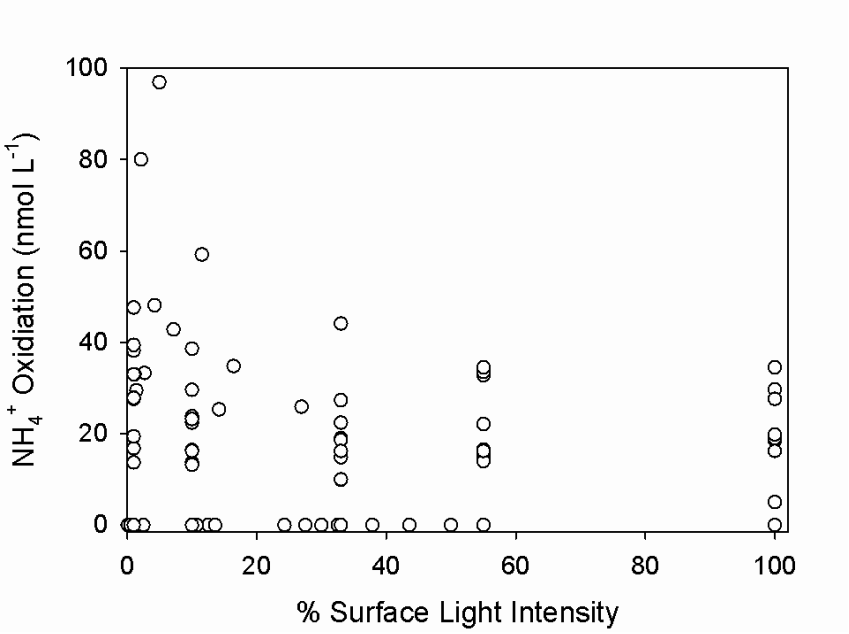

Figure 3.5. Relationship between NH_4^+ oxidation rates and relative light intensity.

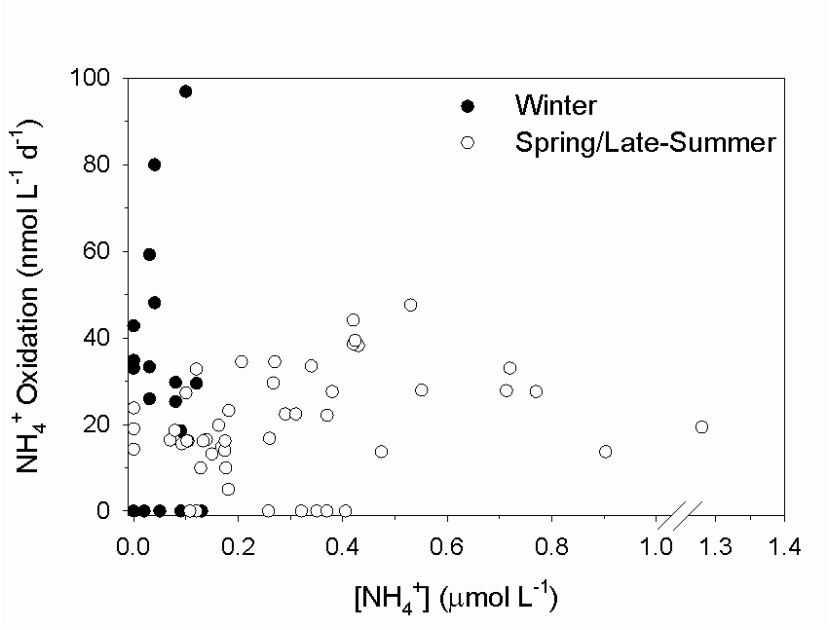

Figure 3.6. Relationship between NH_4^+ oxidation rates and NH_4^+ concentrations during winter (closed circles) and spring/late-summer (open circles).

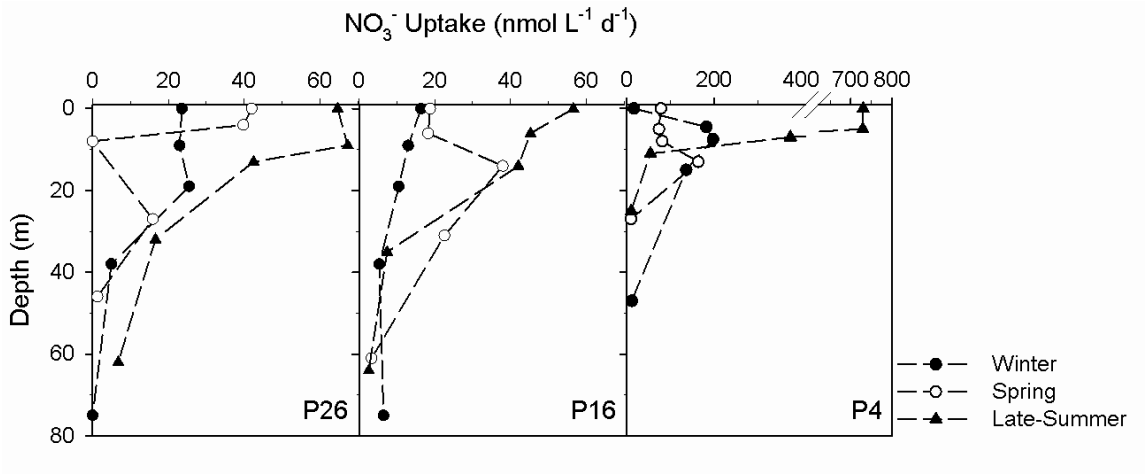

Figure 3.7. Vertical profiles of NO_3^- uptake rates at stations P4, P16 and P26 during winter, spring and late-summer. Note the different scale used to plot NO_3^- uptake rates at P4, compared to P16 and P26, as well as the x-axis line break for the P4 plot.

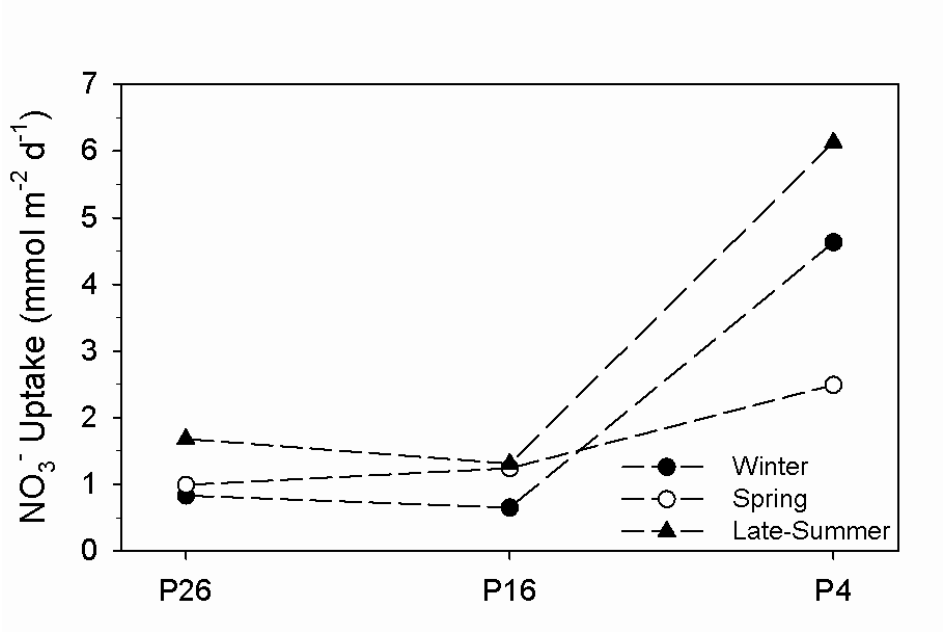

Figure 3.8. Euphotic zone integrated (i.e. surface to depth of 1% I_o integration) NO_3^- uptake rates at stations P4, P16 and P26 during winter, spring and late-summer 2009.

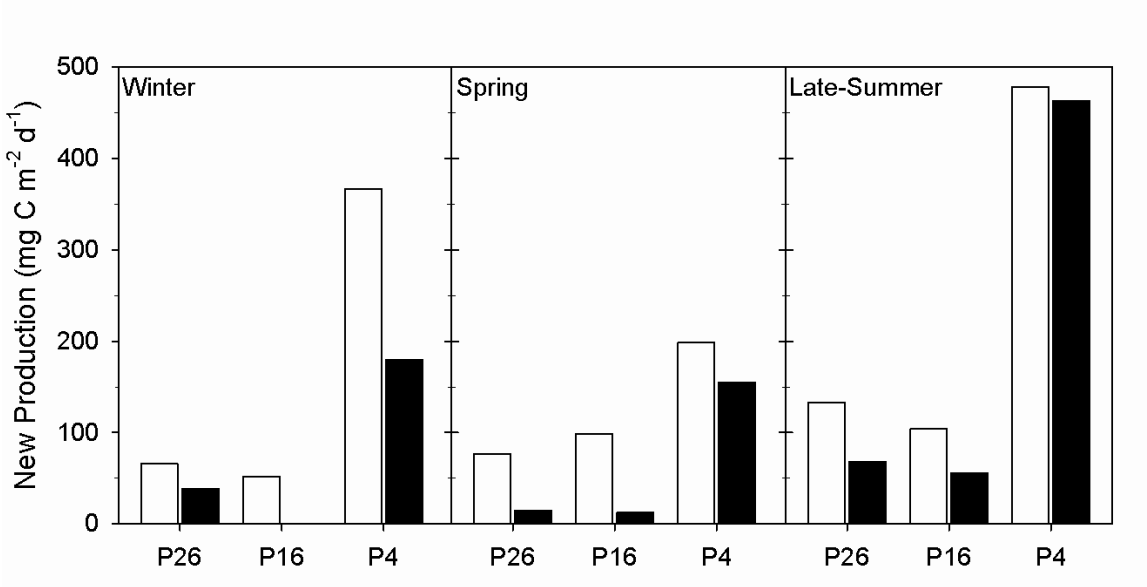

Figure 3.9. Euphotic zone integrated (i.e. surface to depth of 1% I_o integration) new production rates in terms of carbon at stations P4, P16 and P26 during winter, spring and late-summer 2009. The open bars reflect new production rates which were calculated following the traditional assumption of no euphotic zone nitrification, whereas the closed bars represent our revised estimates after subtracting the amount of new production that was potentially based on regenerated NO_3^- (see section 3.3.5.3 for a description of how these revised estimates were calculated).

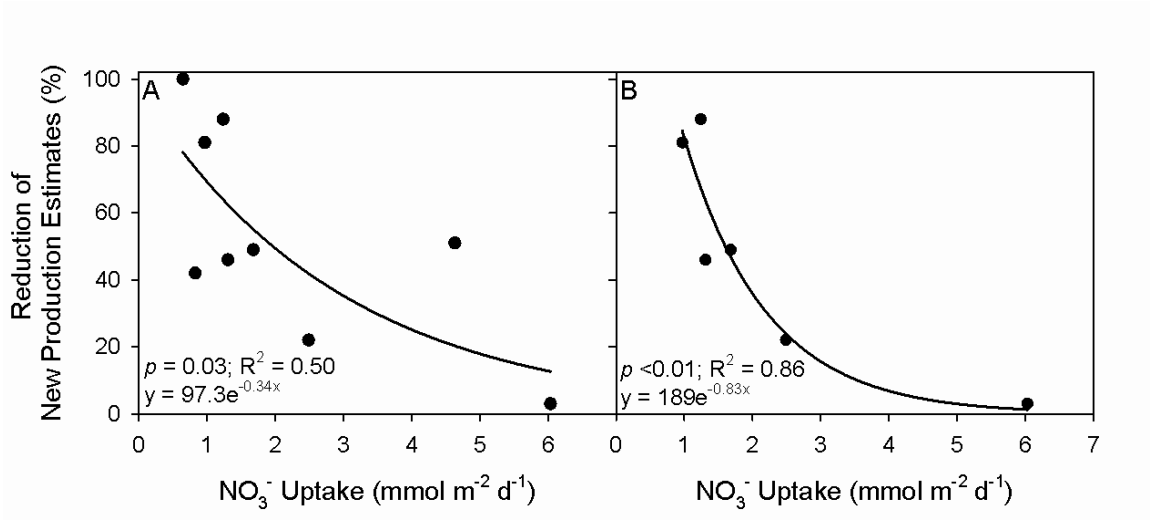

Figure 3.10. The relationship between the relative reduction of depth-integrated new production estimates and depth-integrated NO_3^- uptake rates. (A) includes data from P4, P16 and P26 during winter, spring and late-summer 2009, whereas (B) only includes spring and late-summer 2009 data from P4, P16 and P26. The solid lines represent non-linear exponential decay regressions.

Chapter 4 : Euphotic zone nitrification in the Sargasso Sea: Implications for measurements of new production

Citation:

Grundle, D.S., M.W. Lomas, S.K. Juniper. In prep. Euphotic zone nitrification in the Sargasso Sea: Implications for measurements of new production.

Abstract

Simultaneous ammonium oxidation (AO) and NO_3^- uptake rates were measured for the first time at the Bermuda Atlantic Time-series Study site in the Sargasso Sea during April and November of 2009. AO was detected throughout the euphotic zone, with rates ranging from undetectable to 33 nmol L^{-1} d^{-1}. Light and potentially substrate supply were found to play an important role in controlling AO rates through the euphotic zone, while increases in AO rates and potential NO_3^- supply appeared to positively influence NO_3^- uptake rates. The presence of euphotic zone AO activity has important implications for measurements of new production in the Sargasso Sea. Taking into account the fractions of depth-integrated NO_3^- uptake rates that may have been supported by *in situ* NO_3^- regeneration, caused NO_3^- uptake derived new production rates to be reduced by 62 to 100% (mean, 79%; median 67%). Our results have provided important insights into the role that nitrification plays in recycling NO_3^- in the euphotic zone, and we have demonstrated the need to revise our view of the new production paradigm in the Sargasso Sea.

4.1 Introduction

The microbial oxidation of NH_4^+ to NO_3^-, via NO_2^-, is an important component of the marine nitrogen cycle. It is critical for supporting NO_3^- based primary production and has played a central role in the "new production" paradigm. Early studies of soil nitrifying bacteria (Mueller-Neugluck and Engel 1961; Schon and Engel 1962) and marine nitrifying bacteria (Horrigan et al. 1981) found evidence to suggest that nitrification was photo-inhibited, leading to the general assumption that any NO_3^- present in the euphotic zone of the ocean was a result of upward physical transport mechanisms. This led to NO_3^- in the euphotic zone being classified as a form of "new" nitrogen (N_{new}) and NO_3^- based primary production as "new" production (NP), as opposed to "regenerated" forms of nitrogen (e.g. NH_4^+ and urea; N_{reg}) which can be directly recycled within the euphotic zone and result in "regenerated" production (Dugdale and Goering 1967). Following this, it was pointed out that if the only routes for NO_3^- into the euphotic zone were upward physical transport mechanisms, and for equilibrium to be maintained, any upward flux of NO_3^- into the euphotic zone must be balanced by a downward flux of particulate organic nitrogen (PON) out of the euphotic zone (Eppley and Peterson 1979). Eppley and Peterson (1979) defined the fraction of total primary production attributable to NP as the *f*-ratio, and they concluded that NP, or the *f*-ratio multiplied by total primary production, should be quantitatively equivalent to potential carbon export via the biological pump (hereinafter referred to as C-export). Measurements of NP have since become a widely used proxy for estimating potential C-export from the euphotic zone to deeper waters and sediments, and for determining how various environmental variables impact this

important climate relevant process. Oceanographic time-series stations, where routine, or at least repeat, measurements of NO_3^- based primary production are conducted have played a particularly important role in our understanding of C-export and the factors that regulate it.

The assumption that nitrification is restricted to the aphotic region of the water column is fundamentally imbedded in Dugdale and Goering's view of NO_3^- as a form of N_{new} and NO_3^- based production as NP, and the subsequent conclusion by Eppley and Peterson (1979) that NP should be quantitatively equivalent to potential C-export. More recently, however, studies have demonstrated that marine nitrification can in fact proceed under illuminated conditions (e.g. Clark et al. 2008; Diaz and Raimbault 2000; Dore and Karl 1996; Grundle and Juniper 2011[Chapter 2]; Grundle et al. in revision[Chapter 3]; Ward 1987, 2005). Observational evidence of euphotic zone nitrification highlights that not all euphotic zone NO_3^- should be considered N_{new}, and, as a result, NP and potential C-export rates inferred from NO_3^- uptake measurements may have been overestimated (Yool et al. 2007). Any NO_3^- produced by nitrification within the euphotic zone, should instead be regarded as part of the N_{reg} pool, and any production based on this regenerated NO_3^- should be considered regenerated production. This does not render the NP paradigm redundant; it simply requires that estimates of euphotic zone nitrification be incorporated into calculations of NP. It does, however, raise questions as to the reliability of C-export estimates based on historical measurements of NP where the potential for euphotic zone NO_3^- regeneration was not taken into consideration. Obtaining more meaningful interpretations of both historical and future NO_3^- uptake rate measurements, in terms of NP and C-export, requires a comprehensive understanding as to the magnitude of

euphotic zone nitrification, and the extent to which regenerated NO_3^- supports phytoplankton NO_3^- requirements at regionally specific scales.

Time-series measurements in the Sargasso Sea, starting with Hydrostation S (1954) and later with the Bermuda Atlantic Time-series Station (BATS; 1988), have played a critical role in our understanding of NP and potential C-export rates in subtropical ocean regions (see review by Lipschultz et al. 2002). Indeed, Hydrostation S served as one of the sampling stations for the first measurements of $^{15}N\text{-}NO_3^-$ uptake rates (Dugdale and Goering 1967). It also laid the foundations for our understanding of how the *f*-ratio varies across oceanographic regimes characterized by distinctly different nutrient and light conditions, and changes in *f*-ratio values were linked to changes in total primary production (Eppley and Peterson 1979). This led Lipschultz et al. (2002) to describe the concept of NP as being "intimately tied" to the Sargasso Sea. Improvements in the sensitivity of N isotope measurements, combined with flow cytometric sorting of phytoplankton, has recently fueled new interests in NP in the Sargasso Sea by allowing measurements of NP by specific phytoplankton groups (Casey et al. 2007). The fact that nitrification has now been found to occur within the euphotic zone, however, suggests that NP may have been overestimated in the Sargasso Sea. Indeed, Lipschultz (2001) reported qualitative observations of NO_3^- regeneration during $^{15}N\text{-}NO_3^-$ uptake incubations and suggested that a large portion of phytoplankton NO_3^- uptake must be based on *in situ* NO_3^- regeneration. In the absence of euphotic zone nitrification rate estimates, however, it is difficult to assess the degree to which NP may have been overestimated. To this end, the primary goals of the present study were to determine how prevalent nitrification is in the euphotic zone of the Sargasso Sea, identify factors which

may play important roles in controlling nitrification rates, and quantify the degree to which NP is reduced when euphotic zone nitrification is taken into account. In order to estimate the amount of NO_3^- supplied to phytoplankton by nitrification within the euphotic zone, we followed the protocol used by Grundle et al. (in revison[Chapter3]) and focused on the first and rate limiting step of nitrification (i.e. NH_4^+ oxidation, AO). Before proceeding, it is worth noting that while we have focused on NP arising from phytoplankton NO_3^- uptake, we also recognize that N_2 fixation is also a source of NP. Early stable N isotope ratio measurements indicated that N_2 fixation at BATS was negligible (Altabet 1988; 1989), however, more recent direct rate measurements have shown that N_2 fixation could account for a substantial fraction of the net community production at BATS during the April to November period, particularly when considering the C:N fixation ratios of *Trichodesmium* (Orcutt et al. 2001) and evidence that studies may have underestimated *Thrichodesmium* abundance in the Sargasso Sea (Davis and McGillicuddy 2006) . Nevertheless, our focus here was to examine the implications of euphotic zone nitrification for NO_3^- based estimates of NP in the Sargasso Sea, and, as such, N_2 fixation was not considered. Thus, all further reference to NP strictly infers NP derived from NO_3^- uptake measurements.

4.2 Methods

Sampling in the Sargasso Sea was conducted at BATS (31° 40′N, 64° 10′W) onboard the *RV Atlantic Explorer* during two cruises in April 2009 and two cruises in November 2009. Water samples for AO rate measurements were collected from depths corresponding to ~100, 55, 33, 10 and 1% surface incident irradiance (I_o) on April 1 and 15, and on November 7, 9 and 22. The first three cruises and first four sets of AO rate

measurements were facilitated by the BATS sampling program (Bermuda Institute of Ocean Sciences), while the fourth cruise and final set of AO rate measurements were facilitated by the Ocean Flux Program (Marine Biological Laboratory, Woods Hole). Water samples for the measurement of NO_3^- uptake rates were also collected from the same depths as those outlined above on April 1, and November 7 and 9. All water samples were collected using a rosette configuration of Niskin bottles with an attached SeaBird Electronics SBE 9+ conductivity, temperature and depth (CTD) profiler.

The methods used here to measure biological rate measurements have been described elsewhere in greater detail (see Grundle and Juniper 2011[Chapter 2]; Grundle et al. in revision[Chapter 3]). Briefly, water samples for AO rate measurements were incubated under dark conditions in on-deck polycarbonate incubators with flowing surface supplied seawater to maintain temperature stability. AO rates were calculated based on the difference between NO_2^- concentrations between duplicate 500 ml control samples and duplicate 500 ml treatment samples (treated with the AO inhibitor, allylthiourea; ATU) following an incubation period 24 to 48 hrs. NO_2^- concentrations were measured using the colorimetric method outlined by Bendschneider and Robinson (1952) at 654 nm, using a 10 cm pathlength cell to allow nanomolar detection of NO_2^-. The substrate availability corresponding to each of our AO rate measurements was assessed by measuring NH_4^+ concentrations fresh at sea using the fluorometric technique of Holmes et al. (1999). One exception to the AO rate measurements employed here and those previously described (Grundle and Juniper 2011[Chapter 2]; Grundle et al. in revision[Chapter 3]), involved the addition of NO_2^- to both the control and treatment bottles. During our first set of AO rate measurements on April 1 2009, the NO_2^- pools in

the ATU treated samples collected from 33% I_o were exhausted by the end of a 24 hr incubation period. This could have caused us to underestimate the AO rate at 33% I_o on April 1, however, as the AO rate derived from these samples was the highest of all the AO rates measured at 33% I_o, and at the upper range of AO rate measured at all depth and on all sampling dates (see section 4.3.1), any underestimation was likely minimal. To avoid the possibility of this occurring during subsequent incubations, we equally amended all subsequent control and treatment samples with 100 nmol NO_2^- L^{-1}.

Water samples for phytoplankton NO_3^- uptake rates were collected in 1 L polycarbonate bottles and inoculated with 0.01 µmol ^{15}N-labelled KNO_3 (99 atom% ^{15}N) L^{-1}. Following this, sample bottles were covered with neutral density screening to simulate the light intensities from which the samples originated, and then incubated in the previously described on-deck incubators for ~24 hrs. Absolute NO_3^- uptake rates were calculated from measurements of particulate organic nitrogen (PON) and the atom% ^{15}N content of particulate matter retained on 0.7 µm glass fiber filters at the end of the incubations, and using the equations of Dugdale and Wilkerson (1986). To determine corresponding substrate concentrations and atom% enrichments, water samples were collected and stored at -20°C for post-cruise measurements of NO_3^- concentrations using a SEAL AutoAnalyzer 3 HR.

4.3 Results and Discussion

4.3.1 NH_4^+ Oxidation Rates

AO rates at BATS ranged from undetectable to 33 nmol L^{-1} d^{-1} (Fig. 4.1). The range of rates reported here are lower than those observed within the euphotic zone at higher latitudes of the North Pacific (Grundle et al. in revision[Chapter 3]; Santoro et al. 2010;

Ward 2005), as well as at the Hawaii Ocean Time-series station (Dore and Karl 1996), but are highly similar to those measured in the eastern subtropical North Atlantic (Clark et al. 2008) and in the Mediterranean (Diaz and Raimbault 2000). Depth-integrated (DI; 100 to 1% I_o) AO rates ranged from 0.5 to 1.6 mmol m^{-2} d^{-1}, with the highest rates occurring in April (Fig. 4.2). The mean DI-AO rate in April (1.4 ±0.3 mmol m^{-2} d^{-1}) was more than twice that of November (0.6 ±0.1 mmol m^{-2} d^{-1}). This was not an artifact of our depth integration ranges as our highest observed DI-AO rate (April 1) coincided with the shallowest euphotic zone base (1% I_o) of the study. Although the relative difference between mean DI-AO rates during April and November was high, the absolute difference in DI-AO rates was small in comparison to temporal AO rate variations in regions where AO rates are high (e.g. Grundle and Juniper 2011[Chapter 2]), and the magnitude of AO rate variations across distinct oceanographic regimes (see review by Ward 2005).

4.3.2 Factors Controlling NH_4^+ Oxidation through the Sargasso Sea Euphotic Zone

Our results have shown that AO occurs throughout the euphotic zone of the Sargasso Sea, thus demonstrating that AO is not completely photo-inhibited. This does not rule out partial photo-inhibition or a controlling role of light. Indeed, with the exception of our November 9 sampling date, AO rates were undetectable at the surface (100% I_o); whilst highest AO rates were always observed at the base of the euphotic zone (i.e. 1% I_o; Fig. 4.1), supporting the notion of at least partial photo-inhibition of marine AO. Furthermore, we found that even though low AO rates were observed at all relative light intensities, the highest AO rates were associated with the lowest light intensities, and AO increased exponentially with decreasing relative light intensity through the euphotic zone (p <0.01,

R^2 = 0.35; Fig. 4.3a). These results are consistent with studies from Monterey Bay (Ward 2005) and the NE subarctic Pacific (Grundle et al. in revision[Chapter 3]). Thus, while our AO rate measurements support a growing collection of work which has demonstrated that AO can no longer be thought of as a strictly aphotic zone process (Clark et al. 2008; Diaz and Raimbault 2000; Dore and Karl 1996; Grundle and Juniper 2011[Chapter 2]; Grundle et al. in revision[Chapter 3]; Santoro et al. 2010; Ward 1987, 2005; Yool et al. 2007), we conclude that light still plays an important role in limiting AO rates through the euphotic zone of the Sargasso Sea.

In addition to light, some studies have found evidence for control of AO rates by ambient substrate concentrations (Bianchi et al. 1999; Grundle and Juniper 2011[Chapter 2]; Grundle et al. in revision[Chapter 3]; Olson 1981). During the present study, we found no relationship between ambient substrate concentrations and AO rates. However, with the exception of our April 15, and November 7 and 9 sampling dates, when NH_4^+ concentrations at 1% I_o were ~20 nmol L^{-1}, substrate concentrations were always undetectable. Interestingly, AO rates were positively correlated (Pearson Product Moment Correlation) with PON concentrations (p = 0.03, r = 0.56; Fig. 4.3b). If increased PON results in higher remineralization rates and NH_4^+ supply, this could indicate that substrate supply, which is often more important for regulating AO rates than ambient NH_4^+ concentrations (Clark et al. 2008; Ward 2005), may also play an important role in controlling AO rates in the Sargasso Sea euphotic zone. This would also explain the higher DI-AO rates in April compared to November, as highest PON concentrations were found in April.

Finally, it is important to consider factors which may have led us to systematically over- or under- estimate AO rates during this study. Firstly, our use of dark incubations could have allowed AO communities to recover from photo-inhibition, particularly those in the upper regions of the euphotic zone, thus leading to an overestimation of AO rates. Given that the use of dark incubations did not erase the AO vs. relative light intensity relationship, it is likely that any overestimation would have been minimal. The second factor that may have caused some error and led us to underestimate AO rates is the potential presence and activity of AO archaea (AOA). AOA were only recently discovered (Könneke et al. 2005), and if these organisms were present and actively oxidizing NH_4^+ during the present study it is possible that we may have underestimated AO rates, as although ATU completely inhibits AO bacteria (AOB) it may not completely inhibit AOA. Studies have shown that AOA ammonia monooxygenase subunit A gene (*amoA*) copy numbers may be one to four orders of magnitude higher than AOB *amoA* copy numbers in the ocean (Mincer et al. 2007; Santoro et al. 2011), and Bouskill et al. (2012) recently confirmed this for the Sargasso Sea. Nevertheless, the relative distributions of AOA vs. AOB *amoA* copy numbers cannot be used to estimate the relative contribution of these two groups to total AO activity (Santoro et al. 2011). Additionally, unlike AOB, it is not clear whether AOA are obligate autotrophs (Ward 2008), and, as such, their presence does not necessarily infer AO activity. Furthermore, the degree to which ATU vs. ^{15}N tracer methodology may underestimate AO rates when AOA are present and active appears to be relatively minor in the euphotic zone compared to deeper waters (Santoro et al. 2011). Thus, it is again likely that any error caused by our use of ATU to measure AO rates would have been minimal. Finally, even if systematic

positive and negative errors were introduced as a result of our use of dark incubations and ATU, respectively, the maximum relative magnitude of these two sources of error are somewhat similar, and it is therefore likely that they would have countered each other to some degree (see section 1.7, Chapter 1). This is supported by the high degree of similarity between our AO rate estimates and those of Clark et al. (2008) at similar latitudes in the eastern North Atlantic using ^{15}N tracer methodology and simulated light conditions.

4.3.3 NO_3^- Uptake Rates

Here we report phytoplankton NO_3^- uptake rates and quantify the degree to which NP estimates are reduced when euphotic zone nitrification is taken into consideration. These estimates are based on measurements of AO, and, as such, we are making the assumption that any NH_4^+ oxidized to NO_2^- is oxidized all the way through to NO_3^-. This assumption seems fairly reasonable given observations of night-time NO_2^- depletions in the Sargasso Sea euphotic zone and the suggestion that NO_2^- oxidation is equal to and may even exceed AO.

NO_3^- uptake rates ranged from undetectable to 44 nmol L^{-1} d^{-1} (Fig. 4.4), and these values are within the expected range of our sampling period (Lipschultz et al. 2001). Also consistent with Lipschultz et al. (2001) was the observation that NO_3^- uptake rates were positively correlated with NO_3^- concentrations ($p = 0.02$; $R^2 = 0.33$; Fig. 4.5a), thus indicating that NO_3^- uptake rates were at least partially controlled by substrate availability. A positive correlation was also observed between NO_3^- uptake rates and AO rates ($p < 0.01$, $R^2 = 0.57$; Fig. 4.5b), demonstrating that contemporaneous NO_3^- supply by nitrification also plays an important role in controlling the magnitude of NO_3^- uptake in

the Sargasso Sea. A comparison between corresponding AO and NO_3^- uptake rates (Fig 4.5a) shows that, at times, AO could have supplied amounts of NO_3^- which were far in excess of daily phytoplankton NO_3^- demands. The mean (all depths) relative contribution of AO to phytoplankton NO_3^- requirements was 123%. However, this value was skewed towards the high end by an extreme outlying value on November 7 at 55% I_o when AO was 13 nmol L^{-1} d^{-1} and NO_3^- uptake was only 2 nmol L^{-1} d^{-1}, resulting in a 650% contribution of AO to daily phytoplankton NO_3^- requirements. Instead, the median value of 75% is probably more representative of the general potential contribution of euphotic zone nitrification to phytoplankton NO_3^- uptake.

4.3.4 Implications of Euphotic Zone Nitrification for Measurements of New Production

Our sampling period fell within the Sargasso Sea "oligotrophic" period (April to November), when stratification of the upper water column prevents, or at least minimizes, upward mixing of truly new NO_3^- into the euphotic zone (Lipschultz et al. 2002). An examination of the density profiles measured by the BATS program (http://bats.bios.edu/) during our sampling period confirms this. Still, it is important to note that even during the oligotrophic period mesoscale eddies can also sporadically introduce truly new NO_3^- into the euphotic zone of the Sargasso Sea (McGillicuddy et al. 1998). However, although mesoscale eddies are capable of fuelling large increases in primary production, biological removal of the new NO_3^- introduced by these eddies is fairly rapid (days; McGillicuddy et al. 1998). As a result, for large periods of the Sargasso Sea oligotrophic period, *in situ* nitrification must be the predominant source of NO_3^- to the euphotic zone. It certainly appeared that *in situ* nitrification was the dominant

source of euphotic zone NO_3^- during the sampling dates reported here, as NO_3^- concentrations through the euphotic zone were always low and far below those observed during mesoscale eddy events (McGillicuddy et al. 1998). Further evidence supporting the notion that euphotic zone nitrification was an important source of NO_3^- during the present study comes from the positive NO_3^- uptake vs. AO rate linear relationship (Fig. 4.5b). To this end, observations of euphotic zone AO and large potential contributions of regenerated NO_3^- have important implications for NP and C-export estimates based on NO_3^- uptake measurements. Outside of the oligotrophic period, when convective cooling of the surface water breaks down stratification and allows nutrient rich water to be mixed into the euphotic zone (Lipschultz et al. 2002), or during oligotrophic mesoscale eddy events, the introduction of truly new NO_3^- probably diminishes the importance of euphotic zone nitrification in supporting phytoplankton NO_3^- requirements.

To estimate the overall amount by which NP and potential C-export estimates are reduced once euphotic zone NO_3^- regeneration is taken into account, we estimated the potential degree by which depth-integrated (DI; surface to 1% I_o) NO_3^- uptake would have been supported by euphotic zone nitrification. DI-NO_3^- uptake rates ranged from 1.0 to 1.5 mmol m^{-2} d^{-1}, and using the Redfield C:N ratio of 6.6, this equates to a DI-NP range, in terms of C, of 78.3 to 118.2 mg m^{-2} d^{-1} (Fig. 4.6). The corresponding DI-AO uptake rates suggest that nitrification could have supported between 62 and 110% of DI phytoplankton NO_3^- requirements (mean, 79%; median, 67%). These estimates are in close agreement with those calculated for the euphotic zone at station ALOHA in the N Pacific (Dore and Karl 1996) and for regions of the NE subarctic Pacific characterized by similar NO_3^- uptake rates (Grundle et al. in revision[Chapter 3]). Furthermore, Mongin et

al. (2003) applied a complex upper-ocean biogeochemical model to the BATS site. This model was tuned to reproduce vertical profiles and temporal variations of NO_3^-, NH_4^+, and $Si(OH)_4$ concentrations consistent with the BATS dataset. To prevent unrealistically high NH_4^+ concentrations from accumulating in the model output, the authors needed to invoke substantial rates of euphotic zone nitrification and found that nitrification in the upper 200 m of the water column accounted for 64 to 79% of simulated phytoplankton NO_3^- rates. These modeled estimates are extremely close to my field-based mean and median estimates of the fraction of phytoplankton NO_3^- uptake rates that are potentially supported by euphotic zone NO_3^- regeneration. Clearly, if large fractions of the DI-NO_3^- uptake rates reported here were supported by regenerated NO_3^-, they cannot be used to infer NP and potential C-export. Taking into account the amount of DI-NO_3^- uptake that was potentially supported by nitrification results in a new DI-NP range, in terms of C, of 0 to 29.8 mg m^{-2} d^{-1} (Fig. 4.6).

Finally, because we did not measure all sources of N uptake by phytoplankton, we have not attempted to directly calculate a revised *f*-ratio for the Sargasso Sea. This, however, does not prevent us from indirectly speculating on the impact euphotic zone NO_3^- regeneration may have for *f*-ratio estimates in the Sargasso Sea. As pointed out in a review of NP in the Sargasso Sea (Lipschultz et al. 2002), recent estimates place the total annual primary production at BATS between 114 and 196 g C m^{-2} (Steinberg et al. 2001). Based on the traditional NP paradigm (i.e. no euphotic zone nitrification), and using the canonical view of how *f*-ratio values vary with changes in total production (Eppley and Peterson 1979), Lipschultz et al. (2002) pointed out that the *f*-ratio would be 0.3. Applying this traditional *f*-ratio estimate to the "mid-point" of the annual primary

production range of Steinberg et al. (2001) equates to an annual NP rate of 47 g C m^{-2}. As discussed earlier, truly new NO_3^- is transported into the euphotic zone during the winter convection period, and this likely diminishes the importance of regenerated NO_3^- arising from euphotic zone nitrification. This is not to suggest that euphotic zone nitrification would be "turned off" during winter, but its contribution, relative to truly new NO_3^-, may be significantly reduced. Therefore, to err on the side of caution, we assume that all NO_3^- uptake during winter represents uptake of N_{new}. Winter NO_3^- uptake may account for between 25 and 60% of total annual NO_3^- based production, and we therefore calculate winter NP to be 12 to 28 g C m^{-2} (i.e. 25 to 60% of the 47 g C m^{-2} annual NP rate noted above). This leaves 40 to 75% of annual NP, or 19 to 35 g C m^{-2}, to be accounted for during the oligotrophic period. As noted earlier, however, the presence of euphotic zone nitrification activity means that some fraction of this oligotrophic NP estimate should actually be considered regenerated production. Using our median (i.e more conservative) estimate of the potential contribution of euphotic zone nitrification to DI-NO_3^- uptake (67%), results in a revised oligotrophic period NP estimate of 6 to 12 g C m^{-2}. Combining this with the winter NP estimate results in a conservatively revised annual NP rate of between 24 and 34 g C m^{-2}, or a new *f*-ratio range of 0.15 to 0.22. The principle purpose of our revised *f*-ratio range estimate is to simply demonstrate the potential impact that euphotic zone NO_3^- regeneration may have for NP derived export ratios. Export ratio estimates using ^{15}N tracer techniques, direct measurements of export flux and a suite of geochemical methods have all resulted in high "within" and "between" method variability (see review by Lipschultz et al. 2002), and, as such, assessing how accurately our revised NP derived *f*-ratio reflects export production is difficult.

4.4 Summary

This is the first study to directly quantify and report euphotic zone AO rates in the Sargasso Sea, and it has highlighted that we should adapt the way in which we view upper water column nitrogen cycling in this important time-series region. Our results confirmed that nitrification can support large fractions of NO_3^- based production during the Sargasso Sea oligotrophic period, and we have provided important insights into factors that control euphotic zone AO, as well as the potential role that nitrification may play in supporting and controlling NO_3^- uptake at BATS. Specifically, results from this study have shown that

- nitrification should be considered a relatively ubiquitous process within the euphotic zone of the Sargasso Sea;
- both light and substrate supply appear to play an important role in controlling AO rates;
- NO_3^- supply from euphotic zone nitrification plays an important role in controlling phytoplankton NO_3^- uptake during the Sargasso Sea oligotrophic period; and
- euphotic zone nitrification potentially supports large fractions of NO_3^- based production, and when this fraction is subtracted from total daily phytoplankton NO_3^- uptake rates, DI NP and potential C-export rates are reduced by 62-100% (mean, 79%; median 67%).

This final point demonstrates the critical importance of taking euphotic zone NO_3^- regeneration into account when interpreting historical estimates of NP, and when attempting to infer NP from future measurements of NO_3^- based production.

Figures

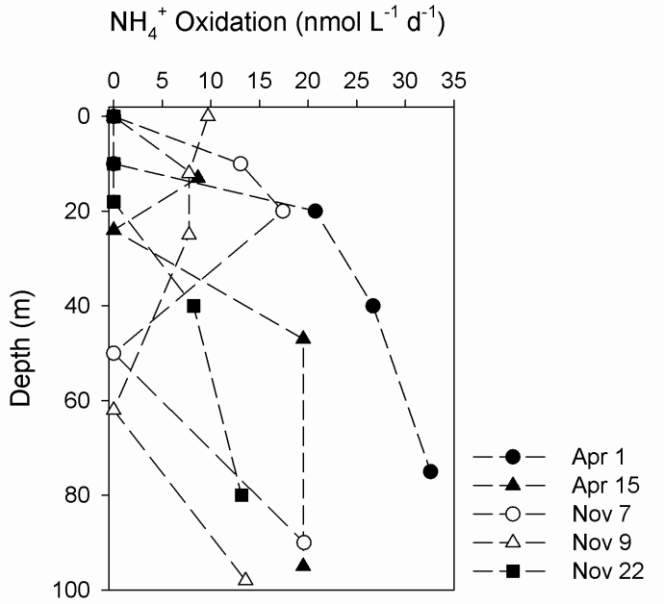

Figure 4.1. Vertical profiles of NH_4^+ oxidation rates at BATS during 2009, and at depths corresponding to ~100, 55, 33, 10 and 1% I_o.

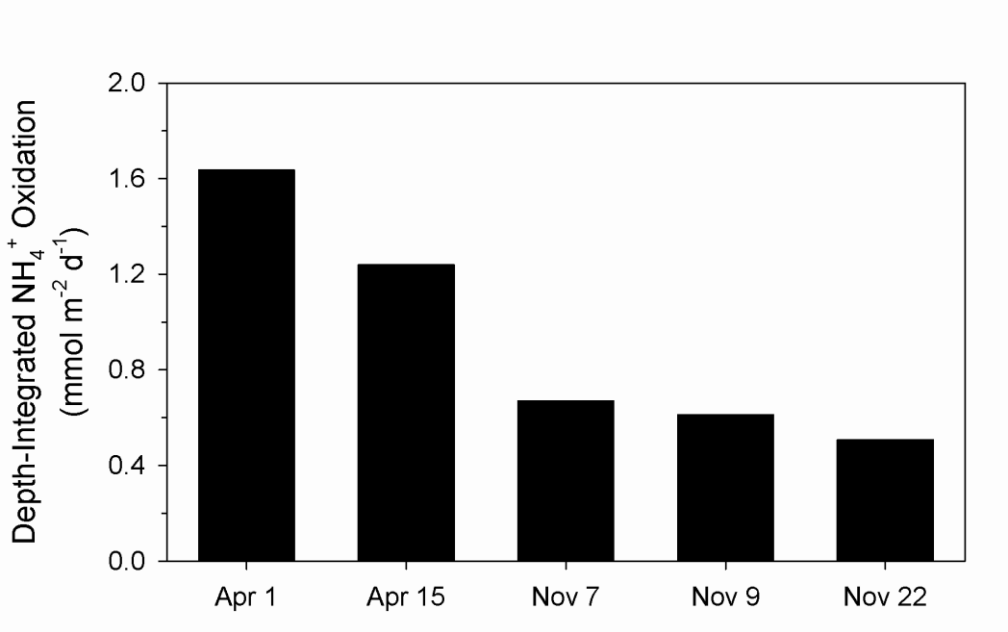

Figure 4.2. Depth-integrated (surface to 1% I_o) NH_4^+ oxidation rates at BATS during 2009.

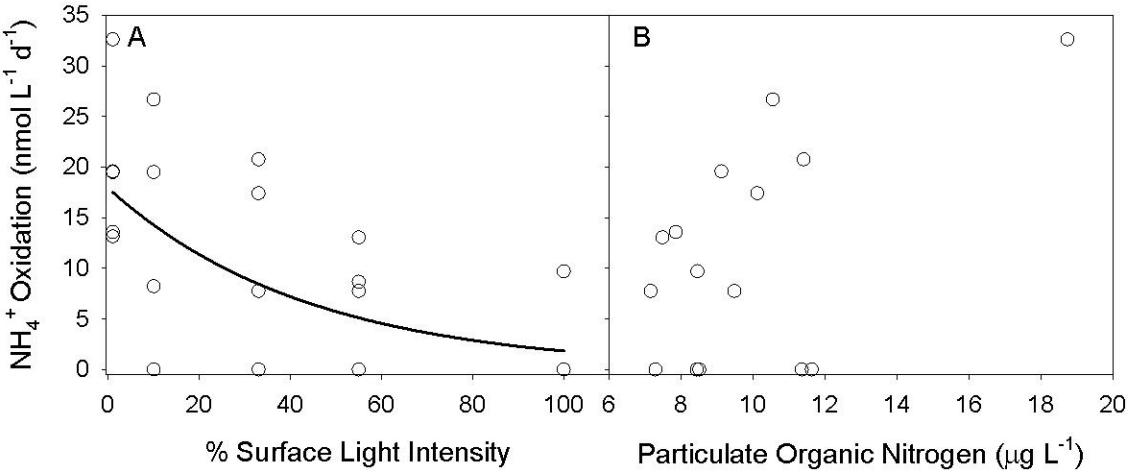

Figure 4.3. (A) NH_4^+ oxidation rates vs. relative light intensity; the solid line represents a non-linear exponential decay regression (p <0.01, R^2 = 0.35). (B) NH_4^+ oxidation rates vs. particulate organic nitrogen concentrations.

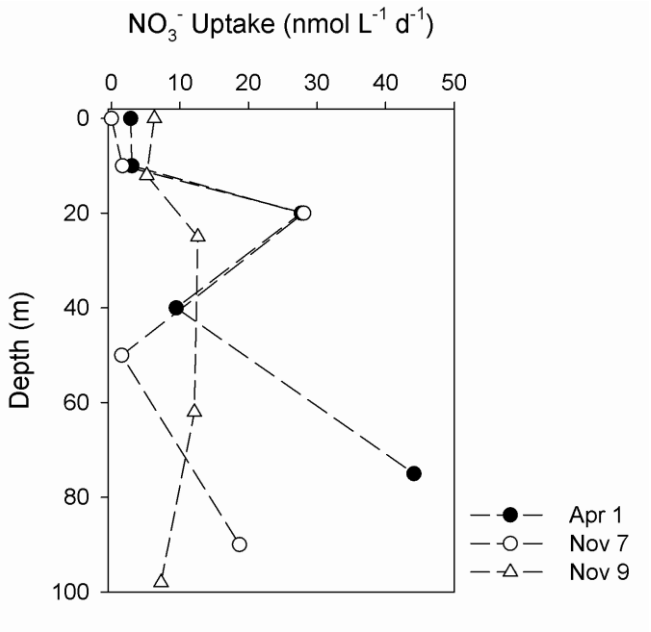

Figure 4.4. Vertical profiles of NO_3^- uptake rates at BATS during 2009, and at depths corresponding to ~100, 55, 33, 10 and 1% I_o.

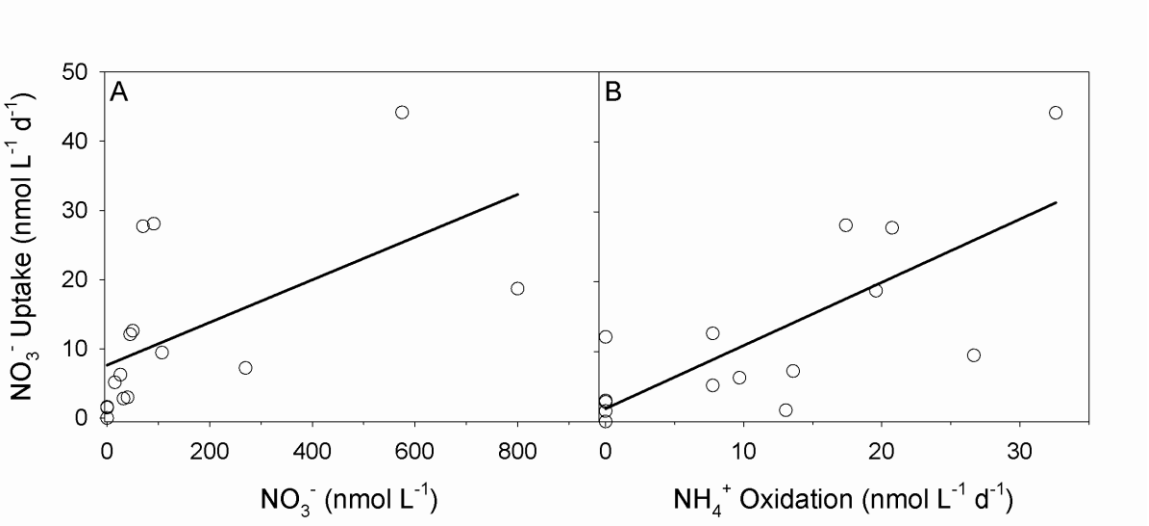

Figure 4.5. NO_3^- uptake rates vs. (A) NO_3^- concentrations and (B) NH_4^+ oxidation rates. The solid lines represent linear regressions ([A] p =0.02, R^2 = 0.33; [B] p <0.01, R^2 = 0.57).

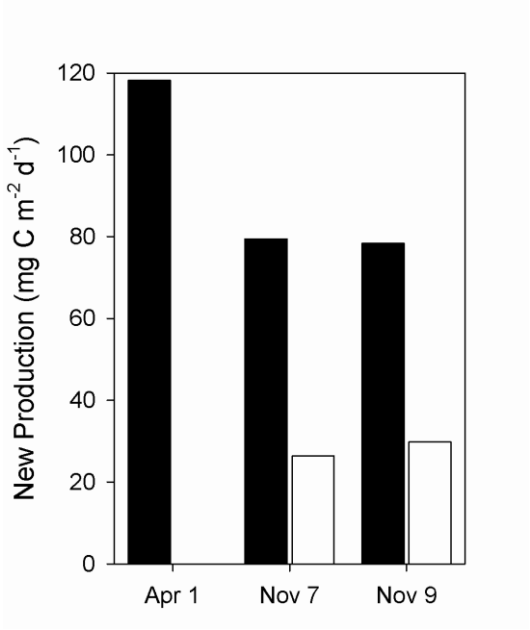

Figure 4.6. Depth-integrated (surface to 1% I_o) new production rates in terms of carbon at BATS during 2009. The closed bars reflect new production rates which were calculated following the traditional assumption of no euphotic zone nitrification. The open bars represent our revised new production estimates after subtracting the amount of production that was potentially based on regenerated NO_3^-.

Chapter 5 : Upper water column nitrous oxide distributions in the northeast subarctic Pacific Ocean

Citation:

Grundle, D.S., R. Maranger, S.K. Juniper. 2012. Upper water column nitrous oxide distribution in the northeast subarctic Pacific Ocean. *Atmosphere-Oceans* 50, 475-486.

Abstract

This is the first study to investigate the magnitude and distribution of N_2O concentrations along the Line P oceanographic transect in the Northeast (NE) subarctic Pacific Ocean. Concentrations of N_2O were measured from the surface to 600 m depth at five stations between 126°W and 145°W. Although nitrification within the mixed layer may produce some N_2O, we conclude that mixing and diffusion processes, which vertically transport N_2O upwards from below the mixed layer, are the primary sources of N_2O to the surface waters of the NE subarctic Pacific Ocean. Below the mixed layer, nitrification appears to be the dominant source of N_2O, and based on correlations of excess N_2O (ΔN_2O) versus apparent oxygen utilization and NO_3^- concentrations, we estimated that the N_2O yield from nitrification was approximately 0.028 to 0.040%. The longitudinal distributions of N_2O concentrations below the mixed layer were variable and we consider the potential role that different transiting water masses may play in contributing to this variability. Finally, we estimated that the regional average sea-to-air N_2O flux was 4.37 mol of N_2O km^{-2} d^{-1}, a value which is approximately four times that of the global average seawater-to-air flux rate. Our N_2O yield estimates are within the range of those expected under oxic conditions, leading us to conclude that decreasing dissolved O_2 concentrations in the NE subarctic Pacific Ocean, and the water masses that influence this region, over the past 50 years have yet to produce a substantial increase in N_2O production. Given the expectation that dissolved O_2 concentrations in the subarctic Pacific Ocean will continue to decrease during this century, this study has provided an important baseline from which future studies will be able to track changes in seawater N_2O concentrations and fluxes to the atmosphere.

5.1 Introduction

Nitrous oxide (N_2O) is an important atmospheric gas that influences the global environment. In the troposphere, N_2O acts as a greenhouse gas and has a global warming potential more than 300 times that of CO_2 per mole; in the stratosphere N_2O can undergo photochemical reactions that deplete ozone (Crutzen, 1970; de Bie, 2002). The open ocean is a significant net source of N_2O to the atmosphere with an emission rate of approximately 4 Tg N yr^{-1} (IPCC, 2007), or approximately 25% of total global emissions (Nevison et al., 1995). Oceanic N_2O production, as a by-product of microbial nitrogen transformations, is largely regulated by dissolved oxygen (DO) concentrations (Codispoti, 2010).

In the ocean, N_2O is formed via two microbial production pathways—denitrification and nitrification (Bange, 2008). During denitrification, typically restricted to DO concentrations approximately $\leq$5 μmol L^{-1} (Codispoti et al., 2001), N_2O is formed as an intermediate in the last step of the reduction of NO_3^- to N_2, and studies have shown that net N_2O yields may be as high as 2% (Bange et al., 2000). Nitrification on the other hand can occur across a wide range of DO boundaries from oxic to sub-oxic and involves the formation of N_2O as a by-product of the oxidation of NH_4^+ to NO_2^- via the intermediate hydroxylamine (NH_2OH), or by the so-called nitrifier-denitrification process which reduces NO_2^- to N_2O (Stein and Yung, 2003). As DO concentrations decrease from oxic to below sub-oxic (less than approximately 10 μmol O_2 L^{-1}), N_2O yields from nitrification can increase by several orders of magnitude (Bange, 2008; Goreau et al., 1980; Codispoti, 2010). Once sub-oxic conditions are reached, additional factors such as the density of NH_4^+ oxidizing cells (Frame and Casciotti, 2010; Goreau et al., 1980) and

the community composition of NH_4^+ oxidizing organisms (i.e., bacteria versus archea; Santoro et al., 2010, 2011) may also play roles of varying importance in the overall regulation of N_2O production by nitrification. Still, a number of studies have demonstrated that N_2O yields from nitrification appear highly non-linear at low DO concentrations, with N_2O production increasing exponentially (e.g., Codispoti and Christensen, 1985; de Bie et al., 2002; Naqvi et al., 2010). While there is still a great deal of uncertainty surrounding the degree to which N_2O production will increase under reduced DO concentrations and the N_2O producing processes and organisms that will predominate, it certainly seems likely that marine N_2O production will increase to some degree as DO concentrations decrease below a certain threshold. Given the accumulating evidence of diminishing DO concentrations in the oceans that can be attributed to various climatic changes (Keeling et al., 2010; Matear and Hirst, 2003; Plattner et al., 2001; Sarmiento et al., 1998; Whitney et al., 2007) and the known climate warming role of N_2O (de Bie et al., 2002), the potential for increased N_2O production and consequent triggering of ocean-atmosphere feedback mechanisms are of particular concern.

The Northeastern (NE) subarctic Pacific Ocean is one region where DO concentrations at intermediate depths have decreased substantially over the past 50 years (Emerson et al., 2004; Whitney et al., 2007). Whitney et al. (2007) provide a detailed description of the origins of this decrease. An important underlying cause is the influence of the subarctic current (SAC; Fig. 5.1) on intermediate depth water throughout much of the subarctic Pacific Ocean. One of the major sources of DO to intermediate depths of the SAC is the Sea of Okhotsk and surrounding waters in the Northwest (NW) subarctic Pacific Ocean. Here, ice formation and brine rejection causes well-oxygenated water to

sink and flow outwards into the southward flowing Oyashio Current (Keeling et al., 2010; Whitney et al., 2007), which eventually diverges from the coast to form the eastward flowing SAC (Fig. 5.1). Recent surface freshening and atmospheric warming, which have led to a reduction in sea-ice formation, have decreased the amount of DO transport from the Sea of Okhotsk to the SAC and so have played a major role in reducing the DO concentration of intermediate depth water throughout much of the subarctic Pacific Ocean (Andreev and Kusakabe, 2001; Ono et al., 2001; Watanabe et al., 2001). In addition, decreased DO concentrations in the northward flowing California undercurrent (CUC; Fig. 5.1), a result of increased stratification and increased advection of low DO water from the eastern tropical North Pacific Ocean (ETNP) into the CUC, have diminished DO concentrations in the more coastal and continental shelf regions of the NE subarctic Pacific Ocean (Bograd et al., 2008; Whitney et al., 2007).

Although intermediate depth DO concentrations throughout much of the subarctic Pacific Ocean have been decreasing, recent estimates in the NE subarctic Pacific Ocean (Whitney et al., 2007) show that intermediate depth DO concentrations are still higher than those which have been shown to promote substantial increases in N_2O production in field and laboratory studies (i.e., less than approximately 10 μmol O_2 L^{-1} (e.g., Bange, 2008; Goreau et al., 1980; Codispoti, 2010). It is unlikely that intermediate depth DO decreases that have occurred to date in the subarctic Pacific Ocean have resulted in increased N_2O production. DO will continue to decrease, however, and this process may even accelerate because DO concentrations have yet to respond fully to the climatic changes that have occurred so far, and precipitation and surface temperatures in the North Pacific Ocean are forecast to increase during this century (Keeling et al., 2010). In order

to understand the degree to which N_2O production and concentrations in the NE subarctic Pacific Ocean may increase in the future, as DO concentrations decline, it is essential that we first determine the present magnitude and distribution of N_2O concentrations and potential yields within this region. To this end, the present study used opportunistic sampling along the Line P oceanographic transect (Fig. 5.2) to determine the spatial (east-west) and vertical (surface to intermediate depths) distribution of N_2O concentrations in the NE subarctic Pacific Ocean. We have also attempted to quantify the present magnitude of nitrification N_2O yields and identify the source waters that contribute N_2O to the intermediate depths of the NE subarctic Pacific Ocean. Finally, N_2O fluxes from surface waters to the atmosphere were also calculated, providing a baseline estimate from which future studies will be able to quantify the impact that decreases in DO concentrations in the NE subarctic Pacific Ocean may have on atmospheric N_2O fluxes.

5.2 Methods

5.2.1 Sampling Regime

Sampling was conducted along the Line P oceanographic transect (Fig. 5.2) during three different research cruises in the winter (February), spring (June) and late-summer (August) of 2009, from the CCGS *John P. Tully* as part of the Line P sampling program of the Institute of Ocean Sciences, Department of Fisheries and Oceans Canada. During each cruise, samples were collected at stations P4, P12, P16, P20 and P26 (Fig. 5.2). Inclement weather during the winter cruise prevented sampling at station P4. All water samples were collected using Niskin bottles on a Rosette sampler with an attached SeaBird Electronics SBE 911 conductivity, temperature and depth (CTD) profiler.

Sampling was conducted somewhat opportunistically resulting in some asymmetry of sampling depths between cruises and stations, while logistics restricted our deepest sampling depth to 600 m. During the winter cruise, water samples were collected at 0, 10, 20, 30, 40, 75, 100, 150, 300 and 600 m; during the spring and late-summer cruises water samples were collected at depths corresponding to 100, 55, 33, 10 and 1% surface incident irradiance (I_o), determined using an integrated Biospherical QSP-400 L photosythetically active radiation (PAR) sensor and from 75, 150, 300 and 600 m.

5.2.2 Automated CTD Measurements and Dissolved NO_3^- Concentrations

Continuous vertical profiles of temperature and salinity were measured using the CTD profiler, and an attached SeaBird Electronics SBE 43 dissolved oxygen sensor provided continuous vertical measurements of DO concentrations. Density (expressed as σ_θ) was derived from temperature and salinity, and the base of the mixed layer was identified as the depth at which a change of 0.125 σ_θ, relative to the surface, was first observed (Levitus, 1982). Dissolved NO_3^- concentrations were measured fresh at sea using an Astoria-Pacific autoanalyzer, following the Barwell-Clarke and Whitney (1996) protocol. These samples were collected, measured, and made freely available by personnel at the Institute of Ocean Sciences, Department of Fisheries and Oceans Canada.

5.2.3 N_2O Measurements and Sea-to-Air Flux Calculations

Samples for N_2O analysis were collected in 60 ml glass Wheaton bottles (Fisher Scientific No. 03-313-11C). To collect seawater samples, one end of a Tygon tube was attached directly to the Niskin bottle spigot, while the other end was placed near the bottom of the sampling vessel. Seawater was then transferred directly into the Wheaton

bottles using the overflow technique until the sample water had been replaced approximately three times. The Tygon tube was then carefully removed and samples were immediately poisoned with 100 µl of a saturated solution of $HgCl_2$ to stop all biological activity in the bottles. Finally, bottles were capped with thick butyl-septa stoppers (Microliter Analytical prod. No. 20-0025), sealed with aluminum O-rings and stored in the dark at 4°C until analyzed ashore. Care was taken during all stages of sample collection to ensure that no bubbles were introduced into the samples.

Immediately prior to the analysis of N_2O concentrations, each water sample was brought to room temperature, after which dissolved N_2O concentrations were measured using a static headspace equilibrium method. Briefly, 12 ml of seawater were carefully removed from each sample and simultaneously replaced with an equivalent amount of helium gas using a gas-tight syringe. Samples were then shaken vigorously for two hours using an orbital shaker to allow for gas equilibration to the headspace. A 9 ml sub-sample of the headspace gas was then removed and immediately injected into a 9 ml pre-evacuated glass vial (Alltech No. 98548) with a thick butyl-septa stopper (Alltech No. 98697) and sealed with an aluminum O-ring. The N_2O concentration of each sample was then measured by gas chromatography using an electron capture detector ECD on a Shimadzu 2014 GC with a Tekmar 7050 autosampler that accommodates the 9 ml glass vials. A Poropaq Q (80/100) column was used to separate gases with P5 (95% argon and 5% methane) as the carrier gas. Standard curves were derived using a range of N_2O gas standards, 0.22, 1.2 and 2.4 ppm, injected into the pre-evacuated 9 mL vials and treated as above. Finally, N_2O concentrations were calculated using corresponding measurements of in situ temperature and salinity, corrected for temperature and pressure

during the headspace equilibration, following the solubility tables of Weiss and Price (1980). The analytical precision of our N_2O measurements (±7%) was determined from the analyses of 46 duplicate samples collected at varying depths, stations and time. Excess N_2O (ΔN_2O) was calculated as the difference between the N_2O concentration of the sample and the concentration of N_2O at saturation following Eq. (1), where the concentration of N_2O at saturation was considered to be the solubility of N_2O at an atmospheric mole fraction of 322 ppb (i.e., the contemporary atmospheric mole fraction of N_2O over the Pacific Ocean; Ryabenko et al., 2011);

$$\Delta N_2O = [\ N_2O_{measured}] - [N_2O_{saturation}]\ . \quad (1)$$

The sea-to-air flux of N_2O was calculated using Eq. (2), where k_{N_2O} is the piston velocity (m d^{-1}) and C is the concentration of N_2O (µmol m^{-3}) in surface samples and at saturation. The piston velocity was estimated using the Wanninkhof (1992) wind speed model corrected using the appropriate Schmidt scaling (Jähne et al., 1987). Wind speeds were continuously measured onboard the CCGS *John P. Tully* and the corresponding daily averages were used for each of our sea-to-air N_2O flux calculations;

$$\text{Flux} = k_{N_2O}\left(C_{sample} - C_{saturation}\right)\ . \quad (2)$$

5.3 Results and Discussion

5.3.1 Physical Characteristics and Hydrography

The mixed layer (ML) was deepest in winter at all stations (Table 5.1). Following winter, the ML shoaled to minimum depths in spring, after which a slight deepening of the ML was observed at all stations during late summer. The ML temperatures displayed

expected seasonal variability at all stations, with the lowest temperatures in winter, intermediate temperatures in spring, and highest temperatures in late summer (Table 5.1). The seasonal variability of ML salinity was minimal (<0.2%) and no seasonal trends were observed (Table 5.1).

A plot of temperature versus salinity below the permanent pycnocline at each station (i.e., below the winter ML depth) to 600 m (hereinafter referred to as intermediate depth water) showed that although there was some similarity in temperature and salinity characteristics between P26 and P16, both of these variables tended to increase along discrete isopycnals from P26 to P16 (Fig. 5.3). Temperature and salinity at P12, for the most part, and at P4 were distinctly different from the other three stations (Fig. 5.3).

Differences in physical characteristics of intermediate depth water along Line P can be explained by examining the transiting water masses that influence this region. The far offshore regions of Line P (i.e., P26 to P16) are largely influenced by the colder, less saline waters of the SAC (Whitney et al., 2007; Fig. 5.1); however, as the SAC flows from the western to the eastern boundary of the subarctic Pacific Ocean there is some mixing of the warmer, more saline subtropical current (STC; Fig. 5.1) into the SAC (Aydin et al., 2004; Mecking et al., 2006). The observed temperature and salinity increases from P26 to P16 indicate an increasing influence of the STC on the physical characteristics of intermediate depth water east of P26. The SAC and STC eventually diverge northward to form the Alaska current (AC) and southward to form the California current (CC), respectively (Fig. 5.1). East of this divergent region, the CUC, which flows counter to the CC, begins to play an important role in influencing intermediate depth water (Thomson and Krassovski, 2010; Whitney et al., 2007). The CUC undoubtedly

plays a role in influencing the physical characteristics at P4 (Whitney et al., 2007), and mesoscale eddies can transport CUC water far enough west to encompass the longitude of P12 (Collins et al., 2004). For the most part, the temperature and salinity characteristics of intermediate depth water at P12 were found to lie between those of P16 and P4. This indicates that while P12 may show some SAC and STC characteristics, a strong CUC influence also appears likely. Finally, in contrast to biogeochemical signatures, temperature and salinity signals are often lost as CUC water is transported to the ocean interior (Whitney et al., 2007). Thus, the observation that P12 temperature and salinity characteristics began to converge with those at the more westerly stations at isopycnals greater than approximately 26.75 σ_θ (Fig. 5.3), does not necessarily indicate that the effect of the CUC on the physical properties of P12 diminishes at greater depths.

5.3.2 Dissolved Oxygen

The DO concentrations were highest at the surface, decreasing to minimum values at our deepest sampling depths (i.e., 600 m); overall, concentrations ranged from 342 µmol O_2 L^{-1} to a low of 16 µmol O_2 L^{-1} (Fig. 5.4). The DO concentrations observed at intermediate depths for each station were similar to those recently reported within this depth range in the NE subarctic Pacific Ocean (Aydin et al., 2004; Whitney et al., 2007).

The spatial distribution of intermediate depth DO concentrations was examined by plotting the average (all three cruises) DO concentration along isopycnals 26.5 and 27.0 σ_θ at each station. At 26.5 σ_θ, DO concentrations showed little spatial variability between P26 and P12; whereas, at 27.0 σ_θ DO concentrations displayed a decreasing trend from P26 to P12 (Fig. 5.5). At both 26.5 and 27.0 σ_θ, DO concentrations at P4 were substantially lower than at all other stations. The portion of the CUC that influences P4

(i.e., that portion which is not transported offshore to more westerly longitudes) is subject to high vertical organic matter export from overlying waters as a result of high primary production driven by upwelling along the coast from California to British Columbia (Whitney et al., 2005). The resulting elevated rates of remineralization and DO consumption provide an explanation for the low intermediate depth DO concentrations at P4 (Whitney et al., 2007).

5.3.3 Nitrous Oxide

5.3.3.1 Vertical Distribution of Nitrous Oxide

The concentrations of N_2O ranged from 8.6 to 33.1 nmol L^{-1}, and the vertical distribution of N_2O was opposite to that of DO, with the lowest concentrations within the surface waters and the highest values typically occurring at 600 m (Fig. 5.6). Our observation that N_2O reached highest concentrations at the depths at which we recorded minimum DO concentrations is consistent with studies from other oceanic regions (e.g., Butler et al., 1989; Cohen and Gordon, 1979; Oudot et al., 1990; Walter et al., 2006). Concentrations of DO continue to decrease slightly to a minimum of approximately 15 µmol L^{-1} near 1000 m (Line P database, Department of Fisheries and Oceans Canada), and it is therefore likely that N_2O concentrations continue to increase to some degree between 600 m and the core of the oxygen minimum zone (OMZ).

Exceptions to the N_2O depth distributions that were most often observed (i.e., highest N_2O concentrations at 600 m) occurred at P12 and P4 in late summer when concentrations decreased between 300 and 600 m, with P12 displaying the most noticeable decrease (Fig. 5.6). Also noteworthy was the somewhat lower late-summer P12 N_2O concentration at 300 m, compared to winter and spring values. The observed

N_2O decrease between 300 and 600 m at P4 and P12 during late summer seems somewhat anomalous given that all of our other vertical profiles showed an increase between these two sampling depths. Denitrification can both produce and consume N_2O, and N_2O consumption by denitrification at these depths is one possible explanation. This seems unlikely, however, as the late-summer DO concentrations observed at 600 m at P4 and P12 were not low enough to support denitrification (Codispoti et al., 2001).

Another potential explanation is far-field transport of denitrification signals to these two stations. Castro et al. (2001) showed that denitrification signals originating in the ETNP could be detected in the CUC. These enhanced denitrification signals were supported by observations of low N^* values. Given that N^* is simply an indicator of NO_3^- removal by denitrification, rather than N_2 or N_2O production, we are unable to determine whether denitrification in the ETNP results in 1) steady-state N_2O production and consumption, 2) net N_2O production, 3) net N_2O consumption (i.e., removal of N_2O produced by both denitrification and nitrification), or 4) simply lower N_2O production compared to the CUC. Another possibility of course, is that each of these scenarios may dominate at different times depending on the DO concentration in the ETNP. If denitrification in the ETNP results in net losses of N_2O, or even just lower N_2O production than in the CUC at least some of the time, then this could certainly cause periods of lower than normal N_2O concentrations in the CUC, which in turn could translate into lower N_2O concentrations at P12 and P4. Furthermore, the denitrification signals observed in the CUC by Castro et al. (2001) occurred at densities $\geq$26.8 σ_θ, with the peak signal being observed at approximately 27.1 σ_θ. The depth of the 27.1 σ_θ isopycnal at P12 and P4 was approximately 600 m and, therefore, offers an explanation

as to why N_2O concentrations decreased between 300 and 600 m at these two stations. On the other hand, while the late-summer 26.8 σ_θ isopycnal was observed at our P12 300 m sampling depth, it was greater than 50 m below our P4 300 m sampling depth. This could also explain why the 300 m N_2O concentration was notably lower at P12 but not at P4 in late summer. Finally, the strongest denitrification signals in the CUC are often observed west of its core, probably the result of an eastward expansion of the CUC by mesoscale eddies (Castro et al., 2001), and this could explain why the decrease in N_2O concentrations was most notable at P12.

5.3.3.2 Nitrous Oxide in the Mixed Layer

The range of ML N_2O and ΔN_2O (i.e., $[N_2O_{measured}] - [N_2O_{saturation}]$) concentrations reported here represent the mean of all N_2O and ΔN_2O concentrations observed within the ML for each station and cruise. Mean ML (MML) N_2O concentrations ranged from 9.1 ±0.3 to 18.2 ±2.4 nmol L^{-1}, while MML ΔN_2O concentrations ranged from -0.7 ±0.3 to 8.4 ±2.3 nmol L^{-1} (Fig. 5.7). The observation that MML ΔN_2O concentrations were typically positive indicates that the NE subarctic Pacific Ocean acts as a source of N_2O to the atmosphere (discussed further in Section 5.3.3.4).

N_2O yields from nitrification, estimated from the molar ratio of N_2O production to NO_3^- production (i.e., nitrification), in the oxic water masses of the North Pacific Ocean range from 0.004 to 0.027% (Yoshida et al., 1989). Based on measured nitrification rates in the ML along Line P (Grundle et al., in revison[Chapter 3]), and using the nitrification N_2O yields of Yoshida et al. (1989), we estimate that it would require at least 1.5 years for in situ nitrification (i.e., nitrification within the ML) to achieve the average ML ΔN_2O concentration observed during this study. Given that N_2O in the ML exchanges with the

atmosphere within approximately three weeks (Najjar, 1992; Nevison et al., 1995), in situ nitrification is an unlikely primary source of N_2O for the ML. Instead, similar to other studies (e.g., Walter et al., 2004, 2006), we conclude that the primary sources of N_2O to the ML are mixing and diffusive processes that transport N_2O vertically from below the ML (Walter et al., 2004, 2006). This conclusion is supported by the observation that MML ΔN_2O concentrations were positively correlated to the ΔN_2O concentration measured at our closest sampling depth below the ML (p <0.001, R^2 = 0.76; data not shown).

5.3.3.3 Nitrous Oxide at Intermediate Depths

Production of N_2O

Intermediate depth (i.e. below the winter ML depth) N_2O concentrations ranged from 10.4 to 33.1 nmol L^{-1}, and ΔN_2O ranged from -1.3 to 19.9 nmol L^{-1}. The N_2O concentrations that we observed at intermediate depths along Line P were higher than those observed in waters of the South Pacific and South and North Atlantic oceans (10–20 nmol N_2O L^{-1}), lower than those observed in the eastern tropical Pacific Ocean (50–70 nmol N_2O L^{-1}), but similar to those observed in tropical Atlantic waters (25–30 nmol N_2O L^{-1}; see synthesis of oceanic N_2O concentrations in Nevison et al. (2003)).

Given that apparent oxygen utilization (AOU; $[DO]_{saturation} - [DO]_{observed}$) is directly linked to nitrification and by extension N_2O production by nitrification, we used simple linear regression to compare ΔN_2O and AOU, and calculated N_2O yields, per mole, of O_2 consumption from the slope of this relationship. The anomalously low N_2O concentrations at our deepest P12 and P4 sampling depths in late summer (discussed in Section 5.3.3.1) were omitted from the regression to avoid confounding of any possible

relationship between ΔN_2O and AOU. Before discussing these results it is worth noting that Nevison et al. (2003) pointed out that horizontal mixing of different water masses can lead to highly variable ΔN_2O versus AOU slopes, and caution should be taken when pooling data collected over large spatial scales. Despite the fact that our different Line P sampling stations are likely influenced by different water masses, an analysis of covariance (ANCOVA) comparing the linear ΔN_2O versus AOU relationship among stations showed that the slopes of the individual regressions were not significantly different (p >0.05), thus enabling us to pool our data. Still, Nevison et al. (2003) recommend using a two-end member mixing model to remove the effects of isopycnal mixing of water masses with different amounts of preformed N_2O and DO concentrations. This requires an understanding of the effect that varying DO concentrations have on N_2O yields, but the validity of extrapolating laboratory estimates of N_2O yields to the field is questionable given the wide range of reported values (Goreau et al., 1980; Frame and Casciotti 2010; Santoro et al., 2011); therefore, we chose not to attempt to remove preformed N_2O from our bulk N_2O measurements. Hence, the ΔN_2O concentrations and the N_2O yields that we report, should not be considered localized N_2O production values and yields but rather integrated values over the history of the water masses.

Simple linear regression analysis of the pooled data revealed that intermediate depth ΔN_2O concentrations were significantly positively correlated to AOU (Fig. 5.8a). This type of relationship has previously been interpreted as indicating that nitrification is the dominant N_2O formation process (Bange, 2008; Nevison et al., 1995). The slope of the ΔN_2O versus AOU relationship indicates that 21,300 moles of O_2 are consumed per mole

of N_2O produced. This is within the range of estimates of DO consumption per mole of N_2O production reported for other oceanic regions (range, approximately 3000 to 33,000; see summary in Nevison et al. (1995)) and is also similar to nearby estimates from the NE Pacific region off Washington State (Cohen and Gordon, 1979). Based on our estimate of DO consumption per mole of N_2O produced, and following Redfield rationale which attributes approximately 17% of total DO consumption to NH_4^+ oxidation (Ward, 2008), we estimate that N_2O yields from nitrification are approximately 0.028% (i.e., approximately 280 nmol of N_2O are produced for every mole of NH_4^+ oxidized). This is near the upper limit of the N_2O yields reported for oxic North Pacific waters (range, 0.004 to 0.027%; Yoshida et al., 1989) but is far below estimated nitrification N_2O yields originally reported for sub-oxic conditions (up to 10%; Goreau et al., 1980). The nitrification N_2O yields calculated by Goreau et al. (1980) employed cultures with NH_4^+ oxidizing bacteria cell densities far higher than expected under in situ conditions. More recent culture studies, using cell densities more characteristic of those found in situ, estimated that the nitrification N_2O yield under sub-oxic conditions was only approximately 0.05 to 0.07% (Frame and Casciotti, 2010). This estimate, however, was based on only one species of marine NH_4^+ oxidizing bacteria. Furthermore, Santoro et al. (2011) recently demonstrated that NH_4^+ oxidizing marine archaea may be responsible for far more N_2O production than their bacterial counterparts. Therefore, nitrification N_2O yields under natural, sub-oxic, mixed assemblage conditions probably lie somewhere between the upper and lower range of these culture estimates.

If the lower range of DO concentrations (i.e., the higher range of AOU) observed during this study had resulted in higher N_2O yields we would have expected a non-linear

relationship between ΔN_2O and AOU (Punshon and Moore, 2004b; Upstill-Goddard et al., 1999), which was not the case. Although we claim that nitrification is the most probable explanation for the observed linear ΔN_2O versus AOU relationship, Yamagishi et al. (2005) showed that diffusion of N_2O produced by denitrification into more oxygenated waters can result in a similar relationship. Denitrification, however, is likely not important within the water column of our study region, as even the lowest DO concentrations along Line P were greater than 15 µmol L^{-1}, and denitrification is typically limited to DO concentrations approximately less than or equal to 5 µmol L^{-1} (Codispoti et al., 2001). Still, it is possible that denitrification could have occurred within sub-oxic microzones surrounding aggregations of organic particles. Nevertheless, we also found that intermediate depth ΔN_2O concentrations were positively correlated with NO_3 (Fig. 5.8b). The slope of the ΔN_2O versus NO_3^- relationship indicates that 2,500 moles of NO_3^- are produced for every mole of N_2O produced, equating to a nitrification N_2O yield of 0.040% (i.e., 400 nmol of N_2O are produced for every mole of NH_4^+ oxidized to NO_3^-). This result is in close agreement with the nitrification N_2O yield estimated from the ΔN_2O versus AOU relationship, and it provides additional evidence to support our conclusion that N_2O in the NE subarctic Pacific Ocean is largely a product of nitrification (Bange, 2008; Nevison et al., 1995; Walter et al., 2006).

Finally, until we have a more precise understanding of the impact of varying DO concentrations on N_2O production it is difficult to accurately separate far-field N_2O production from more localized N_2O production. This, however, does not prevent us from speculating on the impact of DO losses in the NE subarctic Pacific Ocean, and the water masses that influence it, on bulk N_2O concentrations in this region. In the absence of any

historical data it is difficult to determine whether N_2O yields have increased to any degree in conjunction with declining DO. Based on the linear ΔN_2O versus AOU relationship, however, it certainly appears that nitrification N_2O yields at lower DO concentrations (i.e., higher AOU) in the NE subarctic Pacific Ocean, and the water masses that influence it, have not yet begun to increase exponentially to the extent that might be expected under sub-oxic conditions. If DO concentrations continue to decrease in the water masses that influence the NE subarctic Pacific Ocean, as has been predicted (Keeling et al. 2010), then our results have provided an important baseline from which future studies will be able to track potential increases in N_2O within this region.

Spatial Variations

The spatial variability of intermediate depth ΔN_2O was investigated by examining the average (all three cruises) ΔN_2O concentration along isopycnals 26.5 and 27.0 σ_θ (Fig. 5.9). In the majority of cases our sampling depths did not precisely match these discrete isopycnals, obliging us to use linear interpolation between sampling depths to estimate the ΔN_2O concentration that corresponded to 26.5 and 27.0 σ_θ. The highest degree of seasonal variability was found at P12 on the 27.0 σ_θ isopycnal, which can be attributed to the previously discussed anomalously low late-summer P12 ΔN_2O concentration at 600 m (Section 5.3.3.1). A general spatial trend along isopycnals was still evident despite the high degree of variability associated with P12. Along both the 26.5 and 27.0 σ_θ isopycnals, average ΔN_2O concentrations tended to decrease from P26 to P16. East of P16, ΔN_2O concentrations increased at P12 and P4. The finding that P26 ΔN_2O concentrations were higher than those at P20 and P16 was somewhat surprising given that we have demonstrated that ΔN_2O and AOU were positively correlated and that

between these stations AOU showed minimal variability along the 26.5 and 27.0 σ_θ isopycnals (Fig. 5.5). The similarity of ΔN_2O concentrations at P12 and P4 was also unexpected given that AOU increased substantially from P12 to P4 (Fig. 5.5).

We demonstrated earlier that there were no differences between the slopes of the ΔN_2O versus AOU relationships and, therefore, between estimates of nitrification N_2O yield, between stations along Line P. It is unlikely that the higher than expected ΔN_2O concentrations at P26 and P12 were simply a result of higher integrated nitrification N_2O yields to these stations. Instead, we consider the possibility that far-field denitrification processes, which could influence N_2O concentrations without modifying DO concentrations, may have caused the unexpected spatial distribution of intermediate depth ΔN_2O concentrations. Given that the water masses that influence P26 to P16 and P12 to P4 are at least somewhat different, each of these two spatial regions will be discussed separately.

Stations P26 to P16 are largely influenced by the SAC and STC. Following the formation of intermediate depth water in the Sea of Okhotsk, this water can come into contact with denitrifying shelf sediments, whose biogeochemical signatures have been observed in the overlying water column (Yoshikawa et al., 2006). Net N_2O production by benthic denitrification could therefore introduce additional N_2O into the SAC, which in turn could result in higher N_2O concentrations at P26. As the SAC transits farther east towards P20 and P16, this signal would be diluted to some extent as more STC water mixes with the SAC. This scenario could, therefore, explain why intermediate depth water at P26 was characterized by higher ΔN_2O concentrations compared with P20 and P16, despite there being very little difference in AOU among these three stations.

Stations P12 and P4 are, at least in part, both influenced by the CUC. As we discussed earlier (Section 5.3.3.1), denitrification signals originating in the ETNP are transported into the CUC, and we concluded that N_2O consumption by denitrification may have resulted in lower N_2O concentrations at P12 and P4 during late summer. Net N_2O losses from denitrification, however, only occur under extremely low sub-oxic conditions, otherwise denitrification tends to result in a net production of N_2O (Devol, 2008; Punshon and Moore, 2004b). Thus, it is possible that, at times, denitrification in the ETNP can also result in net accumulations of N_2O as DO concentrations fluctuate, and this could translate into periodically higher N_2O concentrations at P12 and P4. Furthermore, as we discussed earlier (Section 5.3.3.1), denitrification signals are often highest west of the CUC core (Castro et al., 2001), and this may translate into a stronger signal at P12 than at P4. This would explain why ΔN_2O concentrations were somewhat similar at P12 and P4, even though AOU was considerably greater at P4 than at P12.

Finally, if benthic denitrification in the NW subarctic Pacific Ocean and water column denitrification in the ETNP do at times augment N_2O concentrations in the NE subarctic Pacific Ocean this should not alter our earlier interpretation of the ΔN_2O versus AOU relationship. The transit times of the SAC from the NW subarctic Pacific Ocean to P26 and of the CUC from the ETNP to P12 and P4 are approximately 5–7 (Ueno and Yasuda, 2003; Whitney et al., 2007) and greater than 3 years (Castro et al., 2001), respectively. Gases diffuse across boundaries from high to low concentrations. Given the transit time of the SAC and CUC it, therefore, seems reasonable that at least some of the additional N_2O added to these water masses by denitrification would have diffused upwards, essentially causing the denitrification signals to be vertically homogenized

through the water column. Thus, any N_2O added to the SAC and CUC through far-field denitrification should not have impacted the slope of the previously described ΔN_2O versus AOU relationship significantly. Any N_2O which was added without modifying DO concentrations (i.e., N_2O from far-field denitrification) would, however, have impacted the *y*-intercepts of station specific ΔN_2O versus AOU relationships. Indeed, station specific simple linear regressions of the data shown in Fig. 5.8a, showed that the *y*-intercepts of the ΔN_2O versus AOU relationships were highest at P26 and P12 (Table 5.2), the two stations we speculate may have been influenced the most by denitrification.

5.3.3.4 Nitrous Oxide Fluxes to the Atmosphere

Estimates of N_2O fluxes from the surface layer of the ocean to the atmosphere (N_2O emissions) are largely dependent on the wind speeds that were measured on each of our sampling dates. Although wind speeds are typically higher along Line P in winter, it is possible for high wind speed events to occur during spring and late-summer cruises (personal observation). Given our sampling regime, it is possible that we may have missed important wind events. This makes it difficult to compare seasonal N_2O emission rates for each station based on single, time-point measurements. Instead, we simply present the average (all three cruises) N_2O emission rate for each station.

Average N_2O emission rates ranged from a low of 0.05 ±0.01 mol km^{-2} d^{-1} at P4 to a high of 11.12 ±8.54 mol km^{-2} d^{-1} at P12 (Fig. 5.10), and the regionally averaged Line P emission rate was 4.37 ±4.20 mol N_2O km^{-2} d^{-1}. The regionally averaged Line P N_2O emission rate was approximately twice the regionally averaged rate calculated for the Bering Sea by Hirota et al. (2009). The relative distribution of N_2O emission rates between the Bering Sea (Hirota et al., 2009) and Line P (this study) is similar to the

north-south N_2O distributions modelled by Nevison et al. (1995) for these latitudinal regions. Our regionally averaged N_2O emission rate was also higher than the estimated global average seawater N_2O emission rate per square kilometre. The total N_2O emission rate from seawater to the atmosphere has been estimated at approximately 4 Tg N yr^{-1} (IPCC, 2007; Nevison et al., 1995). Accounting for the area of the world's oceans, this equates to an average flux of 375 mol N_2O km^{-2} yr^{-1} or 1.03 mol N_2O km^{-2} d^{-1}, thus demonstrating that N_2O emissions from the subarctic Pacific Ocean are higher than regionally scaled global emissions. Estimates from coastal regions provide a broader perspective for the potential importance of the NE subarctic Pacific Ocean as a source of N_2O to the atmosphere. The coastal ocean has long been recognized as an important source of N_2O to the atmosphere, because total N_2O emissions from coastal areas are disproportionately high (Codispoti et al., 2001; Nevison et al., 2004). Despite coastal regions only accounting for approximately 18% of the total ocean area (Punshon and Moore, 2004a), they may be responsible for as much as 45% of the total N_2O emissions from seawater to the atmosphere (Nevison et al., 2004). This results in a coastal average N_2O emission rate of 940 mol km^{-2} yr^{-1} or 2.57 mol km^{-2} d^{-1}, once again highlighting the importance of the NE subarctic Pacific Ocean as a potential hotspot for marine N_2O emissions to the atmosphere.

5.4 Conclusions

This study is the first to report water column N_2O concentrations and emission rates for the Line P region of the NE subarctic Pacific Ocean and its findings have provided critical insights into the magnitude and distributions of N_2O concentrations and emission rates within this region. Results from this study indicate that

- N_2O in the water column of the NE subarctic Pacific Ocean is largely a product of nitrification;
- N_2O yields from nitrification in the NE subarctic Pacific Ocean and the water masses that influence this region are approximately 0.028–0.040%;
- the NE subarctic Pacific Ocean is an important source of N_2O to the atmosphere and the Line P regional average emission rate is higher than the regionally scaled global or coastal N_2O emission rates from seawater; and
- N_2O yields from nitrification are still within the range expected for oxic conditions, and this may indicate that despite the DO losses that have occurred so far in the NE subarctic Pacific Ocean and the water masses that influence it, nitrification N_2O yields have not yet begun to increase substantially. An absence of historical data impedes more definitive conclusions.

Tables

Table 5.1. Depth of 1% I_o (i.e. base of the euphotic zone), mixed layer (ML) depth, ML temperature and ML salinity.

Characteristic	Station	Cruise		
		Winter	Spring	Late Summer
1% I_o depth (m)	P4	_	27	25
	P12	_	57	65
	P16	_	61	64
	P20	_	46	64
	P26	_	46	62
ML depth (m)	P4	55	14	15
	P12	112	21	25
	P16	102	16	38
	P20	103	16	41
	P26	121	24	36
ML Temperature (°C)	P4	7.61	12.62	12.91
	P12	7.60	11.05	15.81
	P16	6.86	10.79	15.47
	P20	6.33	10.21	13.34
	P26	6.01	9.08	12.47
ML Salinity	P4	32.17	32.11	32.21
	P12	32.46	32.43	32.28
	P16	32.43	32.46	32.49
	P20	32.48	32.50	32.48
	P26	32.57	32.56	32.47

Table 5.2. Individual linear regression y-intercept values (± standard error) for the ΔN_2O vs. AOU relationships at stations P4, P12, P16, P20 and P26.

	Station				
	P4	P12	P16	P20	P26
y-intercept	-2.35 ±2.20	2.79 ±2.18	-3.24 ±0.95	-0.57 ±0.68	1.85 ±1.63

Figures

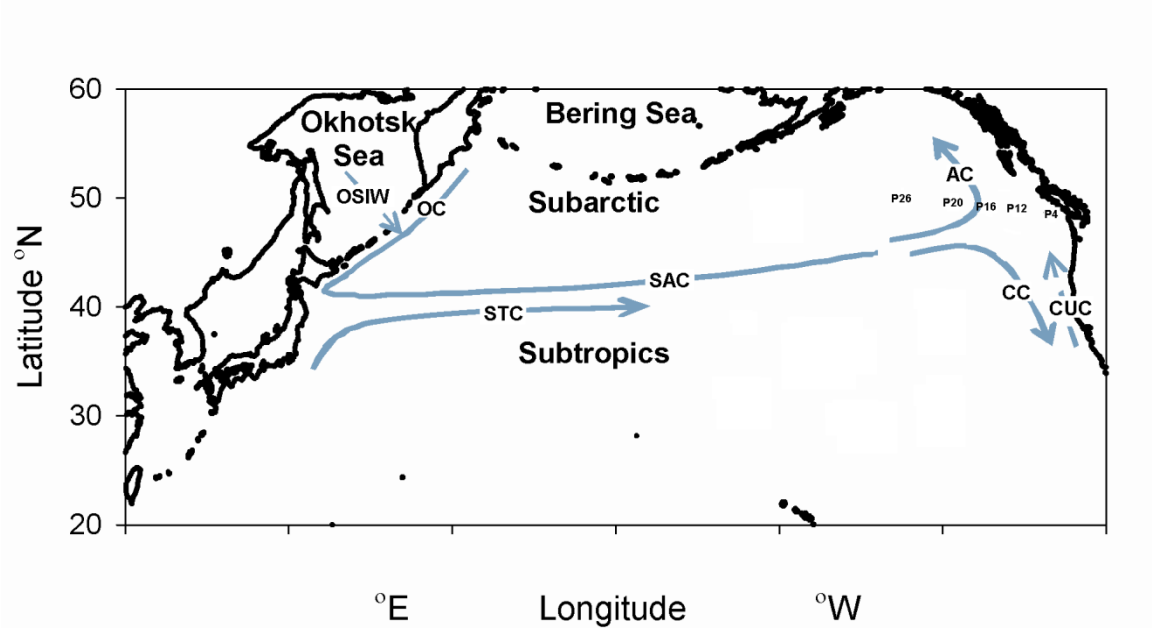

Figure 5.1. Map of the North Pacific Ocean showing major currents (OC, Oyashio Current; SAC, subarctic current; STC, subtropical current; AC, Alaska Current; CC, California Current) and the location of our Line P sampling stations (Whitney et al., 2007). Also shown is the SOIW (Sea of Okhotsk Intermediate Water) which flows into the Oyashio Current, and the northward flowing CUC (California Under Current).

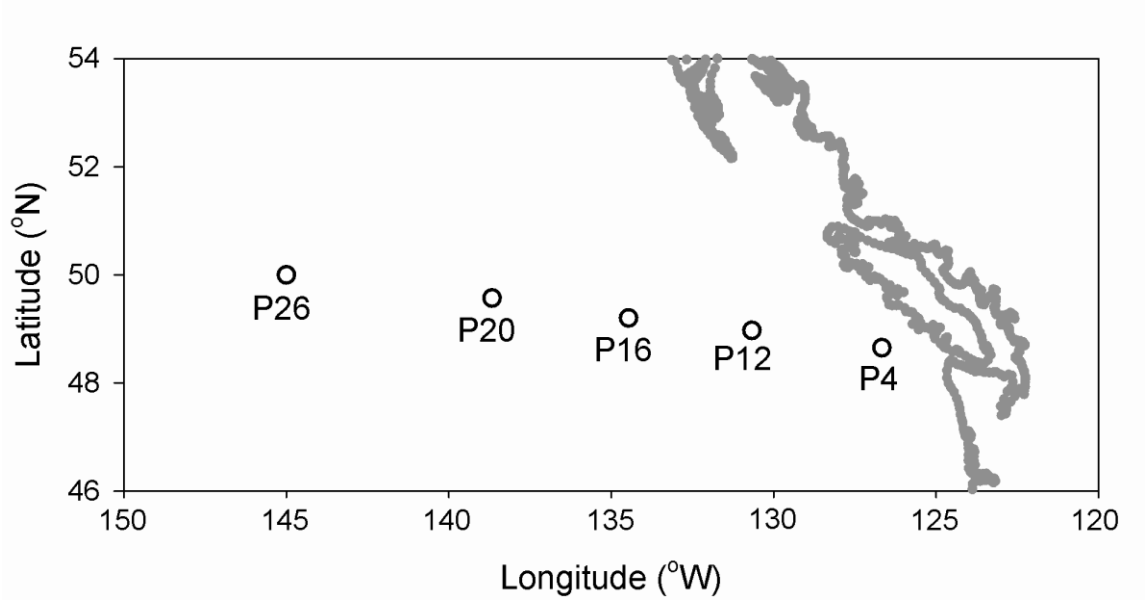

Figure 5.2. Map of the NE subarctic Pacific Ocean showing the locations of the major Line P sampling stations.

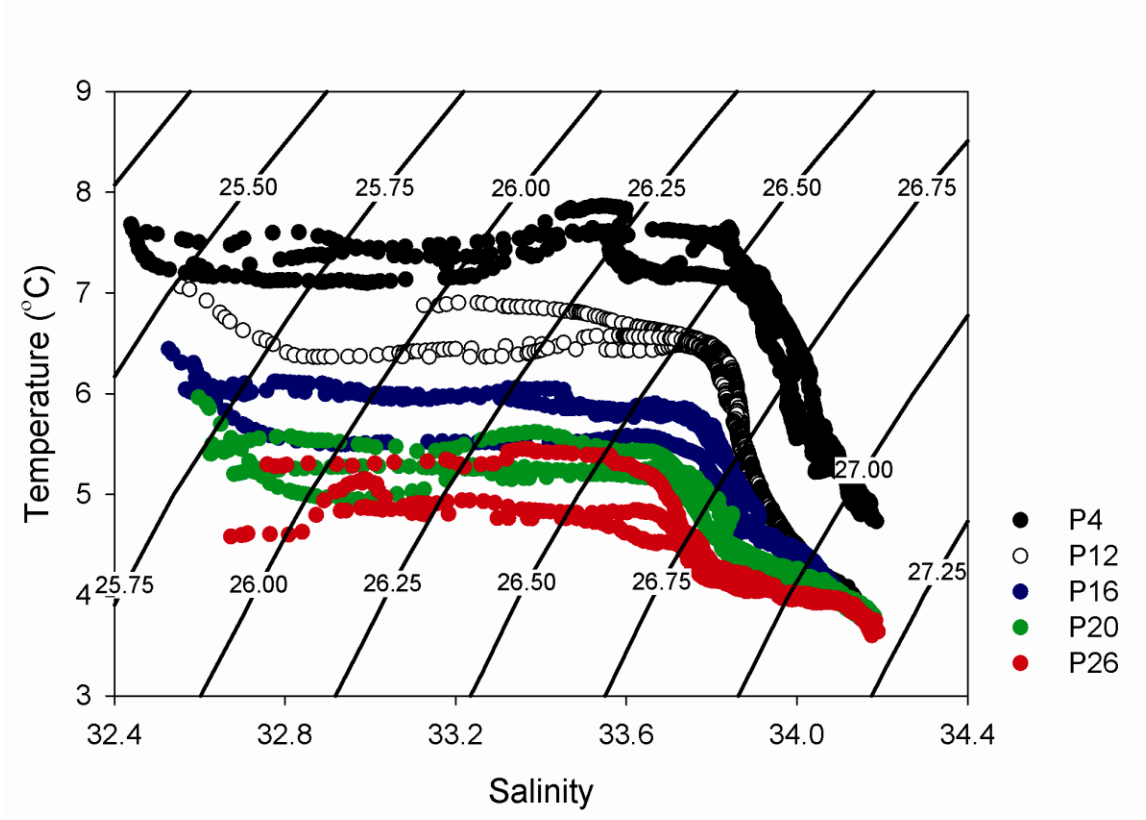

Figure 5.3. Plot of temperature versus salinity for intermediate depth water at stations P4, P12, P16, P20 and P26.

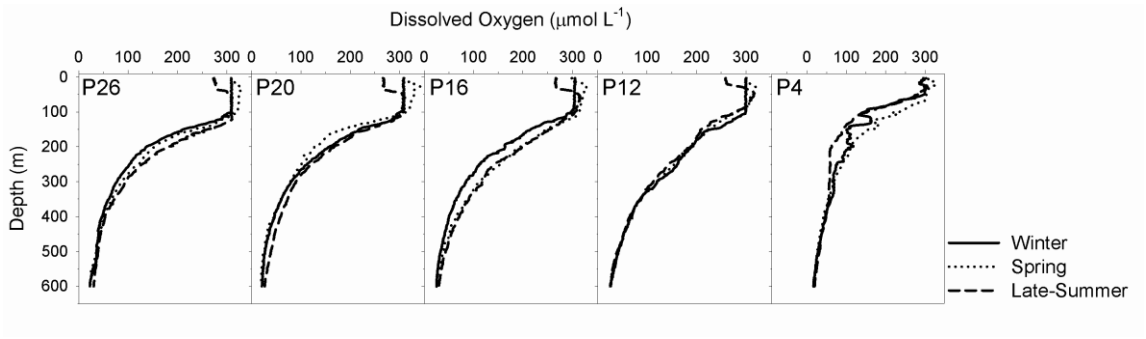

Figure 5.4. Vertical profiles (surface to 600 m) of dissolved oxygen concentrations for stations P4, P12, P16, P20 and P26 during winter, spring and late summer.

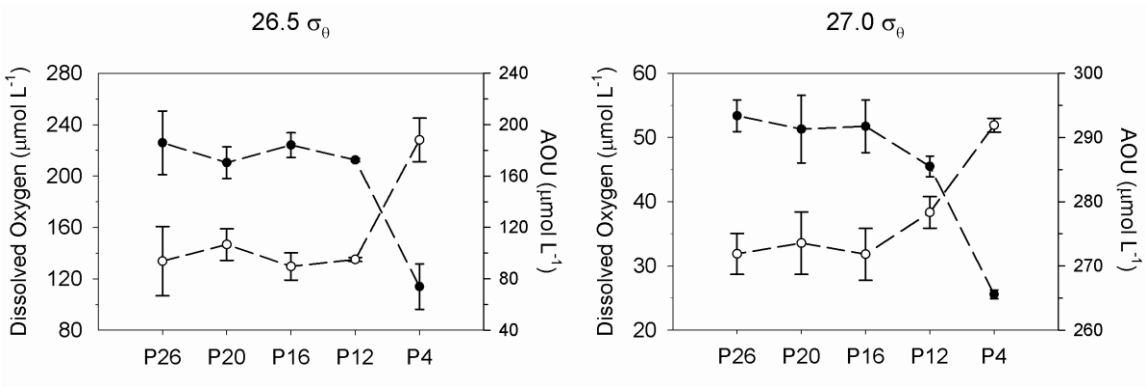

Figure 5.5. Average (all three cruises) dissolved oxygen (closed circles) and apparent oxygen utilization (AOU; open circles) concentrations along isopycnals 26.5 σ_θ and 27.0 σ_θ, at stations P4, P12, P16, P20 and P26.

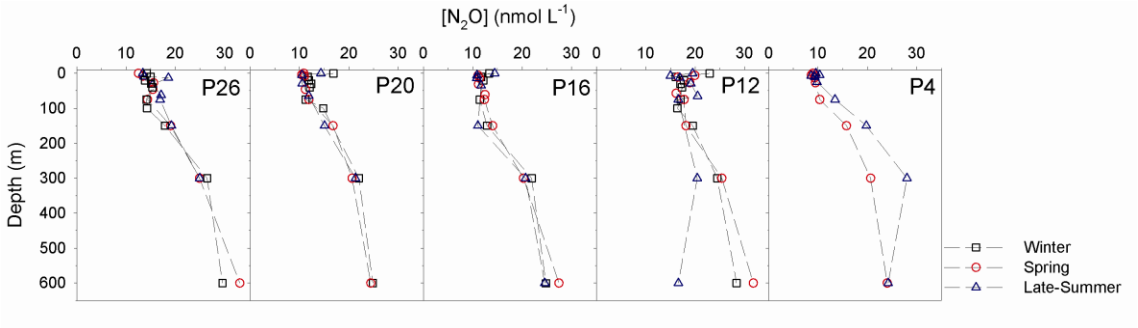

Figure 5.6. Vertical profiles of N_2O concentrations at discrete sampling depths from the surface to 600 m, for stations P4, P12, P16, P20 and P26 during winter, spring and late summer.

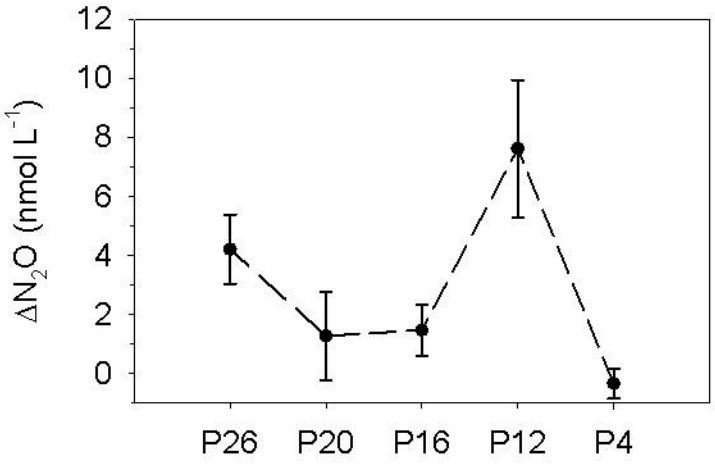

Figure 5.7. The average (all three cruises) mean mixed layer ΔN_2O concentration at stations P4, P12, P16, P20 and P26.

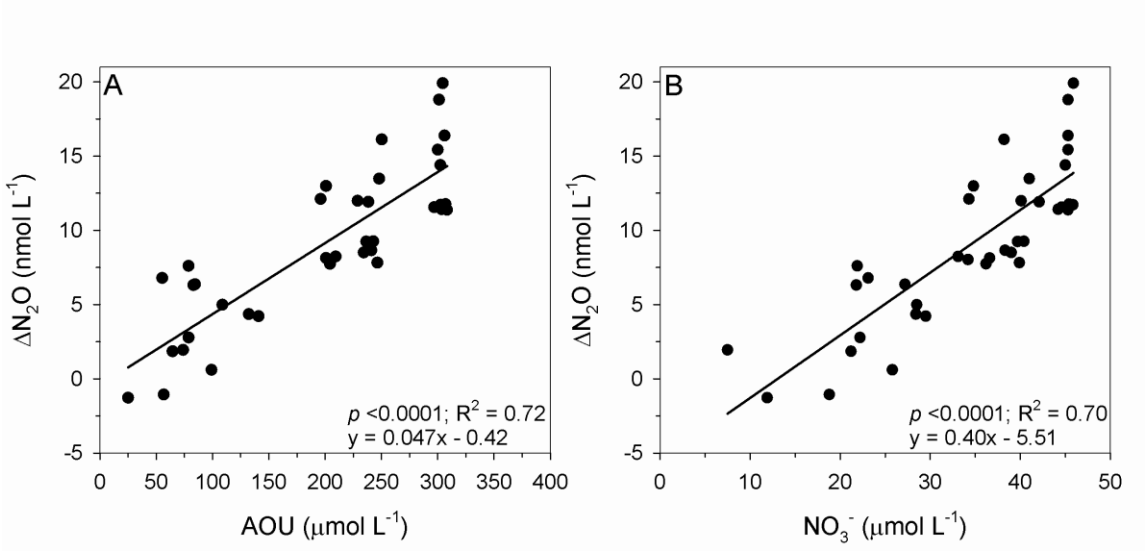

Figure 5.8. Plots of (a) ΔN_2O versus apparent oxygen utilization (AOU) and (b) ΔN_2O versus NO_3^- concentrations (data from all stations and cruises pooled). The solid lines are linear regressions and the results of the linear regression analyses are shown in the lower right corner of each plot.

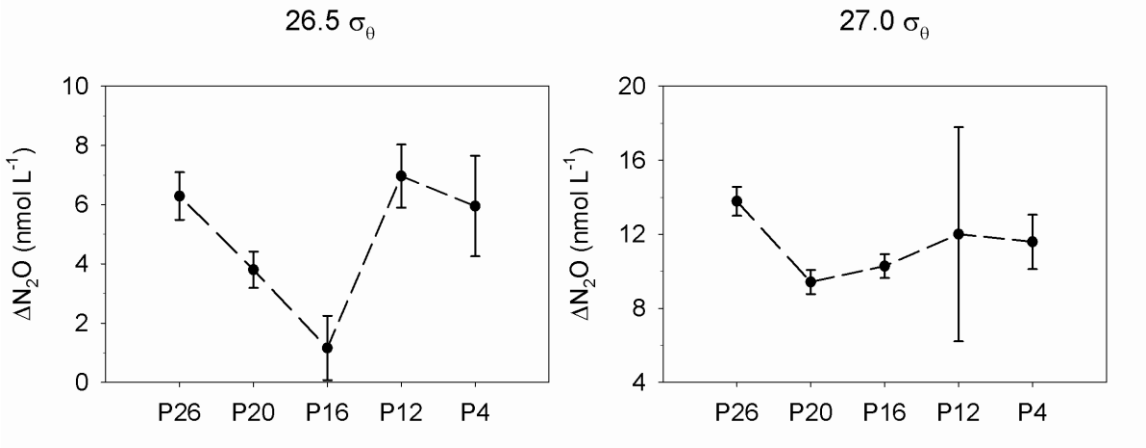

Figure 5.9. Average (all three cruises) ΔN_2O concentrations along isopycnals 26.5 σ_θ and 27.0 σ_θ, at stations P4, P12, P16, P20 and P26.

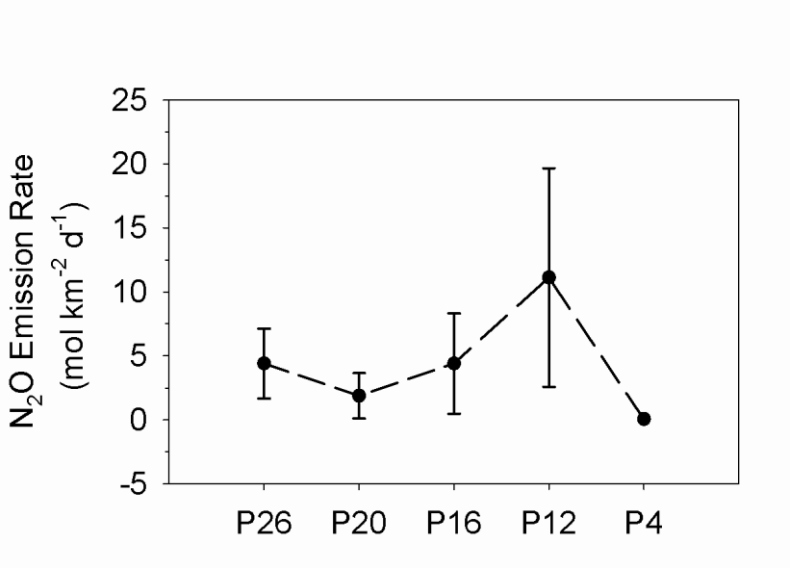

Figure 5.10. Average (all three cruises) N_2O emission rates at stations P4, P12, P16, P20 and P26.

Chapter 6 : Conclusions and Further Discussion

6.1 Summary of Main Findings

Chapter 2: Nitrification from the lower euphotic zone to the sub-oxic waters of a highly productive British Columbia fjord

- NH_4^+ and NO_2^- oxidation rates are, at least some of the time, controlled by substrate concentration.
- NO_2^- oxidation can exceed NH_4^+ oxidation, possibly due to additional NO_2^- supply to Saanich Inlet during spring-tide nutrient renewal events.
- The combined activity of NH_4^+ and NO_2^- oxidation is responsible for ~25% of dissolved oxygen consumption.
- The failure to consider euphotic zone nitrification may have resulted in new production being overestimated by ~15%.

Chapter 3:Euphotic zone nitrification in the NE subarctic Pacific: Implications for measurements of new production

- NH_4^+ oxidation is capable of proceeding throughout the euphotic zone, year-round, and in waters adjacent to the continental shelf to open ocean environments.
- Light plays an important role in controlling NH_4^+ oxidation, with rates increasing as relative light intensity decreases.
- Substrate availability has a positive influence on NH_4^+ oxidation rates, and this influence appears to be stronger in winter when daylight and incident irradiance are lower than in spring or late-summer.
- Potential NO_3^- regeneration within the euphotic zone could have supported between 3 and 100% of the contemporaneous phytoplankton NO_3^- requirements, and thus, the failure to recognize the role that nitrification plays in regenerating

NO_3^- within the euphotic zone could lead to gross overestimates of new production and potential carbon export.

- The relative magnitude by which new production estimates are reduced when taking potential euphotic zone NO_3^- regeneration into account increases exponentially as total NO_3^- uptake decreases.

Chapter 4: Euphotic zone nitrification in the Sargasso Sea: Implications for measurements of new production

- NH_4^+ oxidation is capable of proceeding throughout the euphotic zone even in oligotrophic sub-tropical waters.
- Light plays an important role in controlling NH_4^+ oxidation, with rates increasing as relative light intensity decreases.
- Based on the positive relationship between NH_4^+ oxidation rates and particulate organic nitrogen concentrations, I suggest that the rate of NH_4^+ supply also plays a role in controlling NH_4^+ oxidation rates, and that these two processes are likely to be tightly coupled.
- Potential NO_3^- supply by euphotic zone nitrification plays an important role in controlling phytoplankton NO_3^- uptake rates, at least during the Sargasso Sea oligotrophic period.
- Euphotic zone nitrification potentially supported between 62 and 100% of the contemporaneous phytoplankton NO_3^- requirements, and failure to recognize the importance of *in situ* nitrification as a source of NO_3^- to the euphotic zone could lead to new production and potential carbon export being substantially overestimated.

Chapter 5: Upper water column nitrous oxide distributions in the northeast subarctic Pacific Ocean

- N_2O in the water column is largely a product of nitrification.
- N_2O yields from nitrification in the NE subarctic Pacific and the water masses that influence this region are ~0.028 to 0.040%.
- The NE subarctic Pacific is an important source of N_2O to the atmosphere and the Line P regional average emission rate is higher than regionally scaled global or coastal N_2O emission rates from seawater.
- N_2O yields from nitrification are still within the range expected for oxic conditions, and this may indicate that despite the dissolved oxygen losses that have occurred so far in the NE subarctic Pacific Ocean and the water masses that influence it, nitrification N_2O yields have not yet begun to increase substantially.

6.2 Further Discussion

6.2.1 Chapters 2-4

The research presented in these chapters has provided a significant contribution to the understanding of various factors which can control water column nitrification rates in marine environments. The observation that NH_4^+ oxidation is at least partially controlled by light is of particular importance. Yool et al. (2007) applied the results from a compilation of nitrification studies to a global new production model in order to assess the degree to which new production may have been overestimated on a global scale. While their results provided an excellent baseline understanding of the extent by which

global new production may have been overestimated, there are at least two potential sources of errors that may have arisen.

The first potential source of error which may have been introduced into the model study of Yool et al. (2007) is related to assumptions made about the role of light. Firstly, based on their compilation of upper 250 m depth NH_4^+ oxidation rate data, Yool et al. (2007) found no clear increase in nitrification with increasing depth and alluded to the conclusion that light did not play an important role in controlling nitrification. Two of the four most systematic studies of oceanic nitrification through the euphotic zone are presented in this thesis (Chapters 3 and 4), while the others were conducted by Diaz and Raimbault (2000) and Ward (2005). Collectively, these four studies have conclusively demonstrated that light does indeed affect the rate at which nitrification proceeds through the euphotic zone in four very distinct oceanographic regions (i.e. NE subarctic Pacific [Chapter 3]; Sargasso Sea [Chapter 4]; NW Mediterranean [Diaz and Raimbault 2000]; Monterey Bay [Ward 2005]). There are two principle reasons which may explain why Yool et al. (2007) did not observe an increase in nitrification rates with increasing depth in their data compilation, and neither reflect an inherent failure of the study itself as euphotic zone nitrification rate data are, and were in particular at the time of their paper, sparse at best. The first reason may arise from the fact that a large portion of the nitrification rate data available to Yool et al. (2007; nine studies in total) were measured at depths near or at the 1% I_o depth (in some cases below it), thus making it difficult to detect a relationship between nitrification and light. The second, and perhaps most important reason, is probably related to the use of data collected across distinct oceanographic regimes. As I have demonstrated in this thesis, nitrification rates can vary

substantially, and thus, detecting a relationship between nitrification rates and light (or increasing depth) may not always be possible when pooling data across large spatial scales where NH_4^+ oxidation rates span several orders of magnitude. The second potential source of error which may have been introduced into the Yool et al. (2007) model is linked to assumptions made about the relationship between NH_4^+ oxidation and substrate concentration. The authors scaled their NH_4^+ oxidation rates against substrate concentrations, such that NH_4^+ oxidation proceeded at a constant substrate specific rate ($0.2\ d^{-1}$). As I have shown in this thesis, and as Yool et al. (2007) themselves recognize, applying a constant specific rate may not be appropriate. Moreover, as I discussed in Chapter 4, and as Clark et al. (2008) have demonstrated, the rate of NH_4^+ supply may, at times, be more important than the size of the ambient substrate pool. This, however, would have probably added a level of complexity to the Yool et al. (2007) model that could not be adequately addressed.

At the outset of my Ph.D. research my primary goals were to assess how ubiquitous and important euphotic zone nitrification is when considered in a broad oceanographic sense, and quantify the magnitude to which it may contribute to phytoplankton NO_3^- requirements and the extent by which new production may have been overestimated. Based on the results reported in Chapters 2, 3 and 4, I conclude that euphotic zone nitrification is indeed a ubiquitous process in the ocean, and that it can proceed at rates high enough to support large fractions of phytoplankton NO_3^- requirements. This latter point highlights the extent to which new production in the ocean may have been overestimated when following the traditional assumption of no euphotic zone nitrification. As pointed out in Chapter 3, it is critical that we revise the "*rather stagnated*

view that all euphotic zone NO_3^- represents a source of new nitrogen which has been mixed upwards from the aphotic region of the water column". Future studies of new production should incorporate measurements, or at least estimates, of euphotic zone nitrification into their calculations.

Results pertaining to the extent to which new production is reduced, when euphotic zone NO_3^- regeneration is taken into consideration, have provided a significant contribution to our understanding of upper water column nitrogen cycling and will allow for new and more accurate interpretations of past NO_3^- uptake studies. This is particularly relevant in the case of studies in oceanographic time-series regions which have helped shape our view of marine nitrogen cycling. Another especially intriguing finding was the relationship between the percent by which new production was reduced (%NP-reduction) when considering euphotic zone nitrification, and the overall magnitude of depth-integrated phytoplankton NO_3^- (DI-NO_3^-) uptake rates shown in Chapter 3 (Fig. 3.10). If this type of inverse relationship holds true when data from other regions are incorporated, it may provide another means of modeling the implications of euphotic zone nitrification for estimates of new production. To test this, I pooled data from Chapters 2, 3 and 4 to assess the %NP-reduction vs. NO_3^- uptake relationship that results from the use of data spanning distinct oceanographic regimes. In addition, simultaneous measurements of NO_3^- uptake and %NP-reduction from the NW Mediterranean Sea were also incorporated (Clark et al. 2008). Because NO_3^- uptake rates were not measured during the Saanich Inlet study (Chapter 2), I simply used the mean DI-NO_3^- uptake rate calculated by Grundle et al. (2009) for Saanich Inlet, in conjunction with the %NP-reduction estimated by Grundle and Juniper (2011[Chapter 2]). The exponential decay relationship between

the %NP-reduction and DI-NO_3^- uptake remains significant (p <0.001, R^2 = 0.57; Fig. 6.1), and thus promising, when data from Saanich Inlet, Line P, BATS, and the NW Mediterranean Sea are pooled. It is important to point out, however, that this dataset has a disproportionately larger number of %NP-reduction estimates calculated for the lower end of the DI-NO_3^- uptake range, and it will be interesting to see if this relationship holds when more data from the higher end of the DI-NO_3^- uptake range are included.

Future Recommendations: Given the potential for euphotic zone nitrification to support large fractions of phytoplankton NO_3^- requirements, particularly in regions of relatively low NO_3^- based production, it is imperative that future new production studies account for *in situ* regenerated NO_3^-. For large scale spatial comparisons of new production, a simple estimate based on the %NP-reduction vs. NO_3^- uptake relationship shown in Figure 6.1 may be sufficient. However, given the dearth of results available for regions where NO_3^- uptake rates are >2 mmol m^{-2} d^{-1}, this relationship should be used with caution until more data from regions of higher NO_3^- based production are obtained, and a determination can be made as to whether this relationship holds true. For regions where NO_3^- based production is generally low (i.e. <2 mmol m^{-2} d^{-1}) substantially more data are available (n = 14), and the mean %NP-reduction of the results shown in Figure 6.1 is 75 ±20%. Thus, in regions where NO_3^- based production is low, and where simultaneous euphotic zone nitrification rates are not available, a 75% reduction correction should be applied as long as the error associated with this correction is recognized. For comparison of new production rates at high spatial and temporal resolution scales, or between phytoplankton groups, as has been done through the use of high sensitivity ^{15}N detection combined with flow cytometric sorting (e.g. Casey et al.

2007; Lomas et al. 2011), it will be necessary to conduct direct, contemporaneous measurements of euphotic zone nitrification. The inhibitor based approach I used to measure nitrification rates is well established and has been used under a number of oceanic conditions including the euphotic zone (e.g. reviews by Ward 2005, 2011), and it allows rapid assessment of nitrification rates without the need to perturb substrate concentrations, as is the case with ^{15}N-tracer techniques. Still, given the recent discovery of NH_4^+ oxidizing archaea (Könneke et al. 2005) and the even more recent recognition that ATU may not completely inhibit these organisms (Santoro et al. 2010), I recommend the use of ^{15}N-tracer techniques to obtain the most accurate nitrification measurements. As pointed out above, the principle source of error with the use of ^{15}N-methodology to measure NH_4^+ oxidation is the need for isotope, and thus substrate, enrichment. This has been of particular concern in oligotrophic regions where "trace" additions of ^{15}N-labeled NH_4^+ are not possible. Advances in the sensitivity of ^{15}N detection by mass spectrometry over the past several years, however, have recently begun to alleviate this problem (Ward 2011). Future studies should also be aimed at better understanding the importance of NH_4^+ oxidizing archaea under natural, mixed assemblage conditions. It is currently thought that the relative importance of NH_4^+ oxidizing archaea vs. bacteria is greatest in the oxycline (Santoro et al. 2010). Löescher et al. (2012) recently successfully employed a specific archaea inhibitor to determine the relative contribution of NH_4^+ oxidizing bacteria vs. archaea to N_2O production. Applying this type of approach in combination with ^{15}N methodology to measure NH_4^+ oxidation by bacteria and by bacteria+archaea will greatly improve our understanding of the role that archaea play in oxidizing NH_4^+ under different environmental conditions.

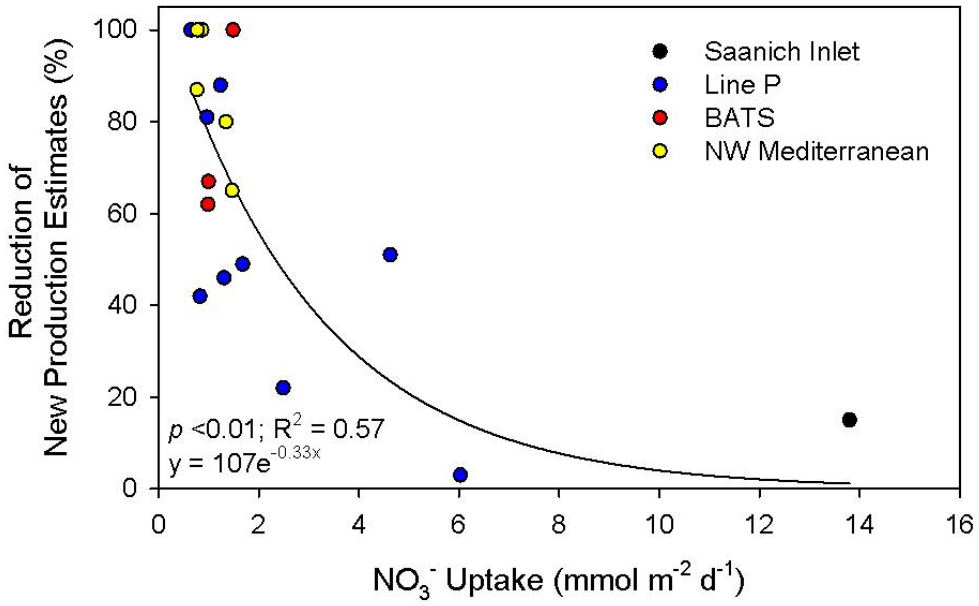

Figure 6.1. The relationship between the relative reduction of depth-integrated new production estimates and depth-integrated NO_3^- uptake rates from Saanich Inlet (NO_3^- uptake rates from Grundle et al. 2009; relative reduction of depth-integrated new production estimate from Grundle and Juniper 2011 [Chapter 2]), Line P (Grundle et al. in revision [Chapter 3]), BATS (Grundle et al. in prep [Chapter 4]), and the NW Mediterranean (Clark et al. 2008). The solid line is an exponential decay regression of the pooled data.

6.2.2 Chapter 5

Measurements of the distribution, magnitude and potential production of N_2O in the NE subarctic Pacific have provided an important baseline, from which future studies will be able to track potential changes in these parameters as dissolved oxygen in the NE subarctic Pacific continues to decrease through this century. Because of the nature of our

measurements (i.e. bulk N_2O pools), however, I was restricted to estimating N_2O production over the integrated history of the water mass, rather than regionally specific N_2O production rates. Furthermore, while I concluded that nitrification was primarily responsible for the bulk of NE subarctic Pacific N_2O pools, I also recognized that far-field denitrification in the sediments of the NW subarctic Pacific and in the water column of the eastern tropical N Pacific could have caused some of the unexpected variability in N_2O concentrations and in the ΔN_2O:AOU ratios.

Future recommendations: Future studies should aim to address some of the unresolved issues alluded to above. For example, what are the regionally specific N_2O production rates in the NE subarctic Pacific, and does far-field denitrification, or even localized denitrification in sub-oxic microzones surrounding particle aggregates play a role in N_2O production or removal in the NE subarctic Pacific and the water masses that influence it? Incubation measurements using ^{15}N tracer methodology will help to identify the importance of different N_2O production pathways at specific locales in the NE subarctic Pacific (Kool et al. 2011), however, they will not provide any indication of the N_2O production pathways that have contributed to the NE subarctic Pacific N_2O pools away from this region. Instead, because of differential kinetic isotope fractionation by the various N_2O producing pathways, isotope ($\delta^{15}N$ and ^{18}O) and isotopomer (i.e. the site preference of ^{15}N in the linear N-N-O molecule, defined as defined as $^{15}N^{\alpha}$-$^{15}N^{\beta}$) measurements of bulk N_2O pools will help identify the contribution of different N_2O producing pathways over the integrated history of the different water masses (Hirota et al. 2010; McIlvin and Casciotti 2010; Toyoda et al. 2005; Yoshida and Toyoda 2000). Work of this nature, conducted in the NE subarctic Pacific and in the water masses that influence it, would significantly improve our understanding of 1) the different production pathways that

contribute to the NE subarctic Pacific bulk N_2O pool, and 2) the relative importance of different water masses as "transport" sources of N_2O into the NE subarctic Pacific. Finally, given the important role that N_2O plays in atmospheric warming, and the prediction that dissolved oxygen concentrations will continue to decline through this century (Keeling et al. 201), it is imperative we gain a better understanding of the role that dissolved oxygen plays in controlling N_2O production via each of the different N_2O producing pathways (i.e. nitrification, nitrifier-denitrification, and denitrification). It has recently been shown that early culture studies (e.g. Goreau et al. 1980) probably overestimated the impact that decreasing dissolved oxygen has for N_2O production in the ocean, due to the use of unrealistically high cell concentrations (Frame and Casciotti 2010). Furthermore, given the recent recognition that NH_4^+ oxidizing archaea may play an important role in N_2O production, particularly in low oxygen environments, the use of species specific, or even domain specific, culture investigations of N_2O production under varying dissolved oxygen concentrations may not be appropriate for extrapolation to natural marine environments. To this end, I recommend that studies aiming to understand how decreasing dissolved oxygen in the ocean will affect marine N_2O production, should make use of well defined, naturally occurring oxygen gradients. Conducting measurements of N_2O production under naturally decreasing dissolved oxygen conditions will help us predict how N_2O production in regions such as the NE subarctic Pacific will respond to declining oxygen concentrations through this century. This would heed Codispoti's (2010) call in *Science* that "future experiments should focus on the controls for marine N_2O production and on potential N_2O production "hotspots"."

Bibliography

Altabet, M.A. 1988. Variations in nitrogen isotopic composition between sinking and suspended particles: Implications for nitrogen cycling and particle transformation in the open ocean. *Deep-Sea Research* 35, 535-554.

Altabet, M.A. 1989. A time-series study of the vertical structure of nitrogen and particle dynamics in the Sargasso Sea. *Limnology and Oceanography* 34, 1185-1201.

Anderson, J.J., and A.H. Devol. 1973. Deep water renewal in Saanich Inlet, an intermittently anoxic basin. *Estuarine and coastal marine science* 1, 1-10.

Andreev, A.G., and M. Kusakabe. 2001. Interdecadal variability in dissolved oxygen in the intermediate water layer of the Western Subarctic Gyre and Kuril Basin (Okhotsk Sea). *Geophysical Research Letters* 28, 2453-2456.

Aydin, M., Z. Top, and D.B. Olson. 2004. Exchange processes and water mass modification along the subarctic front in the North Pacific: Oxygen consumption rates and net carbon flux. *Journal of Marine Research* 62, 153-167.

Bange, H.W., 2008. Gaseous nitrogen compounds (NO, N_2O, N_2, NH_3) in the ocean. In: Capone, D.G., Bronk, D.A., Mulholland, M.R., Carpenter, E.J. (Eds), Nitrogen in the marine environment 2nd addition. Academic Press, Burlington, MA, pp. 51-94.

Bange, J.W., T. Rixen, A.M. Johansen. R.L. Siefert, R. Ramesh, V. Ittekkot, M.R. Hoffmann, and M.O. Andreae. 2000. A revised nitrogen budget for the Arabian Sea. *Global Biogeochemical Cycles* 14, 1283-1297.

Barwell-Clarke, J., and F. Whitney. 1996. Institute of Ocean Sciences nutrient methods and analysis. *Canadian Technical Report of Hydrography and Ocean Sciences*, report no. 182.

Bendschneider, K., and R.J. Robinson. 1952. A new spectrophotometric method for the determination of nitrite in sea-water. *Journal of Marine Research* 11, 96-97.

Bianchi, M., P. Bonin, and Feliatra. 1994a. Bacterial nitrification and denitrification rates in the Rhône River plume (northwestern Mediterranean Sea). *Marine Ecology Progress Series* 103, 197-202.

Bianchi, M. P. Morin, and P. Le Corre. 1994b. Nitrification rates, nitrite and nitrate distribution in the Almeria-Oran frontal systems (eastern Alboran Sea). *Journal of Marine Systems* 5, 327-342.

Bianchi, M., F. Feliatra, P. Tréguer, M-A. Vincendeau, and J. Morvan. 1997. Nitrification rates, ammonium and nitrate distribution in upper layers of the water column and in

sediments of the Indian sector of the Southern Ocean. *Deep-Sea Research II* 44, 1017-1032.

Bianchi, M., Feliatra, and D. Lefevre. 1999a. Regulation of nitrification in the land-ocean contact area of the Rhône River plume (NW Mediterranean). *Aquatic Microbial Ecology* 18, 301-312.

Bianchi, M., C. Fosset, and P. Conan. 1999b. Nitrification rates in the NW Mediterranean Sea. *Aquatic Microbial Ecology* 17, 267-378.

Bograd, S.J., C.G. Castro, E. Di Lorenzon, D.M. Palacios, H. Bailey, W. Gilly, and F.P. Chavez. 2008. Oxygen declines and the shoaling of the hypoxic boundary in the California Current. *Geophysical Research Letters* 35, L12607.

Bouskill, N.J., D. Eveillard, D. Chien, A. Jayakumar, and B.B. Ward. 2012. Environmental factors determining ammonia-oxidizing organism distribution and diversity in marine environments. *Environmental Microbiology* 14 (3), 714-729.

Boyd, P.W., J.A., Berges, and P.J. Harrison. 1998. In vitro iron enrichment experiments at iron-rich and iron-poor sites in the NE subarctic Pacific. *Journal of Experimental Marine Biology and Ecology* 227, 133-151.

Boyd, P.W., D.L. Muggli, D.E. Varela, R.H. Goldblatt, R. Chretien, K.J. Orians, and P.J. Harrison. 1996. In vitro iron enrichment experiments in the NE subarctic Pacific. *Marine Ecology Progress Series* 136, 179-193.

Borckmann, D., and E. Morgenroth. 2010. Evaluating operating conditions for outcompeting nitrite oxidizers and maintaining partial nitrification in biofilm systems using biofilm modeling and Monte Carlo filtering. *Water Research* 44 (6), 1995-2009.

Butler, J.H.. J.W. Elkins, T.M Thompson and K.B. Egan. 1989. Troposheric and dissolved N_2O of the West Pacific and East Indian Oceans during the El Niño southern oscillation event of 1987. *Journal of Geophysical Research* 94, 14865-14877.

Casey, J.R., M.W. Lomas, J. Mandecki, D.E., and D.E. Walker. 2007. *Prochlorococcus* contributes to new production in the Sargasso Sea deep chlorophyll maximum. *Geophysical Research Letters* 34, L10604, DOI: 10.1029/2006GL028725.

Castro, C.G., F.P. Chavez and C.A. Collins. 2001. Role of the California Undercurrent in the export of denitrified waters from the eastern tropical North Pacific. *Global Biogeochemical Cycles* 15, 819-830.

Charette, M.A., S.B. Moran, J.K.B. Bishop. 1999. Th-234 as a tracer of particulate organic carbon export in the subarctic northeast Pacific Ocean. *Deep-Sea Research II* 46, 2833-2861.

Clark, D.R., A.P. Rees, and I. Joint. 2008. Ammonium regeneration and nitrification rates in the oligotrophic Ocean: Implications for new production estimates. *Limnology and Oceanography* 53 (1), 52-62.

Codispoti, L.A., and J.P Christensen. 1985. Nitrification, denitrification and nitrous oxide in the eastern tropical South-Pacific Ocean. *Marine Chemistry* 16, 277-300.

Codispoti, LA. 2010. Interesting times for marine N_2O. *Science* 327, 1339-1340.

Codispoti, L.A., J.A. Brandes, J.P. Christensen, A.H. Devol, S.W.A. Naqvi, H.W. Paerl, and T. Yoshinari. 2001. The oceanic fixed nitrogen and nitrous oxide budgets: Moving targets as we enter the anthropocene? *Scientia Marina* 65, 85-105.

Cohen, Y., and L.I. Gordon. 1979. Nitrous oxide production in the ocean. *Journal of Geophysical Research* 84, 347-353.

Cohen, Y. 1978. Consumption of dissolved nitrous oxide in an anoxic basin, Saanich Inlet, British Columbia. *Nature* 272, 235-237.

Collins, C.A., L.M. Ivanov, O.V. Melnichenko, and N. Garfield. 2004. California Undercurrent variability and eddy transport estimated from RAFOS float observations. *Journal of Geophysical Research* 109, CO5028.

Crutzen, P.J. 1970. Influence of nitrogen oxides on atmospheric ozone content. *Quarterly Journal of the Royal Meteorological Society* 96, 320-327.

Davis, C.S. and D.J. McGillicuddy. 2006. Transatlantic abundance of the N_2-fixing colonial cyanobacteriaum *Trichodesmium*. *Science* 312, 1517-1520.

de Bie, M.J.M., J.J. Middelburg, M. Starink, and H.J. Laanbroek. 2002. Factors controlling nitrous oxide at the microbial community and estuarine scale. *Marine Ecology Progress Series* 240, 1-9.

Devol, A.H. 2008. Denitrification including Anammox. In: D.G. Capone, D.A. Bronk, M.R. Mullholland and E.J. Carpenter (Eds), *Nitrogen in the marine environment 2nd edition* (pp. 263-301). Burlington, M.A.: Academic Press.

Diaz, F., and P. Raimbault. 2000. Nitrogen regeneration and dissolved organic nitrogen release during spring in a NW Mediterranean coastal zone (Gulf of Lions): implications for the stiamte of new production. *Marine Ecology Progress Series* 197, 51-65.

Diaz, R.J., and R. Rosenberg. 1995. Marine benthic hypoxia: A review of its ecological effects and the behavioral responses of benthic macrofauna. *Oceanography and Marine Biology – An Annual Review* 33, 245-303.

Dore, J.W., and D.M. Karl. 1996. Nitrification in the euphotic zone as a source for nitrite, nitrate, and nitrous oxide at Station ALOHA. *Limnology and Oceanography* 41 (8), 1619-1628.

Dore, J.E., B.N. Popp, D.M. Karl, and F.J. Sansome. 1998. A large source of atmospheric nitrous oxide from subtropical North Pacific surface waters. *Nature* 396, 63-66.

Dugdale, R.C., and J.J. Goering. 1968. Uptake of new and regenerated forms of nitrogen in primary productivity. *Limnology and Oceanography* 12, 196-206.

Dugdale, R.C., and F.P. Wilkerson. 1986. The use of ^{15}N to measure nitrogen uptake in eutrophic oceans; experimental considerations. *Limnology and Oceanography* 31, 673-689.

Emerson, S., Y.W. Watanabe, T. Ono, and S. Mecking. 2004. Temporal trends in apparent oxygen utilization in the upper pycnocline of the North Pacific: 1980-2000. *Journal of Oceanography* 60, 139-147.

Eppley, R.W., and B.J. Peterson. 1979. Particulate organic-matter flux and planktonic new production in the deep ocean. *Nature* 282, 677-680.

Falkowski, P.G., R.T. Barber, and V. Smetacek. 1998. Biogeochemical controls and feedbacks on ocean primary production. *Science* 281, 200-206.

Feliatra, F., and Bianchi, M.. 1993. Rates of nitrification and carbon uptake in the Rhône River Plume (Northwestern Mediterranean Sea). *Microbial Ecology* 26, 21-28.

Frame, C.H., and K.L. Casciotti. 2010. Biogeochemical controls and isotopic signatures of nitrous oxide production by a marine ammonia-oxidizing bacterium. *Biogeosciences* 7, 2695-2709.

Gargett, A.E., D. Stucchi, and F. Whitney. 2003. Physical processes associated with high primary production in Saanich Inlet, British Columbia. *Estuarine, Coastal and Shelf Science* 56, 1141-1156.

Giesbrecht, K.E., R.C. Hamme, and S.R. Emerson. In review. Biological Productivity along Line P in the subarctic northeast Pacific: in-situ versus incubation based methods. *Global Biogeochemical Cycles.*

Goreau, T.J., W.A. Kaplan, S.C. Wofsy, M.B. McElroy, F.W. Valois. and S.W. Watson. 1980. Production of NO_2^- and N_2O by nitrifying bacteria at reduced concentrations of oxygen. *Applied and Environmental Microbiology* 40, 526-532.

Gruber, N.. 2008. The marine nitrogen cycle: overview and challenges. In: Capone, D.G., Bronk, D.A., Mulholland, M.R., Carpenter, E.J. (Eds), *Nitrogen in the marine environment 2nd addition*. Academic Press, Burlington, MA, pp. 1-50.

Grundle, D.S., D.A. Timothy, and D.E. Varela. 2009. Variations of phytoplankton productivity and biomass over an annual cycle in Saanich Inlet, a British Columbia fjord. *Continental Shelf Research* 29, 2257-2269.

Grundle, D.S., and S.K. Juniper. 2011. Nitrification from the lower euphotic zone to the sub-oxic waters of a highly productive British Columbia fjord. *Marine Chemistry* 126, 172-181.

Grundle, D.S., S.K. Juniper, and K.E. Giesbrecht. In review. Euphotic zone nitrification in the NE subarctic Pacific: Implications for measurements of new production. *Marine Chemistry*.

Grundle, D.S., R. Maranger, and S.K. Juniper. 2012. Upper water column nitrous oxide distributions in the NE subarctic Pacific. *Atmosphere-Ocean* 50, 475-486.

Guerrero, M.A., and R.D. Jones. 1996a. Photo-inhibition of marine nitrifying bacteria I. Wavelength dependent response. *Marine Ecology Progress Series* 141, 183-192.

Guerrero, M.A., and R.D. Jones. 1996b. Photo-inhibition of marine nitrifying bacteria II. Dark recovery after monochromatic or polychromatic irradiation. *Marine Ecology Progress Series* 141, 193-198.

Herlinveaux, R.H. 1962. Oceanography of Saanich Inlet in Vancouver Island, British Columbia. *Journal of Fisheries Research Board of Canada* 19, 1-37.

Hirota, A., A. Ijiri, D.D. Komatsu, S.B. Ohkubo, F. Nakagawa, and U. Tsunogai. 2009. Enrichment of nitrous oxide in the water columns in the area of the Bering and Chukchi Seas. *Marine Chemistry* 116, 47-53.

Hirota, A., U. Tsunogai, D.D. Komatsu, and K.F. Nakagawa. 2010. Simultaneous determination of $\delta^{15}N$ and $\delta^{18}O$ of N_2O and $\delta^{13}C$ of CH_4 in nanomolar quantities from a single water sample. *Rapid Communications in Mass Spectrometry* 24, 1086-1092.

Holmes, R.M., A. Aminot, R. Kérouel, B.A. Hooker, and B.J. Peterson. 1999. A simple and precise method for measuring ammonium in marine and freshwater ecosystems. *Canadian Journal of Fisheries and Aquatic Sciences* 56, 1801-1808.

Hooper, A.B., and K.R. Terry. 1973. Specific inhibitors of ammonia oxidation in *Nitrosomonas*. *Journal of Bacteriology* 115 (2), 480-485.

Horrigan, S.G., A.F. Carlucci, and P.M Williams. 1981. Light inhibition of nitrification in sea-surface films. *Journal of Marine Research* 39, 557-565.

Horrigna, S.G., and A.L. Springer. 1990. Oceanic and estuarine ammonium oxidation: effects of light. *Limnology and Oeanography* 35 (2), 479-482.

IPCC, 2007. Climate Change 2007. *The physical science basis.* New York, NY: Cambridge University Press.

Iriarte, A., I. de Madariaga, F. Diez-Garagarza, M. Revilla, E. Orive. 1996. Primary plankton production, respiration and nitrification in a shallow temperate estuary during summer. *Journal of Experimental Marine Biology and Ecology* 208, 127-151.

Jähne, B., K.O. Münnich, R. Bösinger, A. Dutzi, W. Huber, and P. Libner. 1987. On the parameters of influencing air-water gas exchange. *Journal of Geophysical Research* 92, 1937-1949.

Keeling, R.F., A. Kortzinger, and N. Gruber. 2010. Ocean deoxygenation in a warming world. *Annual Review of Marine Science* 2, 199-220.

Könneke, M., A.E. de la Tore Bernhard, C.B. Walker, J.B. Waterbury, and D.A. Stahl. 2005. Isolation of an autotrophic ammonia-oxidizing marine archaeon. *Nature* 437, 543-546.

Kool, D.M., J.W. Van Groenigen, and N. Wrage (2011). Source determination of nitrous oxide based on nitrogen and oxygen isotope tracing: Dealing with oxygen exchange. In: Methods in Enzymology 46: Research on nitrification and related processes, Pt B, vol 496; 139-160.

Lam, P., J.P. Cowen, and R.D. Jones. 2004. Autotrophic ammonia oxidation in a deep-sea hydrothermal plume. *Microbiology Ecology* 47, 191-206.

Levitus, S. 1982. In: Climatological Atlas of the World Ocean. *NOAA Professional Paper 13* (pp. 173). Washington, D.C.: US Government Printing Office.

Lipschultz, F. 2001. A time-series assessment of the nitrogen cycle at BATS. *Deep-Sea Research II* 48, 1897-1924.

Lipschultz, F., N.R. Bates, C.A. Carlson, and D.A. Hansell. 2002. New production in the Sargasso Sea: History and current status. *Global Biogeochemical Cycles*, doi: 10.1029/2000GB001319.

Lipschultz, F., S.C. Wofsy, B.B. Ward, L.A. Codispoti, G. Friedrich, and J.W. Elkins. 1990. Bacterial transformations of inorganic nitrogen in the oxygen-deficient waters of the Eastern South Pacific Ocean. *Deep-Sea Research* 37 (10), 1513-1541.

Lomas, M.W., D.A. Bronk, and G. van den Engh. 2011. Use of flow cytometry to measure biogeochemical rates and processes in the ocean. *Annual Review of Marine Science* 3, 537-566.

Lomas, M.W., and F. Lipschultz. 2006. Forming the primary nitrite maximum: Nitrifiers or phytoplankton? *Limnology and Oceanography* 51 (5), 2453-2467.

Maldonado, M.T., P.W. Boyd, P.J. Harrison, and H.M. Price. 1999. Co-limitation of phytoplankton growth by light and Fe during winter in the NE subarctic Pacific Ocean. *Deep-Sea Research II* 46, 2475-2485.

Manning, C.C., R.C. Hamme, and A. Bourbonnais. 2010. Impact of deep-water renewal events on fixed nitrogen loss from seasonally-anoxic Saanich Inlet. *Marine Chemistry 122*, 1-10.

Marchetti, A., P. Juneau, F.A. Whitney, C.S. Wong, and P.J. Harrison. 2006. Phytoplankton processes during a mesoscale iron enrichment in the NE subarctic Pacific: Part II – Nutrient utilization. *Deep-Sea Research II* 53, 2114-2130.

Matear, R.J., and A.C. Hirst. 2003. Long-term changes in dissolved oxygen concentrations in the ocean caused by protracted global warming. *Global Biogeochemical Cycles* 17, doi: 10.1029/2002GH001997.

McGillicuddy, D.J., A.R. Robinson, D.A. Siegel, H.W. Jannasch, R. Johnson, T.D. Dickey, J. McNeil, A.F. Michaels, and A.H. Knap. 1998. Influence of mesoscale eddies on new production in the Sargasso Sea. *Nature* 394, 263-266.

McIlvin, M.R., and K.L. Casciotti. 2010. Fully automated system for stable isotopic analyses of dissolved nitrous oxide and natural abundance levels. *Limnology and Oceanography: Methods* 9, 54-66.

Mecking, S., M.J. Warner, and J.L. Bullister. 2006. Temporal changes in pCFC-12 ages and AOU along two hydrographic sections in the eastern subtropical North Pacific. *Deep-Sea Research I* 53, 169-187.

Mincer, T.J., M.J. Church, L.T. Taylor, C. Preston, and D.M. Karl. 2007. Quantitative distribution of presumptive archaeal and bacterial nitrifiers in Monterey Bay and the North Pacific Subtropical Gyre. *Environmental Microbiology* 9 (5), 1162-1175.

Mongin, M., D.M. Nelson, P. Pondaven, M.A. Brzezinski, and P. Tréguer. 2003. Simulation of upper-ocean biogeochemistry with a flexible composition phytoplankton model: C, N and Si cycling in the western Sargasso Sea. *Deep-Sea Research I* 50, 1445-1480.

Mulholland, M.R., and M.W. Lomas. 2008. Nitrogen uptake and assimilation. In: Capone, D.G., Bronk, D.A., Mulholland, M.R., Carpenter, E.J. (Eds), *Nitrogen in the marine environment 2nd addition*. Academic Press, Burlington, MA, pp. 303-384.

Muller-Neugluck, M., and H. Engel. 1961. Photoinaktivierung von *Nitrobacter winogradskyi* Buch. *Archiv fur Mikrobiologie* 39, 130-138.

Najjar, R.G.. 1992. Marine biogeochemistry. In: K.E. Trenbert (Ed), *Climate system modelling* (pp. 241-280). Cambridge: Cambridge University Press.

Naqvi, S.W.A., H.W. Bange, L. Farias, P.M.S. Monteiro, M.L. Scranton, and J. Zhang. 2010. Marine hypoxia/anoxia as a source of CH_4 and N_2O. *Biogeosciences* 7, 2159-2190.

Nevison, C., J.H. Butler, and J.W. Elkins. 2003. Global distribution of N_2O and the ΔN_2O-AOU yield in the subsurface ocean. *Global Biogeochemical Cycles* 17, doi: 10.1029/2003GB002068.

Nevison, C.D., R.F. Weiss, and D.J. Erickson III. 1995. Global oceanic emissions of nitrous oxide. *Journal of Geophysical Research*, 100, 809-815.

Nevison, C.D., T.J. Lueker, and R.F. Weiss. 2004. Quantifying the nitrous oxide source from coastal upwelling. *Global Biogeochemical Cycles* 18, GB1018,

Olson, R.J. 1981. ^{15}N tracer studies of the primary nitrite maximum. *Journal of Marine Research* 39, 203-226.

Ono, T., T. Midorikawa, Y.W. Watanabe, K. Tadokoro, and T. Saino. 2001. Temporal increase in phosphate and apparent oxygen utilization in the subsurface waters of the western subarctic Pacific from 1968 to 1998. *Geophysical Research Letters* 28, 3285-3288.

Orcutt, K.M., F. Lipschultz, K. Gundersen, R. Arimoto, A.F. Michaels, A.H. Knap, J.R. Gallon. 2001. A seasonal study of the significance of N_2 fixation by *Trichodesmium* spp. At the Bermuda Atlantic Time-series Study (BATS) site. *Deep-Sea Research II* 48, 1583-1608.

Oudot, C., C. Andrie, and Y. Montel. 1990. Nitrous oxide production in the tropical Atlantic Ocean. *Deep-Sea Research I* 37. 183-202.

Parson, T.R., I.R. Perry, E.D. Nutbrown, W. Hsieh, and C.M. Lalli. 1983. Frontal zone analysis at the mouth of Saanich Inlet, British Columbia, Canada. *Marine Biology* 73, 1-5.

Peña, M.A., and D.E. Varela. 2007. Seasonal and interannual variability in phytoplankton and nutrient dynamics along Line P in the NE subarctic Pacific. *Progress in Oceanography* 75, 200-222.

Plattner, G.K., F. Joos, T.F. Stocker, and O. Marchal. 2001. Feedback mechanisms and sensitivities of ocean carbon uptake under global warming. *Tellus Series B – Chemical and Physical Meteorology* 53, 564-592.

Punshon, S. and R.M. Moore. 2004a. A stable isotope technique for measuring production and consumption rates of nitrous oxide in coastal waters. *Marine Chemistry* 86, 159-168.

Punshon, S. and R.M. Moore. 2004b. Nitrous oxide production and consumption in a eutrophic coastal embayment. *Marine Chemistry* 91, 37-51.

Raven, J.A. and P.G. Falkowski. 1999. Oceanic sinks for atmospheric CO_2. *Plant Cell and Environment* 22, 741-755.

Raimbault, P., G. Slawyk, B. Boudjellal, C. Coatanoan, P. Conan, B. Coste, N. Garcia, T. Moutin, and M. Pujo-Pay. 1999. Carbon and nitrogen uptake and export in the equatorial Pacific at 150°W: Evidence of an efficient regenerated production cycle. *Journal of Geophysical Research* 104, 3341-3356.

Ryanbenko, E., A. Kock, H.W. Bange, M.A. Altabet, and D.W.R. Wallace. 2011. Contrasting biogeochemistry of nitrogen in the Atlantic and Pacific Oxygen Minimum Zones. *Biogeosciences Discussions*, doi: 10.1126/science.1208239.

Santoro, A.E., C. Buchwald, M.R. McIlvin, and K.L. Casciotti. 2011. Isotope signature of N_2O produced by marine ammonia-oxidizing archaea. *Science Express Online Publication*, doi:20.1126/science.1208239.

Santoro, A.E., K.L. Casciotti, and C.A. Francis. 2010. Activity, abundance and diversity of nitrifying archaea and bacteria in the central California Current. *Environmental Microbiology* 12, 1989-2006.

Sarmiento, J.L., T.M.C. Hughes, R.J. Stougger, and S. Manabe. 1998. Simulated response of the ocean carbon cycle to anthropogenic climate warming. *Nature* 393, 245-249.

Schon, G., and H. Engel. 1962. Det Einfluss des Lichtes auf *Nitrosomonas europaea* Win. *Archive fur Mikrobiologie* 42, 415-428.

Stein, L.Y., and Y.L. Yung. 2003. Production, isotopic composition, and atmospheric fate of biologically produced nitrous oxide. *Annual Review of Earth and Planetary Sciences* 31, 329-356.

Steinberg, D.K., C.A. Carlson, N.R. Bates, R.J. Johnson, A.F. Michaels, and A.H. Knap. 2001. Overview of the U.S. JGOFS Bermuda Atlantic Time-series Study (BATS): A decade-scale look at ocean biology and biogeochemistry. *Deep-Sea Research II* 48, 1405-1447.

Takahashi, M., D.L. Seibert, and W.H. Thomas. 1977. Occasional blooms of phytoplankton during summer in Saanich Inlet, BC, Canada. *Deep-Sea Research* 24, 775-780.

Takahashi, T., S.C. Sutherland, C. Sweeney, A. Poisson, N. Metzl, B. Tilbrook, N. Bates, R. Wanninkhof, R.A. Feely, C. Sabine, J. Olafsson, and Y. Nojiri. 2002. Global sea-air CO_2 flux based on climatological surface ocean pCO_2, and seasonal biological and temperature effects. *Deep-Sea Research II* 49, 1601-1622.

Thomson, R.E., and M.V. Krassovski. 2010. Poleward reach of the California Undercurrent extension. *Journal of Geophysical Research* 115, C09027, doi: 10.1029/2010JC006280.

Timothy, D.A., and M.Y.S. Soon. 2001. Primary production and deep-water oxygen content of two British Columbia fjords. *Marine Chemistry* 73, 37-51.

Timothy, D.A., M.Y.S. Soon, and S.E. Calvert. 2003. Settling fluxes in Saanich and Jervis inlets, British Columbia, Canada: sources and seasonal patterns. *Progress in Oceanography* 59, 31-73.

Toyoda, S., H. Mutobe, H. Yamigishi, N. Yoshida, and Y. Tanji (2005). Fractionation of N_2O isotopomers during production by denitrificaiton. *Soil Biology and Biochemistry* 37, 1535-1545.

Ueno, H., and I. Yasuda. 2003. Intermediate water circulation in the North Pacific subarctic and northern subtropical regions. *Journal of Geophysical Research* 108, doi: 10.1029/2002JC001372.

Upstill-Goddard, R.C., J. Barnes, and N.J.P. Owens. 1999. Nitrous oxide and methane during the 1994 SW monsoon in the Arabian Sea/northwestern Indian Ocean. *Journal of Geophysical Research* 104, 30067-30084.

Vanzella, A., M.A. Guerrero, and R.D. Jones. 1989. Effect of CO and light on ammonium and nitrite oxidation by chemolithotrophic bacteria. *Marine Ecology Progress Series* 57, 69-76.

Vanzella, A., M.A. Guerrero, and R.D. Jones. 1990. Recovery of nitrification in marine bacteria following exposure to carbon monoxide or light. *Marine Ecology Progress Series* 60, 91-95.

Varela, D.E., and P.J. Harrison. 1999. Seasonal variability in nitrogenous nutrition of phytoplankton assemblages in the northeastern subarctic Pacific Ocean. *Deep-Sea Research II* 46, 2505-2538.

Walter, S., H.W. Bange, and D.W.R. Wallace. 2004. Nitrous oxide in the surface layer of the tropical North Atlantic Ocean along a west to east transect. *Geophysical Research Letters* 31, L23S07, doi: 10.1029/2004GL019937.

Walter, S., H.W. Bange, U. Breitenback, and D.W.R. Wallace. 2006. Nitrous oxide in the North Atlantic Ocean. *Biogeosciences* 3, 607-619.

Wankel, S.D., C. Kendall, J.T. Pennington, F.P. Chavez, and A. Paytan. 2007. Nitrification in the euphotic zone as evidenced by nitrate dual isotopic composition: Observations from Monterey Bay, California. *Global Biogeochemical Cycles* 21, doi:10.1029/2006GB002723.

Wannikhof, R.. 1992. Relationship between wind-speed and gas-exchange over the ocean. *Journal of Geophysical Research-Oceans* 97, 7373-7382.

Ward, B.B.. 1987. Nitrogen transformations in the Southern California Bight. *Deep-Sea* Research 34, 785-805.

Ward, B.B.. 2005. Temporal variability in nitrification rates and related biogeochemical factors in Monterey Bay, California, USA. *Marine Ecology Progress Series* 292, 97-109.

Ward, B.B., 2008. Nitrification in Marine Systems. In: Capone, D.G., Bronk, D.A., Mulholland, M.R., Carpenter, E.J. (Eds), *Nitrogen in the marine environment 2nd addition*. Academic Press, Burlington, MA, pp. 199-262..

Ward, BB. 2011. Measurement and distribution of nitrification rates in the oceans. In: Klotz, M.G. (ed), *Methods in Enzymology, Vol 48*. Academic Press, Burlington, MA, pp. 307-323.

Ward, B.B., H.E. Glover, and F. Lipschultz. 1989. Chemoautotrophic activity and nitrification in the oxygen minimum zone off Peru. *Deep-Sea Research* 36 (7), 1031-1051.

Ward, B.B., and K.A. Kilpatrick. 1990. Relationship between substrate concentration and oxidation of ammonium and methane in a stratified water column. *Continental Shelf Research* 10 (12), 1193-1208.

Ward, B.B., M.C. Talbot, and M.J. Perry. 1984. Contributions of phytoplankton and nitrifying bacteria to ammonium and nitrite dynamics in coastal waters. *Continental Shelf Research* 3 (4), 383-398.

Ward, B.B., R.J. Olson, and M.J. Perry. 1982. Microbial nitrification rates in the primary nitrite maximum off Southern California. *Deep-Sea Research* 29 (2A), 247-255.

Watanabe, Y.W., T. Ono, A. Shimamoto, T. Sugimoto, M. Wakita, and S. Watanabe. 2001. Probability of a reduction in the formation rate of the subsurface water in the North Pacific during the 1980s and 1990s. *Geophysical Research Letters* 28, 3289-3292.

Weiss, R.F., and B.A. Price. 1980. Nitrous oxide solubility in water and seawater. *Marine Chemistry* 8, 347-359.

Whitney, F.A., C.S. Wong, and P.W. Boyd. 1998. Interannual variability in nitrate supply to surface waters of the Northeastern Pacific Ocean. *Marine Ecology Progress Series* 170, 15-23.

Whitney, F.A., H.J. Freeland, and M. Robert. 2007. Persistently declining oxygen levels in the interior waters of the eastern subarctic Pacific. *Progress in Oceanography* 75, 179-199.

Whitney, F.A., W.R. Crawford, and P.J. Harrison. 2005. Physical processes that enhance nutrient transport and primary productivity in the coastal open ocean of the Subarctic NE Pacific. *Deep-Sea Research II* 52 681-706.

Yamagishi, H., N. Yoshida, S. Toyoda, B.N. Popp, M.B. Westley, and S. Watanabe. 2005. Contributions of denitrification and mixing on the distribution of nitrous oxide in the North Pacific. *Geophysical Research Letters* 32, L04603, doi: 10.1029/2004GL021458.

Yool, A., A.P. Martin, C. Fernández, and D.R. Clark. 2007. The significance of nitrification for oceanic new production. *Nature* 447, 999-1002.

Yoshida, N., H. Morimoto, M. Hirano, I. Koike, S. Matsuo, E. Water, T. Saino, and A. Hattori. 1989. Nitrification rates and ^{15}N abundances of N_2O and NO_3^- in the western North Pacific. *Nature* 342, 895-897.

Yoshida, N., and S. Toyoda. 2000. Constraining the atmospheric N_2O budget from intramolecular site preference in N_2O isotopomers. *Nature* 405, 330-334.

Yoshikawa, C., T. Nakatsuka, and M. Wakatsuchi. 2006. Distribution of N* in the Sea of Okhotsk and its use as a biogeochemical tracer of Okhotsk Sea Intermediate Water formation processes. *Journal of Marine Systems* 63, 49-62.

Appendix 1

Table A1. Monthly NH_4^+ oxidation (AO) and NO_2^- oxidation (NO) rates at station SI-2 in Saanich Inlet, from April to October 2008. Depths are either reported as % surface light intensity (I_o) or in metres.

Month	Depth	AO (μmol L^{-1} d^{-1})	AO (μmol L^{-1} d^{-1})
April	10% I_o	0.108	0.164
	1% I_o	nd	nd
	30 m	0	0.092
	60 m	nd	nd
	90 m	0.071	0.187
	120 m	nd	nd
May	10% I_o	0.047	0
	1% I_o	0.017	0.059
	30 m	0.081	0
	60 m	0.039	0.177
	90 m	0.057	0.047
	120 m	0.012	0.122
June	10% I_o	0	0.030
	1% I_o	0.043	0.023
	30 m	0.085	0
	60 m	0.115	0.189
	90 m	0.089	0
	120 m	0	0
July	10% I_o	0.102	0.096
	1% I_o	0.078	0.150
	30 m	0.133	0.236
	60 m	0.096	0.096
	90 m	0.090	0.188
	120 m	0.024	0.016
August	10% I_o	0.229	0.223
	1% I_o	0.176	0.229
	30 m	0.071	0.170
	60 m	0	0
	90 m	0	0
	120 m	0	0.129
September	10% I_o	0.042	0.168
	1% I_o	0.048	0.210
	30 m	0.084	0
	60 m	0	0.182
	90 m	0.138	0.154
	120 m	0.078	0
October	10% I_o	0.263	0.457
	1% I_o	0.131	0.478
	30 m	0.150	0.403
	60 m	0.319	0.103
	90 m	0.225	0
	120 m	0.113	0

Table A2. NH_4^+ oxidation (AO) rates at stations P4, P12, P16, P20 and P26 during winter, spring and late-summer 2009. Depths are either reported as % of surface light intensity (I_o) or in metres.

		AO (nmol L-1 d-1)				
Season	Depth	P4	P12	P16	P20	P26
Winter	0 m	76	0	19	30	63
	10 m	25	0	26	0	0
	20 m	97	0	59	0	0
	30 m	80	0	48	0	35
	40 m	30	0	33	43	0
	75 m	0	0	0	33	0
Spring	100% I_o	19	0	45	28	35
	55% I_o	14	33	34	22	35
	33% I_o	19	27	22	44	15
	10% I_o	24	16	22	39	30
	1% I_o	48	38	17	28	39
Late-Summer	100% I_o	0	0	20	5	16
	55% I_o	0	16	17	14	16
	33% I_o	0	19	10	10	16
	10% I_o	14	0	13	23	16
	1% I_o	14	28	33	28	19

Table A3. NH_4^+ oxidation (AO) rates at BATS during cruises in April and November 2009. Depths are reported as % of surface light intensity (I_o).

	AO (nmol L-1 d-1)				
Depth	Apr 1	Apr 15	Nov 7	Nov 9	Nov 22
100% I_o	0	0	0	10	0
55% I_o	0	9	13	8	0
33% I_o	21	0	17	8	0
10% I_o	27	19	0	0	8
1% I_o	33	19	20	14	13